WIDE-AREA CONTROL FOR LOW FREQUENCY

OSCILLATIONS IN MULTI-MACHINE POWER SYSTEMS

BY

AHMED HUSHAM AHMED MOHAMED

A Thesis Presented to the

DEANSHIP OF GRADUATE STUDIES

KING FAHD UNIVERSITY OF PETROLEUM & MINERALS

DHAHRAN, SAUDI ARABIA

In Partial Fulfillment of the
Requirements for the Degree of

MASTER OF SCIENCE

In

ELECTRICAL ENGINEERING

April 2018

KING FAHD UNIVERSITY OF PETROLEUM & MINERALS

DHAHRAN- 31261, SAUDI ARABIA

DEANSHIP OF GRADUATE STUDIES

This thesis, written by **AHMED HUSHAM AHMED MOHAMED** under the direction

of his thesis advisor and approved by his thesis committee, has been presented and accepted

by the Dean of Graduate Studies, in partial fulfillment of the requirements for the degree

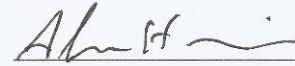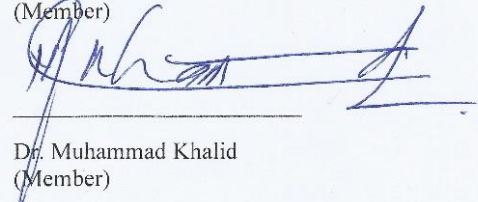of **MASTER OF SCIENCE IN ELECTRICAL ENGINEERING.**

Dr. Mohammad A. Abido
(Advisor)

Dr. Ali A. Al-Shaikhi
Department Chairman

Dr. Alaa El-Din Hussein
(Member)

Dr. Salam A. Zummo
Dean of Graduate Studies

Dr. Muhammad Khalid
(Member)

9/9/18

Date

iii

Dedicated to

My Beloved Mother

ACKNOWLEDGMENTS

In the name of Allah, the Most Gracious and the Most Merciful. Prayers and peace be upon Him prophet Mohammed, the last messenger for all humankind.

First and foremost, all praise and deep thanks are due to Allah, who helped and guided me through the challenges of my study. Glory is to Allah who has given me the strength, patience and knowledge to continue and complete my thesis.

> Allah said:
>
> *"He is the Ever-Living; there is no god except Him, so call upon Him, being sincere to Him in religion. All praise is due to Allah, Lord of the worlds"* *(Qur'an 40:65)*

I would like to acknowledge all those who help me to complete this thesis. I would like to express my sincere gratitude to my advisor, Prof. Mohammad Abido for his guidance and constant support in helping me to conduct and complete this research. I would like also to thank my thesis committee members, Dr. Alaa El-Din Hussein, and Dr. Muhammad Khalid. for their involvement and the time they spare to review this thesis.

Acknowledge is due to my University, King Fahd University of Petroleum and Minerals for giving me the opportunity and the support to obtain this achievement.

My deepest gratitude goes to my beloved family for their endless care, love, prayers and encouragement. May almighty God give them health and wellness, happiness, and long life of obedience to God.

I reserve this last acknowledge to my mother for her emotional support, encouragement and patience throughout the long journey of this thesis. The completion of this thesis wouldn't have been possible without her monumental support and love.

<div dir="rtl">

وآخر دعوانا أن الحمد لله رب العالمين.

والصلاة والسلام على سيد المرسلين وعلى آله وصحبه أجمعين.

</div>

TABLE OF CONTENTS

LIST OF TABLES

LIST OF FIGURES

LIST OF ABBREVIATIONS

AVR	Automatic Voltage Regulator
FACTS	Flexible AC Transmission Systems
GPS	Global Positioning System
LFO	Low Frequency Oscillation
LQG	Linear Quadratic Gaussian
NCS	Networked Control System
PMU	Phasor Measurement Unit
PSS	Power System Stabilizer
RTDS	Real Time Digital Simulator
ST-WADC	Scattering Transformation-based Wide-Area Damping Controller
SVC	Static VAR Compensator
TCSC	Thyristor Controlled Series Compensator
WAC	Wide Area Control
WADC	Wide Area Damping Controller
WAMS	Wide-Area Measurement System

ABSTRACT

Full Name   :   AHMED HUSHAM AHMED MOHAMED

Thesis Title   :   [WIDE-AREA CONTROL FOR LOW FREQUENCY
                          OSCILLATIONS IN MULTI-MACHINE POWER SYSTEMS

Major Field   :   ELECTRICAL ENGINEERING

Date of Degree   :   April 2018

With the continuous expansion of power systems today, they became more exposed to a massive stress than they were before. That is due to the rapid increase of population size which means an inevitable growth of power demands and market needs. Because of these undeniable facts, transmission system is approaching its operating limit, and this shall bring a lot of stability issues which could lead to a series of unwelcomed consequences. With the advent of new wide-area measurements technology, those problems seem to be eventually solved, this new orientation could reinforce the power grid and help to make it more secure. This work aims to design a wide-area damping controller based on robust control theory to improve small-signal dynamic stability. The approach that has been used here is based on linear quadratic gaussian theory. The proposed method has demonstrated its capability to improve system stability and offer an acceptable system performance for a wide range of operating conditions. This methodology has been experimentally verified via real-time digital simulation.

Since wide area signals are utilized, therefore, the delay impact should be considered as well. Moreover, this work proposes a novel design of scattering transformation-based wide-area damping controller to ensure power system stability with large constant and

variable time delay. The performance of the proposed controller is compared with a classical lead-lag structure-based wide-area damping controller. The proposed controller offers a great compensation of time delay and thus, improving the system damping performance. A set of case-studies is considered to verify the effectiveness of the proposed controller under different disturbance scenarios. The results confirm the efficacy of the proposed design approach to overcome the time delay and enhance power system stability.

ملخص الرسالة

الاسم الكامل: احمد هشام احمد محمد

عنوان الرسالة: تصميم نظام تحكم واسع المدى للذبذبات ذات التردد المنخفض في نظام طاقه متعدد المولدات

التخصص: الهندسة الكهربائية

تاريخ الدرجة العلمية: أبريل 2018

مع التمدد المستمر لنظم القدرة الكهربية هذه الايام, اصبحت هذه النظم اكثر عرضة للاجهاد (stress) اكثر مما كانت عليه من قبل, و هذا قد يعزى الى الزيادة المطردة في اعداد السكان مما يعني نموا حتميا في الطلب على الكهرباء و احتياجات السوق. و نتيجه لهذه الحقائق التي لا يمكن انكارها, اصبح نظام النقل (Transmission System) يعمل قريبا من حده الاقصى, مما قد يجلب كثير من المشاكل المتعلقه باستقرارية النظام, وهذا بدوره قد يؤدي لكثير من العواقب الغير مرغوب فيها. مع ظهور تكنولوجيا القياسات ذات المدى البعيد (wide-area measurements technology) , اصبح من الممكن التغلب على هذه العقبات, و هذا التوجه الجديد قد يقوي الشبكه الكهربيه اكثر و يساعد في جعلها اكثر امانا.

هذا البحث يهتم بتصميم متحكم يعمل على الاشارات بعيدة المدى, معتمدا في طريقة عمله على نظريات التحكم المتين للزياده من استقرارية النظام. للحصول على أفضل أداء للمُثبت المُقترح, يتم تطبيق طريقة التحليل الخطي في تفاصيل تصميم المُثبت لتحديد أمثل موقع للمُثبت, ويتم اختيار مجموعة الإشارات المُدخلة بالاعتماد على المُولدات ذات المشاركة المُؤثرة في النطاق.

لتقدير مدى قدرة و كفاءة المُثبت المقترح, يتم دراسة نظام طاقة متعدد المكائن و يجري اختبار المُثبت عن طريق تحليل معامل التحول الخطي و مضائلة الشكل الكهروميكانيكي, إضافةً الى المحاكاة الزمنية غير الخطية لإشارات الشبكة.

بما انه يتم استخدام الاشارات بعيدة المدى, يجب ايضا الاخذ بالاعتبار التاخير الزمني المتعلق بارسال هذه الاشارات. في هذا البحث تم تصميم متحكم بطريقه جديده لضمان استقرارية النظام مع وجود تاخير زمني ثابت او متغير. تم عمل مجموعة من الاختبارات لضمان كفاءة المتحكم المقترح تحت ظروف مختلفه. النتائج اثبتت قابليه المتحكم المقترح لتجاوز مشكلة التاخير الزمني و اثبتت فاعليتها في تحسين استقرارية النظام في حالات تشغيل مختلفه.

يهدف هذا البحث أيضاً لتطبيق النظام المُختبر و المُجهز بالمُثبت المُقترح على منصة محاكاة بالزمن الحقيقي. جهاز المحاكاة بالزمن الحقيقي يعكس ديناميكية النظام و يعطي السلوك او الإستجابات الحقيقية لمكونات النظام في حال تعرض النظام الى إضطراب بسيط او خطأ. بعد الحصول على نتائج المحاكاة بالزمن الحقيقي يتم التحقق من صحتها و فعاليتها و ذلك عن طريق مقارنتها بالبحوث السابقة.

CHAPTER 1

INTRODUCTION

1.1   Overview

With the rapidly evolving of world economy, the consumption of electrical power energy has been greater than it was thirty years ago. Due to the exaggerated profiteering and utilization of natural resources such as gas and coal, a deficiency of energy reserve has been noticed worldwide, and no doubt this usage of the fundamental energy resources is turning into a colossal threat to maintain this increasing energy demand, aside from that, the new world trend towards carbon emissions reduction has wined a lot of awareness during the last decade [1].

Due to continual global growth of electrical demands ruled by the desire of having a reliable operation, power systems transmission infrastructure has remarkably evolved. Such systems experience a significant drift in several dynamical properties, and system stability margins. This evolution accompanied with high complexity to handle various operating circumstances. Multiple power system utilities therefore are interconnected. This interconnection, however, is vulnerable to undesired incoherence between generation resources, thus, a well-defined time-scale decomposition into fast and slow electro-mechanical modes represented in what so-called low frequency oscillations [2]. Damping of such oscillations has become a major concern for improving power system stability as

it would reduce the reserve margin of transmission capacity, and limit transfer ability of large-scale interconnected systems.

Extensive studies have been and continued to be conducted to better understand the modal traits of such oscillatory modes. Interarea oscillation can be damped by means of power system stabilizers (PSSs) and flexible AC transmission system (FACTS) [3]–[7]. With the advent of new wide area measurements (WAMs) technology, these control devises can utilize remote signals, overcoming the limitation of using local measurements which lacks to observe some interarea modes. Unlike SCADA (Supervisory control and data acquisition), WAMs include higher sampling frequency which provides more accurate measurements of system states for a faster remedial action [8].

An interconnected system needs to be controlled, this can be achieved manually by a group of operators to control and adjust the power supply. That would be, however, in the condition of normal operation. In the up normal conditions which usually last for less than 10 secs, it's necessary to have an automatic control [9].

Interconnected power system stability is sorted into three main classes: frequency stability, voltage stability and rotor-angle stability [9]. The overall capability of the interconnected generators can be evaluated by the rotor-angle stability. As soon as the synchronous machines has been connected in large numbers; oscillation frequency in the range between 1-2 Hz is initiated between the machines that are fairly close to each other. These oscillations could be partially resolved by using damper winding located on the machine rotor. These winding produce a damping torque proportional to the rotor speed to reduce the oscillation amplitude by absorbing the propagating kinetic energy caused by the

disturbance incidence. Since reliability issue is the main concern of any electrical company; its necessarily to have a fast system recovery from disturbances. Therefore, some specific designs were added. Automatic voltage regulators were introduced to maintain generators synchronism after faults.

Basically, the oscillations that have a detrimental impact on the power system stability, take place between multiple areas. Special kind of stabilizing controllers were designed to mitigate these oscillations [9]. Low frequency oscillations (LFOs) could be sorted into two kinds according to the swinging modes of the generators, local mode and inter-area mode. Local mode is associated with the machines which are fairly closed to each other and they swing against each other. This mode has a range of frequency between 1-2 Hz. In the case of interconnected system that linked by a weak tie-lines, the system may exhibit oscillations in the range of 0.1-0.7 Hz (Interarea oscillations) represented by the oscillations between one or more machines in one area against the rest of the areas.

1.2   Research Motivation

Interarea oscillations have become the area of great interest since it has a great impact on large-scale inter-connected power systems in term of its operation, because it limits the available transfer capability (ATC). Conventional power system stabilizers (PSSs) are installed to damp local modes but they are not effective on damping interarea oscillation since these oscillations are less controllable and less observable compared to local modes [10]. This Limitation brings up the use of wide-area controllers (WAC) which use the global signals instead of local signals. Phasor measurement units (PMU) used for on-line

monitoring of power system dynamics could provide simultaneous measurements of the system states, synchronized through GPS (Global Positioning System).

1.3 Thesis Objectives

The prime objective of this research is to design a controller based on remote area signals and compare its performance with the conventional controller. Four-machine system as well as ten-machine system are used to conduct the study. Modal analysis is used to identify low frequency oscillation. The selection of the controller location is done using controllability measure, participation factors specify which generator participates in a certain oscillation mode. To validate the controller performance, non-linear simulation is carried out using MATLAB.

To summarize the main objectives:

1. Design of wide-area damping controller based on robust control theory.
2. Hardware implementation of the proposed robust control strategy.
3. Design of new wide-area controller that capable of handling communication delays imperfections.

1.4 Thesis Contributions

This thesis proposes a novel design of scattering transformation-based wide-area damping controller to enhance power system stability. The salient feature of the proposed design approach is that it is delay-independent. The proposed controller offers a great compensation of time delay and thus, improving the system damping performance. A set of case-studies is considered to verify the effectiveness of the proposed controller under

different disturbance scenarios. The results confirm the efficacy of the proposed design approach to overcome the time delay and enhance greatly the power system stability.

1.5   Thesis Breakdown

Chapter 2 presents a relevant literature review which includes a detailed explanation of interarea oscillation nature and some of the control strategies that has been used to mitigate those oscillations. The modeling of power system and the procedure of the controller design is addressed in chapter 3. Chapter 4 discusses the design of WADC based on LQG. The design of WADC based on scattering transformation for a better time delay handling is discussed in chapter 5.

Chapter 6 presents the simulation results of the proposed methods. Real-time implementation of the proposed controller in RSCAD as well as dSPACE and a comparison between the simulated and experimental results is presented in chapter 7. Chapter 8 concludes the thesis and offers some ideas that could be applied in future.

CHAPTER 2

LITERATURE REVIEW

2.1   Nature of Inter-Area Oscillation

As the power systems became more complex, the need of a reliable and flexible operation of the power grid became a necessity. Therefore, an efficient damping of interarea oscillations is needed to maintain the available transfer capacity (ATC) within the transmission system limits [11].

Large inter-connected systems linked with weak tie-lines which transmit heavy power most probably initiate swinging modes between two groups of generators in different areas which, in turn, produce low frequency oscillations (LFOs). This type of oscillations might not be early detected, However, over a period of time, it could propagate and lead to a system collapse. Figure 2.1 and Figure 2.2 illustrates the famous August 10,1996 blackout in the WSCC (western US/Canada interconnected system). Figure 2.1 (a) shows the power response of one of the main lines under small disturbance. The system exhibits a decaying oscillation of 0.26 Hz. The decaying oscillations in Figure 2.1 (b) and Figure 2.2 (b) eventually turned into growing oscillations which caused the final system collapse as shown in Figure 2.2 (b), this has resulted in disconnecting the system regions, causing power loss to many customers [9].

Conventionally power system stabilizer (PSS) is used to suppress power system low frequency oscillations by providing a supplemental control action through the excitation system [12][13].
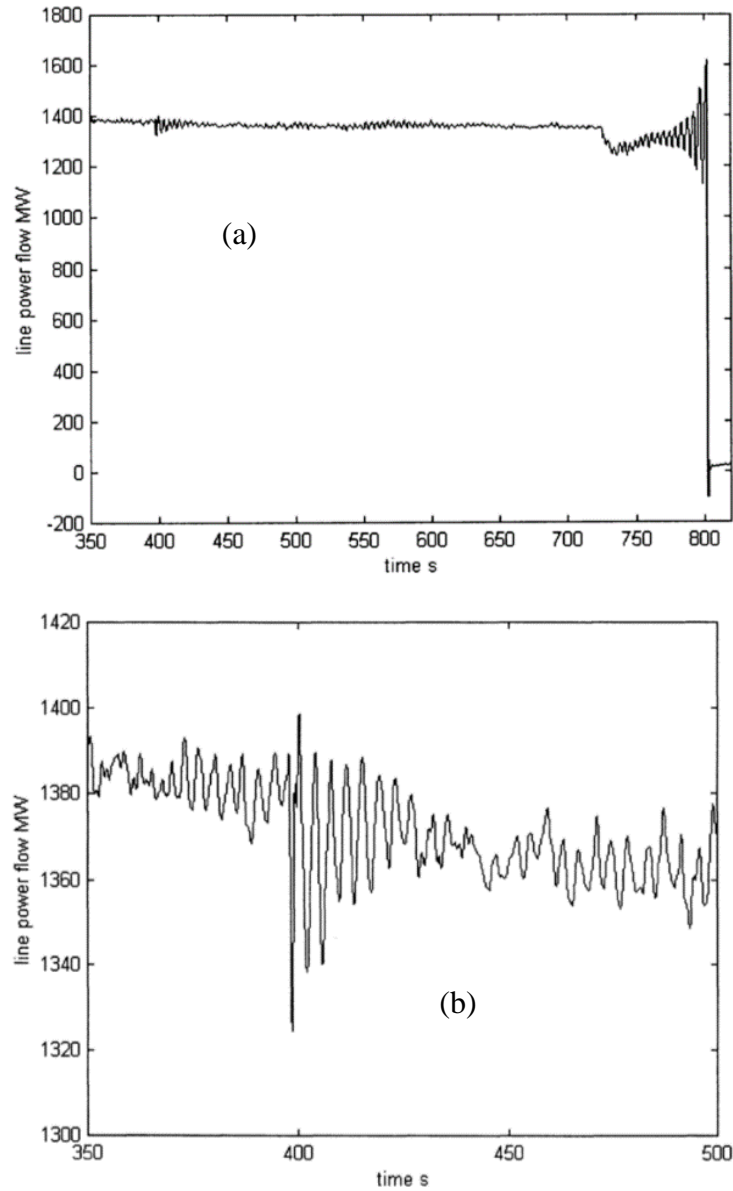
Figure 2.1. Details of 1996 blackout [9] **(a)Tie-line power flow/MW. (b) details of degrading oscillations following the system fault.**

7
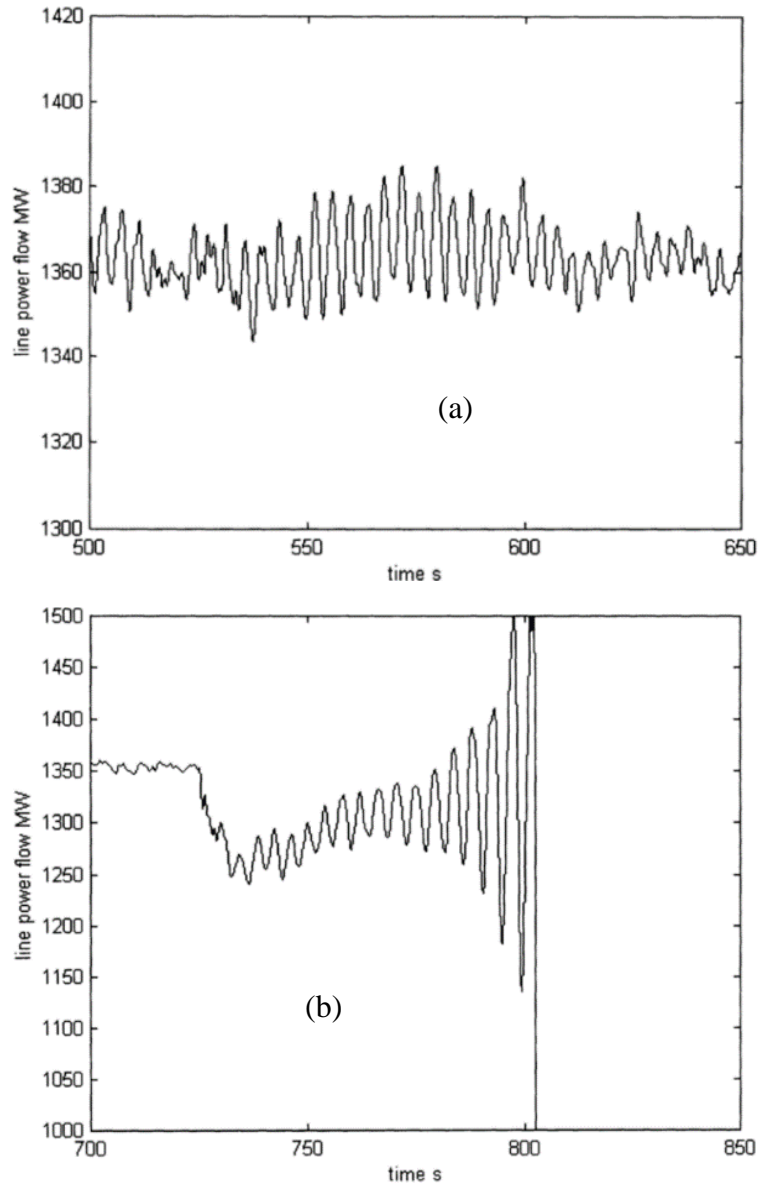
Figure 2.2. Details of 1996 blackout [9] **(a) breakers operations causing small disturbances following fault incidence. (b) Details of growing oscillations causing final system collapse**

However, previous controllers usually use local signals as inputs. This might limit the capability in damping the inter-area oscillations [14]. The solution is to use a combination of local and wide area signals, as demonstrated by some researcher [15]. This could improve the ability of the controller to give the desired control action.

Recently, the appearance of wide area measurements (WAMs) technology, remote signals can be measured and transmitted anywhere in the system with maximum accuracy, so, designing a controller based on synchronized measurements will not be a problem anymore.

2.2   Wide-Area Measurement System

The so-called phasor measurement units (PMUs) are used to measure the voltage, current and frequency. These Phasors are time synchronized by GPS that why they are called synchro-phasors. Some additional information could be delivered such as active power, reactive power, and frequency variation as well as digital information such as devices status. The measured phasors must be communicated to a centralized center, which collects these measurements (information) and make the required processes.

Conventional PSS is effective on damping local oscillation modes, it uses an input signal came from the same generator in which it has been located. Therefore, it is locally measured. Those local signals usually suffer from lack of observability in the interarea oscillation mode. However, in the case of wide area PSS the input signal is a combination of global signals measured by PMUs and synchronized by GPS, then transmitted through telecommunication links to the controller which provides the required control signal. Figure 2.3 depicts the wide area monitoring scheme.

The controller design is either based on the global signals only, this approach is not the commonly used, because it needs many wide area signals, which will increase the communication cost. The other approach is formulated by adding global controller

coordinated with the local one, and this one is usually used in the literature, it will used as reference approach in our research.
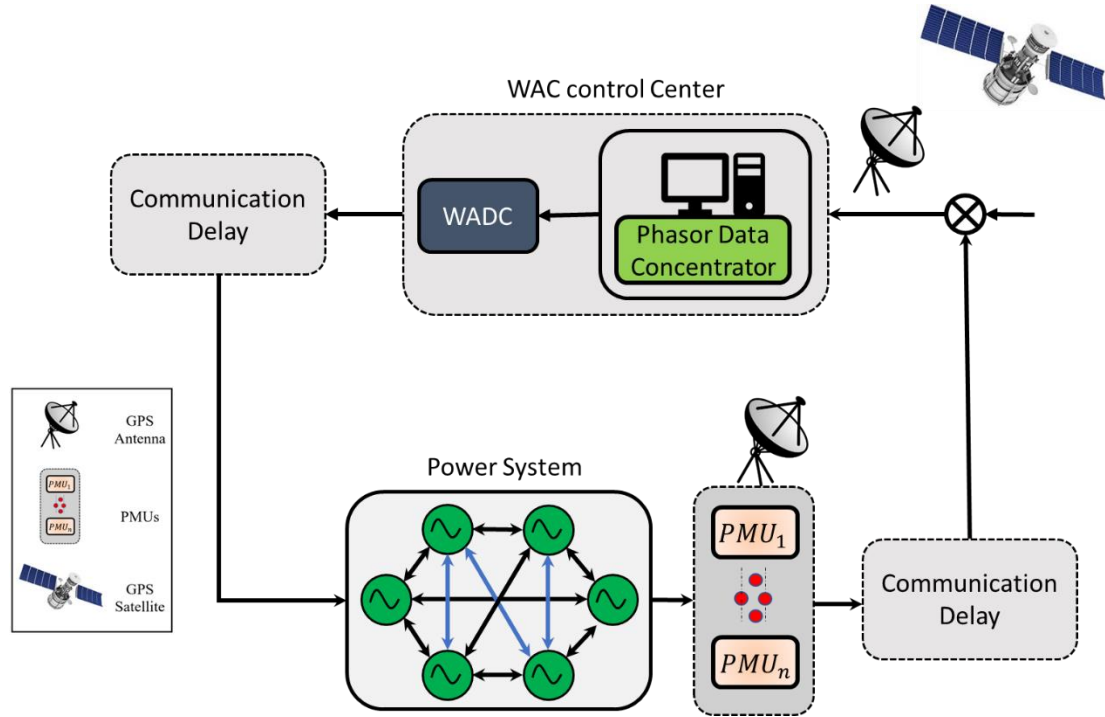
Figure 2.3 Wide-area System scheme

2.3   Identification of Low Frequency Oscillations (LFO)

Many techniques have been proposed to analyze LFOs and to find the dominant modes, either to be eigen-value based techniques (modal analysis) or data measurements-based techniques.

2.3.1 Eigenvalue Based Techniques

Modal analysis could be considered the most suitable way to perform LFO identification [16]. In the case of small disturbances (e.g., load changes) the transient response of non-

linear systems is almost similar to the linear systems [17] [18]–[23]. Even though the fault response is not linear, it settles around post-fault steady-state point. This indicates that the non-linear systems could be linearized around the equilibrium operating point to deal with it like any normal linear system, this provides a useful tool to analyze electro-mechanical oscillations [24]–[27].

In addition to identifying the mode of oscillations, modal analysis also used to trace the source of this oscillations, furthermore, to identify the parameters used in the control design [28].

2.3.2   Data Measurements-Based Techniques

Extracting model information using signal processing techniques is considered to be more advanced than using modal analysis. Here, we might not even look inside the model, however, by some measurements we could identify the unknown black box model, unlike the previous technique which is model-based method. These techniques can be classified according to the number of disposed signals into two groups. The first one is to identify the oscillatory parameters of a single signal, this includes wavelet transform [29], discrete Fourier transform, Hibert-Huang transform [30]. The second group in to identify the dynamic oscillation information, such as Prony algorithm [31], improved Prony method [32].

Fourier Transform (FT) can determine the oscillation frequency based on its spectrum, however, it is not applicable for analyzing the characteristic of the damping. Wavelet algorithm is based on Fourier algorithm but with variable size windowing technique in order to overcome the drawbacks of fixed size widowing in FT [33].

11

Hilbert-Huang Transform (HHT) is based on Empirical Mode Decomposition (EMD) which is used to analyze multi-components signals [34], it has some advantages over Fourier algorithm which is restricted on linear systems and periodic or stationary data, these crucial restrictions could be avoided by HHT. Therefore, it's an excellent technique to extract the properties of non-linear and non-stationary signals. Nevertheless, after a deep experimental work, this algorism has exhibited some deficiencies, so new technique has been proposed to improve the result as shown in ref [35].

Prony algorithm is a linear combination of complex exponential functions to identify the mathematical model (usually known as Prony model) of an equal interval sampling data, it's able to obtain damping, amplitude, phase and frequency from measured signals, unlike Fourier algorithm, it has high spectral resolution even for small data samples, however, its sensitive to noise, so an improved one need to be used as shown in ref [32].

2.4 Power System Stabilizer

Low frequency oscillation damping control is considered one the most sensitive topics in power system stability improvement. Based on years of theoretical and practical research, we can conclude that the damping control could be achieved by a supplemental control equipment such as power system stabilizers and flexible AC transmission system (FACTS).

The first scheme of power system stabilizer was proposed in 1960 for damping synchronous generator rotor speed oscillations by providing a supplementary feedback signal to the generator exciter [36]–[40]. Power system steady-state stability and

transmission capacity has been highly ameliorate with the advent of fast excitation systems, however, it deteriorates the damping torque [41]–[43]. Therefore, to overcome this problem, a use of the power system stabilizer is introduced. By the suitable selection of the input signal, PSS could generate an electrical damping torque to retrieve the diminished damping torque on the generator rotor [44]. Rotor speed deviation Δw could be an appropriate input signal , besides some other candidate signals such as line power flow and the rotor angle deviation, however Δw is the most widely used signal [45].

2.5   Robust Control theory for Wide-Area Control

Ref [46] has developed linear matrix inequality (**LMI**) approach for designing wide area controller tested on New England 39-bus/ten-machine system. The selection of the appropriate   input   signals   is   based   on   geometric   measures   of   joint controllability/observability. The controller has been synthesized as mixed H_2/H_∞ output feedback control problem with regional pole placement constrains.

Ref [47] suggested a use of a supervisory level robust controller using wide area measurements for interarea oscillations damping. The controller was designed based on LMI approach. Multi-agent system theory was used to coordinate supervisory level power system stabilizer (SPSS) and local PSS.

In ref [48] Deng and Zhang proposed a design of a robust damping controller for a thyristor-controlled series compensator (TCSC) under different operating conditions. The control problem was formulated as a multi-objective optimization problem described by a set of bilinear matrix inequalities (BMI), taking into consideration both regional pole placement

13

and H_2 performance for a guaranteed robustness and control effort minimization. real time digital simulation (RTDS) has been used to evaluate the proposed controller performance.

However, the previous references did not consider the communication delay problem which has a significant impact in deteriorating the controller performance [49]–[62]. Ref [63] discussed this issue. Anew robust centralized controller was proposed, the design is LMI-based. The control system comprised of two layers. The first one consists of a decentralized controller which is the PSS that was installed independently in each machine, this layer guarantees the power system stability with a minimum rate of damping. The second layer represent a robust centralized controller which receive the delayed machine signals and send it back as a control signal. Even if the second layer fails to perform this mission and somehow remote signals get lost, the PSS could guarantee an acceptable damping performance. The communication delay is represented by second order Padé approximation.

Ref [64] used a novel method to analyze the delay-dependent stability of a wide-area controlled power system. After reducing the model using Schur method for balanced-truncation model reduction [65]. The maximum delay that allows the system to be stable is calculated based on linear matrix inequality (LMI) theory, considering both constant and time-varying delays resulted from wide area signals transmission. The relationship between WADC parameters and the delay-margin was investigated. Comparison was conducted between the traditional lead-lag WADC and the proposed WADC. Simulation studies were carried out on Kundur four-machine/two-area system. In the case of using the conventional controller, results showed that when the WADC gain increases a little bit, this could lead to a decrement of the delay margin effect. However, a considerable rise of the

delay margin can be achieved by a tiny gain decrement, resulting in a small deterioration in the damping performance.

In [46], a robust approach to coordinate high-voltage direct-current (HVDC) and FACTS based on wide area measurements is reported for damping multiple interarea modes in large-scale power networks. After the selection of the most effective candidate signals which are given to HVDC and FACTS controllers, a sequential robust design approach is used to coordinate HVDC and FACTS devices. Robust control theory is used to formulate the proposed approach as a standard problem of a multi-objective mixed H_2/H_∞ output feedback control constrained with regional pole placement. The problem has been solved using LMI theory. The study has been conducted on 16-machine 5-area system modified with one HVDC transmission, one SVC, and one TCSC, to validate the feasibility of the proposed approach under multiple interarea modes.

Kishor [66] has presented a fixed order H_∞ controller for damping interarea oscillation in large systems. The generators coherency is determined using mutual information (MI) theory, then every area network is reduced to a lower order using square-root variant of balanced truncation technique. The dominant oscillation modes are identified in the reduced form. The local decentralized controller along with the centralized one are designed based on minimizing the H_∞ norm of the closed loop transfer function as far as possible. The effectiveness of the controller has been tested under different load conditions. A new scheme of interarea oscillation damping based on linear quadratic Gaussian (LQG) control is presented in [67]. The model used to conduct the study is 135th order has been reduced to 9th order. The system is equipped with a thyristor-controlled series capacitor (TCSC) which receives the wide area control signal from the LQG centralized controller

for improving the damping of the risky interarea modes. The paper also proposes the use of loop transfer recovery to enhance the controller robustness over the desired frequency range when the system is subjected to any kind of unknown disturbances. Time domain simulation has been used to assess the controller performance.

By the same way, Ref [68] presents a design of LQG-WADC in both, continuous and discrete modes. The paper considered the communication imperfections such as noises exhibited either in the process or in the measurements, information lost, and communication latency due to wide area signal transmission. Modal analysis has been used to select the controller location and the appropriate control signal. The communication delay has been modeled using Padé approximation and a Gaussian random noise has been inserted to represent the communication deficiency. The controller robustness has been evaluated in frequency and time domain using MATLAB/SIMULINK.

2.6   Delay Consideration in Wide-Area Communication System

Due to the High complexity of power system infrastructure, conventional communication methods have become less guarantee of control design requirements of modern power grids. Recently, the advent of phasor measurement units (PMUs) emerged with satellite time service systems has laid to the foundation for wide-area measurement systems (WAMSs) [69]. Unlike conventional communication systems, WAM communication is based on powerful wide area network (WAN)/local area network (LAN) technology [70]–[72]. WAMs technology enabled by broad deployment of phasor measurement units (PMUs) has opened the floor to develop wide-area damping controllers (WADCs) to gain an effective damping for low frequency oscillations (LFOs), compared with the locally

measured signals which lack observing some critical interarea modes [73]–[75]. With WAMs data, the observable space becomes wider. In addition, PMUs signals are time-synchronized and correlated at any point of a geographically spread electric network by global positioning system (GPS) which provides an accurate timing pulses for PMU signals [76], [77]. Since wide-area control system includes a communication channels in the control loop, such system could be considered as a typical network control system (NCS).

With the outstanding growth of communication technologies, communication networks have become more appealing for signal transmission in control systems compared to traditional point-to-point connections which are considered more complex, expensive, and less reliable. Networked control systems (NCSs) have presented a new type of spatially distributed control system, in which sensors, actuators and controllers are spatially separated and linked physically through a limited-bandwidth digital communication network. Remote signals transmission, however, would constitute a major challenge in term of time delay (or latency) induced in the control loop of the WADC.

Communication latency usually referred to the time demanded to render PMU data towards control center (uplink latency) through phasor data concentrator (PDC) in addition to the time required to transfer the control commands to control devices (downlink latency), since the designed wide-area controller (WAC) in a centralized level. Wide-area signal transmission latency in wide area control (WAC) differ from few to hundreds of milliseconds due to some factors such as: transmission media, router selection, transmission protocols [56], and communication loads [78], [79]. Generally, latency can be fixed or variable for each data transmission. Communication latency would cause linear phase shifts that limit the control bandwidth, degrade closed-loop stability, and deteriorate

the damping performance of WADC and, thus, lead to control failure. Time-delays, therefore, should be considered during WADC design.

In the literature, various methodologies have been used to handle the time delay impact. In [80], a hardware implementation of wide-area damping controller is carried out for stability enhancement of power systems based on bilinear transformation. Dynamic output-feedback wide area damping control of HVDC transmission considering signal time-varying delay is addressed in [53]. Ref [47] presented power system stability agents using robust wide area control to ensure a guaranteed system performance with time delay existence. Delay-dependent stability analysis of the power system with a wide-area damping controller embedded is addressed in [81] wherein the design is formulated as an optimization algorithm with a set of linear matrix inequality constrains. Ref [82] discussed a new method of continuous time delay compensation based on rotating coordinates adjustment using adaptive phasor power oscillation damping (POD). In [83] the communication delay impact of HADC-based WADC has been reported as a practical experience in China southern power grid. In [50] Padé approximation is used to compensate for time delay in a wide-area power system as a second level control design. Ref [84] proposed the design of excessive regeneration detector (ERD) for stability augmentation by smoothly shifting the gain of the system when high delay in wide-area damping system arise.

These techniques require a full knowledge of the plant and time-delay. However, the impracticality of having an accurate plant model makes the whole design prone to modeling errors. Moreover, most of these methods are based on robust control theories which are complex as they require a proper selection of weighing matrices.

Scattering transformation is one of the delay-independent procedures, originally derived from classical network theory [85], and applied for the first time in control context in reference [86]. Matiakis et al. [87] presented a new strategy to overcome the restrictive passivity assumption of the plant and controller and extended the notion of scattering transformation to include non-passive LTI systems (A system is called passive system if it's all interconnected subsystems are passive and, thus, stable) to be stabilized independently-of-time-latency, in order to guarantee gracefully degradation of control performance with time-latency increasing. Since Communication delay can easily ruin system passivity, this method is able to passivate the communication subsystem with large latencies via scattering transformation and ensures low sensitivity to time-delays, it can guarantee an acceptable performance for a wide range of delays.

2.7   Summary

The literature review has presented various methods of identification techniques either based on system model, or system measurements. Further, a brief survey regarding the conventional controllers that are based on linear control theory has been highlighted. The robust control theory application in power system control, particularly, in wide-area control has been presented as well. Eventually, the impact of the communication delay is addressed and some of the delay-compensation methods have been discussed.

The gaps that have been filled in this work are summarized as follows:

- Most of the relevant work has considered the design of WADC based on the accurate model of the system. The difficulty of having a precise power system modeling without any parameters uncertainties would pose some limitations.

19

- Commonly obstacle encountered with the relevant delay-compensation methods approaches is that WADC design is based on the linearizing the plant around a certain set of nominal operating conditions. In fact, power systems are inherently nonlinear. In this work, however, the controller design is based on a complete nonlinear model to overcome this drawback.

CHAPTER 3

MODELING AND RESEARCH METHODOLOGY

3.1   Introduction

Electromechanical oscillation damping falls within small signal stability problems. By proper design of the supplemental controller, the closed-loop system performance can be enhanced. For further explanation of the nature of this harmful oscillation, it's necessary to look over the power system model**.** This chapter explains the modeling of the main components of power systems, which include synchronous machines, excitation system, power system stabilizers…. etc. These components are coupled implicitly with the power grid. Having a linear model of power system will transcend the problem of high nonlinearity of the power systems, which makes it unwieldy to design a controller over the whole system operating points. The practical controllers are designed to take actions under a certain range of system perturbations around a certain equilibrium point, so, linearization is performed to get a state-space representation of the system, thus, linear control theories could be applied to extract the eigenvalues which identify the oscillatory modes. Furthermore, observability, controllability, residue measures, and participation factors are explained. This chapter also address the wide area damping controller design and how global signals from PMUs can be used instead of local signals. WADC placement is discussed as well.

3.2   Dynamical System Representation

The system behavior either static or dynamic is prescribed by a set of algebraic and n-first order nonlinear ordinary differential equations.

$$\dot{x} = f(x, y, u) \tag{3.1}$$

$$0 = g(x, u) \tag{3.2}$$

Where x and y represent the vectors of state and network variables respectively; f represents the set of differential equations which describe the dynamical part of the system; g is the vector of algebraic equations describes the static part; u is control signals vector. In a very general sense, these equations describe time evolution of state vector, so, in terms of modeling the power grid this could voltages, currents frequency and phase of a particular synchronous generator. The dynamical systems have been used in the past to effectively model components of power systems, so this tool set has a lot of power, it can be -in some context- has formalism, it allows for variable granularity depending on the model order, and the level of system's nonlinearity.

3.2.1   Generator

Synchronous generators are the main source of energy of power grids, the challenge is to safeguard the synchronism between the interconnected generators, this represent the main power system stability problem. Therefore, complex mathematical representation of the system is required to get an accurate simulation of system's dynamic behavior, the order used in machine representation reflects the dynamic behavior. The machine can be modeled either in a simple classical model or a detailed complex model of orders up to eight. Here,

a 6th order machine is used; thus, the system could be represented more accurately compared with classical models. Following differential equations represent the model of ith machine [88]:

$$\dot{\delta}_i = (\omega_i - \omega_s) \tag{3.3}$$

$$\dot{\omega}_i = \frac{\omega_s}{2H_i}\left(T_{Mi} - D_i(\omega_i - \omega_s) - \frac{X''_{di}-X_L}{X'_{di}-X_L}E'_{qi}I_{qi} - \frac{X''_{qi}-X_L}{X'_{qi}-X_L}E'_{di}I_{di} - \right.$$

$$\left. \frac{X'_{di}-X''_{di}}{X'_{di}-X_L}\varphi_{1di}I_{qi} + \frac{X'_{qi}-X''_{qi}}{X'_{qi}-X_L}\varphi_{2qi}I_{qi} + (X''_{qi} - X''_{di})I_{di}I_{qi}\right) \tag{3.4}$$

$$\dot{E}'_{qi} = \frac{1}{T'_{doi}}\left[E_{fdi} - E'_{qi} - (X_{di} - X'_{di})\left(-I_{di} - \frac{X'_{di} - X''_{di}}{(X'_{di} - X_L)^2}(\varphi_{1di}\right.\right.$$

$$\left.\left. - (X_{di} - X_L)I_{di} - E'_{qi})\right)\right] \tag{3.5}$$

$$\dot{E}'_{di} = \frac{1}{T'_{qoi}}\left[-E'_{di} - (X_{qi} - X'_{qi})\left(I_{qi} - \frac{X'_{qi} - X''_{qi}}{(X'_{qi} - X_L)^2}(-\varphi_{2qi} - (X_{qi} - X_L)I_{qi}\right.\right.$$

$$\left.\left. - E'_{di})\right)\right] \tag{3.6}$$

$$\dot{\varphi}_{1di} = \frac{1}{T''_{doi}}\left[-\varphi_{1di} + E_{qi} + (X'_{di} - X_L)I_{di}\right] \tag{3.7}$$

$$\dot{\varphi}_{2qi} = \frac{1}{T''_{qoi}}\left[-\varphi_{2qi} + E_{di} + (X'_{qi} - X_L)I_{qi}\right] \tag{3.8}$$

Where;

i	Generator Index
m	Total Generators Number
δ_i	Rotor Angle
φ_{1di}, φ_{2qi}	Sub-transient Induced electromagnetic force (EMF)

23

I_{di}, I_{qi}	Stator current (d-q axis)
$X_{qi}, X'_{qi}, X''_{qi}$	Synchronous, transient, sub-transient reactance (q-axis)
$X_{di}, X'_{di}, X''_{di}$	Synchronous, transient, sub-transient reactance (d-axis)
T'_{doi}, T''_{doi}	Transient and sub-transient time constant (d-axis)
T'_{qoi}, T''_{qoi}	Transient and sub-transient time constant (q-axis)
X_L	Armature Leakage reactance
E_{fdi}	Field Voltage
T_{Mi}	Mechanical Torque Input
H_i	Machine Inertia
ω_s	Nominal Speed

The following algebraic equations represent the static part of the system:

$$V_i \sin(\delta_i - \theta_i) - \frac{X'_{qi} - X_L}{X'_{qi} - X_L} E'_{di} + \frac{X'_{qi} - X''_{qi}}{X'_{qi} - X_L} \varphi_{2qi} + R_{si} I_{di}$$
$$- X''_{qi} I_{qi} = 0 \tag{3.9}$$

$$V_i \sin(\delta_i - \theta_i) - \frac{X'_{di} - X_L}{X'_{di} - X_L} E'_{qi} + \frac{X'_{di} - X''_{di}}{X'_{di} - X_L} \varphi_{1di} + R_{si} I_{qi}$$
$$- X''_{di} I_{di} = 0 \tag{3.10}$$

Where;

R_{si}	Armature Winding Resistance
V_i	Terminal Voltage Magnitude
θ_i	Terminal Voltage Phase Angle

3.2.2 Excitation System

Whenever synchronous machine dynamics has been considered, Excitation system dynamics should come along with it. The Impact of the excitation system on power system small signal stability is obvious when different models are used. However, to avoid sophistications, static AC excitation system has been used in this research, a simple diagram describing this system is depicted in Figure 3.1. The following first order ordinary deferential equation represent the dynamics of the excitation system:

$$\dot{E}_{fd\imath} = [K_{Ai}(V_{refi} - V_i - V_{PSS}) - E_{fdi}]/T_{Ai} \qquad (3.11)$$
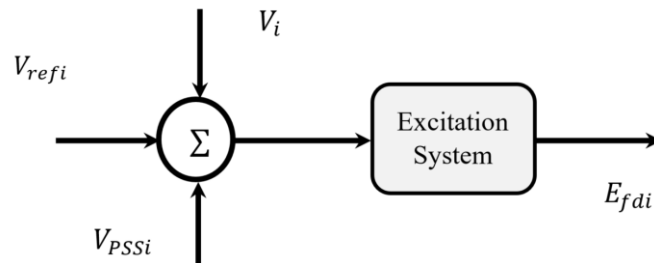
Figure 3.1. Static AC Excitation System

Where;

V_{refi}	Voltage Reference
T_{Ai}	Exciter Time Constant
K_{Ai}	Voltage Regulator Gain
V_{pssi}	PSS Control Signal

3.2.3 System Linearization

As mentioned previously, power systems experience some large variations in operating point conditions, therefore, it's tedious to design a controller that could handle all these conditions. Thus, to test the small signal stability, its required to linearize the system around a certain operating point and form the state-space model of my system, so that it could be able to use linear control techniques to design the controller. Generally, any nonlinear system is described by a set of deferential equations, either ordinary or partial. In this study, a set of nonlinear ordinary differential equations describes the power system can be expressed by the following form:

$$\dot{x}_i = f_i(x_1, x_2, \dots, x_n; \ u_1, u_2, \dots, u_r; \ t) \tag{3.12}$$

Where $i = 1, 2, \dots, n$ and r is the number of the inputs.

If the derivatives are not function of time, the previous equation can be reduced to:

$$\dot{x} = f(x, y) \tag{3.13}$$

Where;

$$x = [x_1, x_2, \dots, x_n]^T$$

$$u = [u_1, u_2, \dots, u_r]^T \tag{3.14}$$

$$f = [f_1, f_2, \dots, f_n]^T$$

The vectors **u, x** *and* **ẋ** represent the inputs, state variables vector and derivatives of state variables. The outputs can be described as:

$$\dot{y} = g(x, u) \tag{3.15}$$

To describe (3.15) in the state-space representation, linearization is performed around a certain operating point **x₀** and **u₀**, this yields the following equations:

$$\Delta \dot{x} = A\, \Delta x + B\, \Delta u$$

$$\tag{3.16}$$

$$\Delta y = C\, \Delta x + D\, \Delta u$$

Where;

$$\Delta x = \begin{pmatrix} \Delta \delta_i & \Delta \omega & \Delta E'_{qi} & \Delta E'_{di} & \Delta \varphi_{1di} & \Delta \varphi_{2qi} & \Delta E_{fdi} & \Delta V_{Pss1} & \Delta V_{Pss2} & \Delta V_{Pss3} \end{pmatrix}^T$$

$$\Delta u = \begin{pmatrix} \Delta T_{Mi} & \Delta V_{refi} & \Delta V_{Pss3} \end{pmatrix}^T$$

3.2.4 Participation Factor

Participation factor defines the amount of contribution gained by a generator to a particular mode. In other word, it shows how this generator state influences this particular mode [89]. This factor specifies the optimal controller location in the multi machine system. For fulfilling the purpose of an effective oscillation damping, the highest state participation factor can be used as an input to the controller. This will reduce the control effort exerted by the controller as well as giving the required damping performance. Nevertheless, this candidate signal has a lack of observation the interarea mode, in addition to the that, some of the generator states such as rotor angle are not directly measured, even though, they might have higher observability index compared with generator speed which is commonly

used. However, participations factors still important for identifying the mode shapes of the interarea modes, i.e. how different generator groups have involved in this mode.

When state matrix has been implemented, the critical oscillatory modes could be identified by calculating the eigen-values, left and right eigenvectors in addition to the participation factors. The largest participation factor indicates the largest contribution in LFO modes. Participation factors are obtained as follows:

$$P = [P_1 \quad P_2 \quad \cdots \quad P_n] \tag{3.17}$$

$$P_i = \begin{bmatrix} p_{1i} \\ p_{2i} \\ \vdots \\ p_{ni} \end{bmatrix} = \begin{bmatrix} \Phi_{1i} \Psi_{i1} \\ \Phi_{2i} \Psi_{i2} \\ \vdots \\ \Phi_{ni} \Psi_{in} \end{bmatrix} \tag{3.18}$$

$$p_{ki} = \Phi_{ki} \Psi_{ik} \tag{3.19}$$

Where;

P Participation matrix;

Φ_{ki} , Ψ_{ik} Right and Left eigenvectors associated with K^{th} state variable and i^{th} oscillatory mode respectively.

3.2.5 Controllability, Observability, and Residue Measures

Since participation factors deal with system states only without system inputs and outputs, its ineffectual to designate the optimal feedback signals based on participation factors only without considering input/output information [90]. This could be obviously seen in equation (3.19 which is used to calculate the participation factors. This equation, however, don't consider input matrix (B) or output matrix (C), it only considers state matrix (A) via its left and right eigenvectors. Therefore, new equations that incorporates both system

inputs and system outputs need to be introduced. These equations are represented by so-called modal (geometric) controllability/observability measures.

Appling control theories with an inappropriate system input/output, could lead to some numerical difficulties, therefore, modal controllability and observability are used to select the proper input/output signals.

Generally, a strictly proper open-loop system $(D = 0)$ is described by the following transfer function:

$$G(s) = C(sI - A)^{-1}B \tag{3.20}$$

The system modal controllability to a certain mode λ_i is calculated through the eigenvectors of the system matrix A, and the input matrix B. Similarly, the system modal observability to the mode λ_i is calculated through the eigenvectors of the system matrix A, and the output matrix C.

In the case of multi-input/multi-output (MIMO) systems, the modal controllability and observability will differ. So, one must calculate the system modal residue to evaluate numerically those modal indexes. The transfer function G(s) in (3.20 can be described in the following partial fraction form:

$$G(s) = \sum_{i=1}^{n} \frac{C v_i w_i B}{s - \lambda_i} = \sum_{i=1}^{n} \frac{R_i}{s - \lambda_i} \tag{3.21}$$

Where;

v_i, w_i Right and Left eigen vectors, respectively

λ_i The ith eigenvalue of matrix A

Due to the proportionality between the magnitude of the system transfer function $|G(s)|$, and the system residues, we can use the largest modal residue R_i for a particular mode to select the system input/output to achieve the less control effort needed to control this mode. The following equations describes the controllability and observability measures, respectively

$$CONT_i = \|\Psi_i^T B_j\|$$
$$OBS_i = \|C_j \Phi_i\|$$

(3.22)

Where;

OBS_i and $CONT_i$ is the observability and controllability measures of the ith mode respectively.

The interpretation of (3.22) is that if $OBS_i \neq 0$ that means the ith mode is visible or observable in the ith output. if $CONT_i \neq 0$ that means the ith mode is controllable by the jth input.

Modal residues are defined as

$$R_i = OBS_i * CONT_i$$

(3.23)

Where;

R_i Residue measure for i^{th} mode.

If $R_i = 0$ that means the mode is either not controllable or not observable.

3.3   Summary

This chapter addresses a comprehensive modeling of the power systems considered at the electromechanical transient level. The system dynamic behavior was represented by the differential equations of synchronous generators' dynamics (including excitation system and PSS), while the algebraic equations of stator output voltages and system network power flows described the static behavior. Linearization is performed to get a state-space realization of the system; thus, linear control theories could be applied to identify the oscillatory modes. Observability, controllability, residues measures, and participation factors are further explained.

CHAPTER 4

LQG-BASED WIDE AREA CONTROL

4.1   Introduction

After presenting the mathematical formulation of the power system and oscillatory modes identification procedure in chapter 3. This chapter highlights the application of linear quadratic Gaussian (LQG) theory in wide-area controller design and discuss its effectiveness. The design will guarantee robust system stability with an acceptable performance compared to the conventional lead-lag structure for a wide range of operating conditions.

4.2   LQG Control

Consider a linear time-invariant (LTI) system that is controllable and observable, one can develop an optimal full state feedback controller using linear quadratic regulator (LQR), in addition to optimal common filter or linear quadratic estimator (LQE) using system matrixes A and C [91]. What's amazing, is that when these two filters are combined, they remain optimal. Therefore, LQR is selected to place the eigenvalues of the close-loop system, and LQE to place the eigenvalues of the estimator dynamics. When this combination happens, the same dynamics can be retained. LQG is a pretty neat control, however, it has some limitations due of this combination. Sometimes the controller could suffer from some robustness issues when the system is arbitrary fragile, in other word, if

the system has a little bit of uncertainty or some nonlinear dynamics that haven't been modeled, the controller might fail stabilizing the system. The general representation of LQG control scheme is depicted in Figure 4.1.
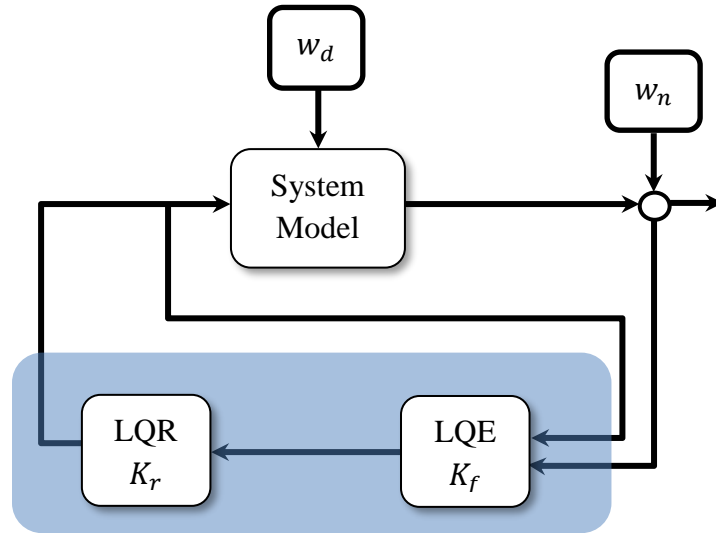
Figure 4.1   LQG control scheme

Where;

K_r LQR gain matrix

K_f LQE gain matrix (Kalman filter)

w_n Sensor noise input

w_d Prosses noise input (System disturbance)

Generally, any linear system with random white noise could be described by a state-space model as:

$$\dot{x} = Ax + Bu + \Gamma w_d$$

(4.1)

$$y = Cx + w_n$$

The estimation error (ϵ) is expressed as:

33

$$\epsilon = x - \hat{x} \qquad (4.2)$$

Step 1. LQR design:

The optimal state-feedback control law is expressed by:

$$u = -K_r x \qquad (4.3)$$

Where;

$$K_r = R^{-1} B P_c \qquad (4.4)$$

And P_c is a unique symmetric positive semi-definite matrix solution of algebraic Riccati equation (ARE);

$$A^T P_c + P_c A + Q - P_c R^{-1} B^T P_c = 0 \qquad (4.5)$$

There is one important condition, is that, (A, B) should be controllable, (Q, A) should be observables for all system modes, where; R, Q, are positive definite and semi-definite ($R > 0, Q \geq 0$), respectively;

Step 2. Kalman Filter:

In equation (4.2) the estimate of x ($\hat{x}$) is used because there is no access to the full system states, or it's unwieldy to measure all plant states. Therefore, an estimator (Kalman filter) is utilized to provide the desired states. Note that, Kalman filter has a similar synthesis to a common filter, with a state estimation formula described as:

$$\dot{\hat{x}} = A\hat{x}(t) + Bu(t) + K_f[y(t) - C\hat{x}(t)] \qquad (4.6)$$

Where;

$$K_f = P_f C^T \theta^{-1} \tag{4.7}$$

And P_f is a unique symmetric positive semi-definite matrix solution of algebraic Riccati equation (ARE);

$$P_f A^T + A P_f - P_f C^T \theta^{-1} C P_f + \Gamma \varphi \Gamma^T = 0 \tag{4.8}$$

The condition is: (C, A) has no unobservable modes (detectible), $\theta > 0, \varphi \geq 0$, and (A, $\Gamma \varphi \Gamma^T$) is controllable. Eventually, the optimal control law could be written as:

$$u = -K_r \hat{x} \tag{4.9}$$

The selection of the weighing matrixes (Q, R, θ, φ) is based on the trial and error, that means they should be adjusted until it gives a satisfactory controller performance, because there is no direct method for selection. However, one can provide initial guess based on the states participation factor on the system critical modes, and the highest participated state will be given the highest weigh, and this might require some experience. More details could be found in [92], where a number of thoughts has been discussed regarding state weighting matrixes selection.

$$\dot{x} = Ax - BK_r \hat{x} + w_d \tag{4.10}$$

$$\dot{\epsilon} = (A - K_f C)\epsilon + w_d - K w_n \tag{4.11}$$

By combining (4.10(4.10and (4.11, we will get:

$$\begin{bmatrix} \dot{x} \\ \dot{\epsilon} \end{bmatrix} = \begin{bmatrix} (A - BK_r) & BK_r \\ 0 & (A - K_f C) \end{bmatrix} \begin{bmatrix} x \\ \epsilon \end{bmatrix} + \begin{bmatrix} I & 0 \\ I & -K_f \end{bmatrix} \begin{bmatrix} w_d \\ w_n \end{bmatrix} \tag{4.12}$$

Where;

x	Actual state
$\hat{x}$	Estimated state
ϵ	Estimation error

What is remarkable here is that when the full state estimated from Kalman filter is combined with an LQR optimal feedback control, one can derive the dynamics for x and ϵ, and what can be observed is the eigenvalues of $(A - BK_r)$ and the eigenvalues of $(A - K_f C)$. Therefore, with this combination, the eigenvalues of the full state x are still stabilized with LQR, and the estimator dynamics retain the exact same Kalman filter eigenvalues or LQE eigenvalues. In control theory this is called the separation principle, which essentially means, the design of LQR and LQE controllers and estimators -respectively- could be done in isolation. When they are combined, the combined system retains the desired properties of each filter. Figure 4.2 depicts the LQG based wide area controller. The separation principle is summarized as follows:

- Determining the optimal state-feedback control law $u(t)$ by LQR control theory.
- Estimation the desired states via Kalman filtering.

There are no restricted guidelines of which subproblem to solve first. However, previously the solution of LQR problem has been considered first.

Basically, for a strictly proper LTI system that is completely controllable and observable, LQG control can be applied, which aim to find the optimal control $u(t)$ that minimizes the quadratic performance index J expressed by:

$$J = \lim_{T=\infty} \frac{1}{T} E\{\int_0^T [z^T(t)Qz(t) + u^T(t)Ru(t)]dt\} \tag{4.13}$$

Where; z(t) is a linear combination of system states x(t) (practically, it is better penalizing certain outputs rather than full system states to have feasible solutions). Q, R, are constant weighing matrixes, they are appropriately selected in a way that Q is positive semi-definite ($Q = Q^T \geq 0$), and R is positive definite ($R = R^T > 0$). There is no fixed form for Q and R, however, usually they are in a diagonal form.

4.3   General Design Procedures

The complete design procedures of robust LQG-based wide-area damping controller are presented in the following steps:

Step 1. Building a detailed full-order model of the power system case, including generators, exciters, turbine/governors, and power system stabilizers in MATLAB/SIMULINK.

Step 2. System Linearization: linearize the full-order nonlinear system around the chosen operating point, to extract the LTI state-space representation. Then calculate the participation factors, frequency, and damping ratios of the system oscillatory modes.

Step 3. Critical Modes Identification: Identify the open-loop power system critical modes (Local or interarea) through either eigenvalue analysis or Fast Fourier Transform (FFT).

Step 4. Candidate signals/optimal location selection: according to the highest modal controllability/observability indexes, the controller location as well as the feed-back signal will be chosen.

Step 5. Convectional Method: a WAC based on a conventional lead-lag controller designed by residue method is presented.

Step 6. Model Reduction: the designed controller will have the order of the power system model. From practical consideration, this order is very high, and its impractical to implement a controller of serval hundreds of states in a hardware framework. Therefore, one need to use some model reduction techniques to gain a lower order model. The model reduction technique that has been used here is Schur method for balanced-truncation model reduction [65].

Step 7. Formulate the LQG controller synthesis as explained in this chapter. The proposed controller is expected to match the desired requirements of damping interarea oscillations.

Step 8. Performance Test: The validation of the proposed controller is carried out through eigenvalue analysis and MATLAB nonlinear simulation.

Step 10. RTDS: Another validation of the proposed controller is carried out through real time digital simulation in order to demonstrate the feasibility to practical implementations.
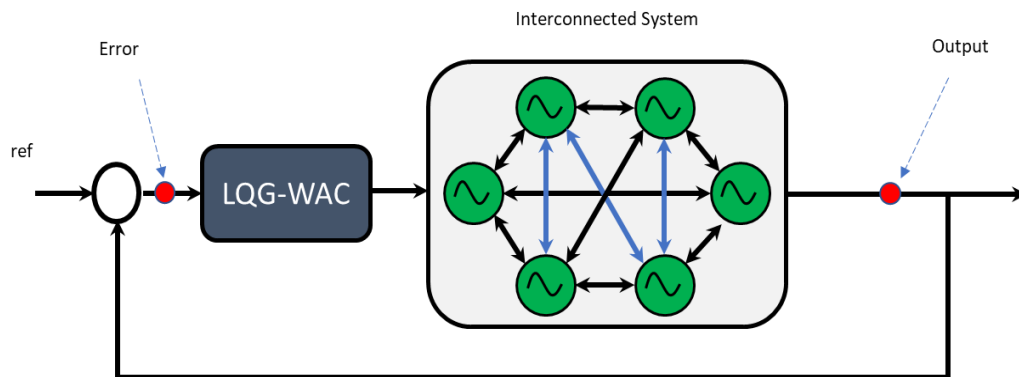
Figure 4.2. LQG based wide area controller

4.4   Summary

In this chapter, a procedure to design a robust LQG controller for wide-area damping control is presented to deal with the problem of system oscillations. The conventional lead–lag WADC is unable to deal with these problems and hence the overall system may become unstable. However, the designed LQG controller is robust enough to nullify the effects of interarea oscillations and also improves system damping performance. Moreover, some important control concepts such as Kalman filtering and separation principle have also been discussed.

CHAPTER 5

WIDE-AREA CONTROL USING SCATTERING

TRANSFORMATION

5.1   Introduction

The utilization of communication network to transmit remote signals might introduce time delay into the control loop [93], [94]. In this chapter, a novel design of scattering transformation-based wide-area damping controller is discussed. The proposed controller is capable to ensure power system stability with large constant and variable time delays. The proposed design is comprised of a classical structure in addition to two scattering transformation ports. These ports are inserted between the power system and WADC to regulate the signal exchanging between these two sides (the plant side and the controller side). Since the proposed WADC is in a centralized level, the time delay imperfections should be considered in the design. The proposed controller offers a great compensation of time delay and thus, improving the system damping performance.

5.2   Preliminaries [95]:

Some of the main design concepts are discussed in this section, as follows:

5.2.1 Passive Systems

A system is called passive system if it's all interconnected subsystems are passive and, thus, stable. Here, the goal is to passivate the communication subsystem with large fixed-latency via scattering transformation. Any passive system has the following properties:

- Passive systems do not produce energy on its own (only consume or dissipate energy), i.e. at $time = 0$, the energy generated should be equal to zero.

- No initial stored energy or it should be dissipated.

- Any increase in the input u is offset by an increase in the output y.

- Any two passive subsystems connected in series, parallel or in feedback connection will result in a passive system.

A simple example of passive systems is PID controller. This system is passive as the control signal (output signal) follows the same direction of the error signal (controller input). Delayed-PID, however, is non-passive system, as the direction of the control signal could oppose the error signal direction, which leads to system instability. Communication delay can easily ruin system passivity. LTI system $H(s) = Y(s)/U(s)$ is passive if the following property holds:

$$\int_0^T P_{in}(t) = \int_0^T Y^T(t)U(t)dt > 0, \qquad \forall T > 0 \tag{5.1}$$

Where $P_{in}(t)$ represents the instantaneous system input power. In frequency domain, a system is passive if and only if it is positive-real (PR), this notion is explained in the following section.

5.2.2 Positive Real Functions

The notion of positive-real functions (PR functions) has arose for the first time in electrical network analysis as a kind of complex functions of complex variables. A Proper rational function matrix with a positive real part in the right-half plane is considered to be PR. Symbolically, a transfer function $H(s)$ is PR if the following conditions holds:

1- The poles of all elements of H(s) are in $\text{Re}(s) \leq 0$.

2- The matrix $H(s) + H^*(s)$ positive semi-definite, i.e. , $\forall \mathcal{R}e[H(s)] \geq 0, \ \forall \sigma > 0.$ (the Nyquist plot lies in the right half plane).

3- Any pure imaginary pole $j\omega$ of any elements of H(s) is a simple pole.

4- The residue for this simple pole   is positive semidefinite Hermitian (A positive semidefinite   matrix   is   a Hermitian   matrix all   of   whose eigenvalues are nonnegative), mathematically, the following inequality must hold:

$$\lim_{s \to \infty} (s - j\omega)H(j\omega) \geq 0$$

5.2.3 Strictly Positive Real Functions

A rational transfer function $H(s)$ is said to be strictly positive real (SPR) if:

1- for some $\gamma > 0, Re[H(s - \gamma)] \geq 0 , \forall \mathcal{R}e(s) \geq 0.$

2- H(s) is Hurwitz (every eigenvalue of H(s) has strictly negative real part, i.e., $Re(\lambda) < 0$)

3- $H(j\omega) + H^*(j\omega) > 0, \forall \omega \in \mathbb{R}$

The forgoing definition indicate that SPR functions are strictly stable. The main deference between PR and SPR is that the PR can tolerate poles in the imaginary axis if they are simple.

5.3 Scattering Transformation-Based WADC (ST-WADC) Design

Consider the power system plant $H(s) = Y_p(s)/U_p(s)$. Figure 5.1 shows a scattering transformation-based wide area damping control. Scattering transformation is inserted between WADC, power system plant, and the communication network. $H_1(s)$ represents the right-hand side scattering with plant $H(s)$. $H_2(s)$ represents the left-hand side scattering with the controller. H_1 and H_2 are given as follows:

$$H_1(s) = \frac{V_r(s)}{U_r(s)} = \frac{H(s) - \beta}{H(s) + \beta} \tag{5.2}$$

$$H_2(s) = \frac{U_l(s)}{V_l(s)} = \frac{1 - \beta.H_{WADC}(s)}{1 + \beta.H_{WADC}(s)} \tag{5.3}$$

Where;

$H_{WADC}(s)$ represents WADC transfer function. $V_r(s)$ and $U_r(s)$ are the right-hand scattering values, $V_l(s)$ and $U_l(s)$ are the left-hand scattering values. β is scattering-parameter, $\beta \in \mathbb{R}$

The measured plant output will be either speed signals or power signals. Scattering-values either right (Port-I) or left (Port-II) are communicated via two-port delayed network. This delayed two-port produces energy as shown in reference [86], and thus the passivity condition is violated. Scattering transformation, therefore, is used to passivate the communication subsystem when arbitrarily large delay is introduced as demonstrated in reference [96].
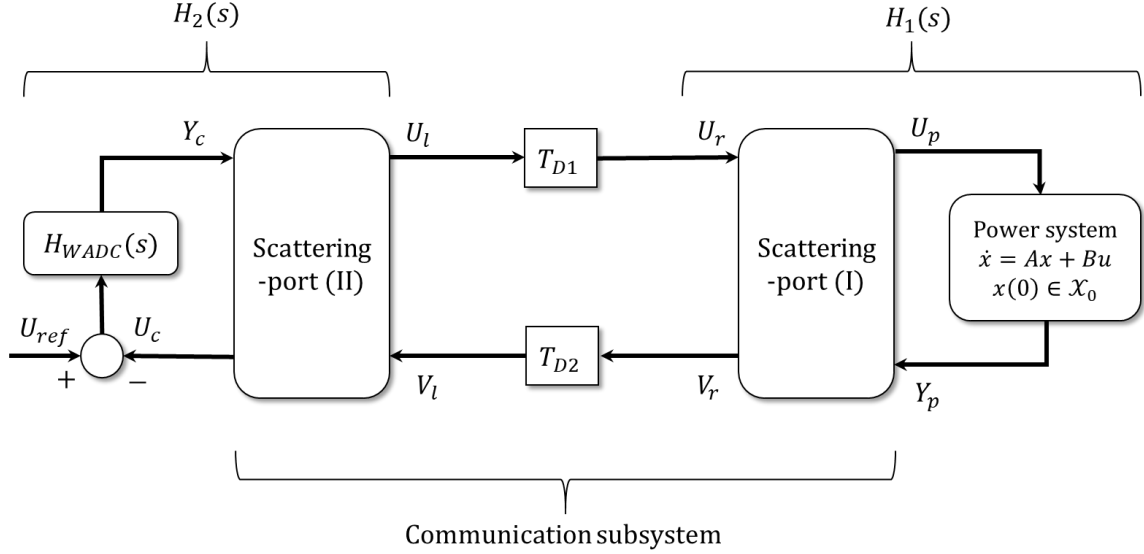
Figure 5.1. Scattering Transformation Based-Wide Area Damping Control Scheme

The round-trip communication delay T is equal to $T_{\text{D}1} + T_{\text{D}2}$, where $T_{\text{D}1}$ is forward delay, and $T_{\text{D}2}$ is backward delay. T is further assumed to be fixed unknown latency. The two forward and backward delays are assumed to be equal, i.e. $T_{D1} = T_{D2}$. Scattering-variables are related as follows:

$$\begin{cases} u_r(t) = u_l(t - T_{D2}) \\ v_l(t) = v_r(t - T_{D1}) \end{cases} \tag{5.4}$$

To mitigate delay impact, the system could be extended by scattering transformation which represents a simple linear transformation of the signals exchanged between the plant and controller over the network in the following form:

$$\begin{cases} U_l = \dfrac{1}{\sqrt{2\beta}}(U_c + \beta Y_c) \\[2mm] V_l = \dfrac{1}{\sqrt{2\beta}}(U_c - \beta Y_c) \\[2mm] U_r = \dfrac{1}{\sqrt{2\beta}}(Y_p + \beta U_p) \\[2mm] V_r = \dfrac{1}{\sqrt{2\beta}}(Y_p - \beta U_p) \end{cases} \tag{5.5}$$

or equivalently

44

$$\begin{cases} \begin{pmatrix} U_l \\ U_c \end{pmatrix} = S \cdot \begin{pmatrix} V_l \\ Y_c \end{pmatrix} \\ \begin{pmatrix} V_r \\ U_p \end{pmatrix} = S^{-1} \cdot \begin{pmatrix} U_r \\ Y_p \end{pmatrix} \end{cases}$$ (5.6)

such that

$$S = \begin{pmatrix} \dfrac{1}{\sqrt{2\beta}} & \sqrt{2\beta} \\ \sqrt{2\beta} & \beta \end{pmatrix} ; \quad S^{-1} = \begin{pmatrix} -1 & \sqrt{\dfrac{2}{\beta}} \\ \sqrt{\dfrac{2}{\beta}} & -\dfrac{1}{\beta} \end{pmatrix} ; \quad \forall \beta > 0$$

Where;

U_p and Y_p are the plant input and output, respectively.

U_c and Y_c are the controller input and output, respectively.

The design aims to minimize the H_∞ norm of $H_1(s)$ to be less than or equal one. If this condition is satisfied, the system $H(s)$ is positive-real (PR), and consequently stable.

Independent of delay-stability analysis: Suppose there exists a $\beta > 0$, so that:

$$\text{K}(s) = \frac{1}{\beta} \frac{\beta^2 \cdot H_{WADC} + H}{1 + H_{WADC} \cdot H}$$ (5.7)

is positive-real (PR), then the closed-loop system stability is independent of delay. For more details see [87].

Our design purpose is to find a scattering-parameter β in a way that $\text{K}(s)$ is PR for a wide range of frequencies, while keeping an acceptable closed-loop system performance without scattering transformation in delay-free case. Particle PSO is used to search for this scattering-parameter β.

When there is no delay, the two scattering transformation ports cancels each other, and the basic feedback interconnection form is resembled. When delays are present,

however, (U_l, V_l) is no longer equal to (U_r, V_r) and this scattering transformation alters the properties of the closed-loop system.
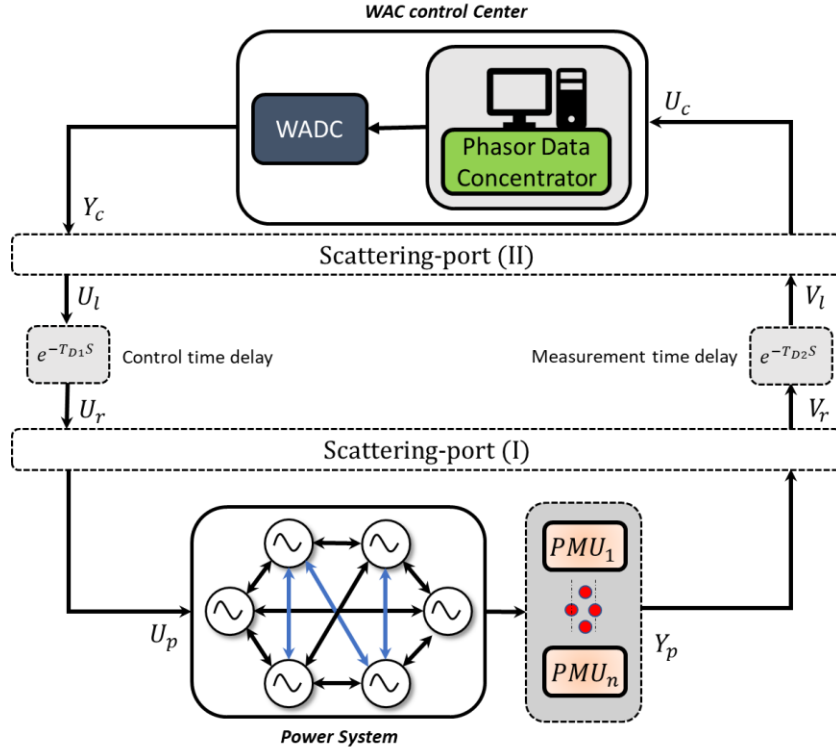
Figure 5.2. Schematic diagram of proposed scattering transformation-based wide area control system

The practical implementation of ST-WADC could be done in two levels. The right-hand scattering port (port I) can be considered as a part of the plant implemented as local controller. Whereas the left-hand scattering port (port II) can be implemented along with the classical lead-lag structure. As shown in Figure 5.2.

5.3.1 Particle Swarm Optimization

Particle swarm optimization (PSO) is population-based metaheuristic intelligent searching method that tackles heavy computational optimization problems which could be partially irregular, discontinuous, noisy, or change over time. The solution is computed iteratively by improving a candidate solution (called particles) based on a given measure of quality.

Each particle is an σ-dimensional, where σ is the number of optimized parameters. It was introduced by Kennedy and Eberhart [97] in 1995, for studying the social behavior of bird flocking or fish schooling. It solves the problem by moving a candidate population (called a swarm) in multidimensional search-space according to a few simple mathematical formulae to dynamically regulate the position and velocity of each particle. Particles trajectory in the search-space is ruled by their own best-known position (personal best position) denoted as P_{best}, in addition to the entire swarm's best-known position (group best position) denoted as g_{best}. The discovered-improved positions will be the movement guidance of the entire swarm. By repeating this process, hopefully (but not guaranteed), the optimal solution will be discovered at the end.

Traditional optimization techniques such as gradient procedure require heavy computation efforts, in addition to that, the solution might be trapped in local minima (or local maxima), and thus, losing the optimal solution. In contrary, PSO is used to search for global optimal solution with minimum computational burden. Furthermore, it does not require a prior knowledge of the problem and does not rely on the initial population guess.

PSO procedure is described as follows:

Step 1) *(Initialization):*

1- Set the time counter $t = 0$.

2- Generate randomly n particles by a random selection of value with a uniform probability over parameters search-space.

3- For each particle in the initial population, the objective function J is evaluated, and the best objective function value is taken J_{best}. This value will be considered as a global best function J_{best} and the associated global best particle as $xbest$.

47

4- Set the initial value of the inertia weight that is a control parameter used to control the impact of the previous velocity on the current velocity. Set the initial value of the inertia weight $\omega_{initial}$.

Step 2) (Time updating): Update the time counter $t = t + 1$.

Step 3) (Weight updating): Update the inertia weight by $\omega(t) = \alpha\omega(t-1)$, where α is a decrement constant smaller than but close to 1. Where ω is the inertia weight factor.

Step 4) (Velocity updating): Using the global best and individual best. One can update the velocity associated with the j_{th} particle the σ_{th} dimension by:

$$\mathcal{V}_{i,\sigma}(t+1) = \omega(t+1)\mathcal{V}_{j,\sigma}(t) + c_1 r_1\big(P_{best}(t) - \mathcal{X}_{i,\sigma}(t)\big) + c_2 r_2\big(g_{best}(t) - \mathcal{X}_{i,\sigma}(t)\big) \tag{5.8}$$

Where σ number of the particles in the group. c_1 and c_2 are positive constants used to alter the particle velocity toward P_{best} and g_{best} and represent the cognitive and social acceleration factors, respectively. r_1 and r_2 are two uniformly distributed random numbers between in [0,1]. t is the iteration number [98] .

Step 5) (Position updating): Based on the updated velocities, each particle changes its position according to the following equation:

$$\mathcal{X}_{i,\sigma}(t+1) = \mathcal{X}_{i,\sigma}(t) + \mathcal{V}_{i,\sigma}(t+1) \tag{5.9}$$

Where $\mathcal{X}_{i,\sigma}$ is the position of the ith particle in σ^{th} dimention.

Step 6) (Individual best updating): Each particle is evaluated according to the updated position. If the cost function of this particle at this moment is less than the global best J_j^* , then update individual best as a global best and go to step 7; else go to step 7.

Step 7) (Global best updating): Search for the minimum value among the global best J_j^* where min is the index of the particle with minimum objective function value, i.e., if

$J_{min} > J^{**}$ then update global best as $X^{**} = Xmin$ and $J_{min} = J^{**}$, and go to step 8; else go to step 8.

Step 8) *(Stopping criteria):* If one of the stopping conditions are satisfied, then the process could be terminated, or else go to step 2.

5.3.2 Objective Functions

The objective function J is represented by the selected signal-deviation from its reference value (ΔE), either to be speed or power signal. The main goal is to minimize J at a nominal delay $50\ ms$ for two different approaches. The proposed method is anticipated to offer the best minimization performance. The chosen objective function might be in various forms depending on the system under study. In this paper, the cost function which need to be minimized by PSO is integral time absolute error (ITAE) performance index, which is an integral of time times the absolute value of the signal-deviation over the time interval of simulation run-time, i.e., from 0 to final simulation time (tf), defined as follows:

$$J = \int_0^{t_f} t.|\Delta E|\, dt \qquad (5.10)$$

5.3.3 Implementation

For the proposed ST-WADC, the optimization problem is formulated to include the scattering-parameter β in order to minimize the adverse impact of the communication delay. This parameter is taken in the design prosses and optimized by PSO along with the parameters of lead-lag compensator, which are adjusted in a way that the phase shift between the speed deviation and resulting electrical damping torque is minimized. The optimization problem formulated as follows;

$$Minimize \;\; J$$

Subjected to the parameters bounds;

$$
\begin{cases}
K^{\min} \leq K \leq K^{\max} \\
T_1^{\min} \leq T_1 \leq T_1^{\max} \\
T_2^{\min} \leq T_2 \leq T_2^{\max} \\
T_3^{\min} \leq T_3 \leq T_3^{\max} \\
T_4^{\min} \leq T_4 \leq T_4^{\max} \\
\beta^{\min} \leq \beta \leq \beta^{\max}
\end{cases}
\tag{5.11}
$$

Where;

$$
\begin{cases}
K \in [0.01 - 40] \\
T_1, T_2, T_3, T_4 \in [0.01 - 2] \\
\beta \in [0.01 - 1]
\end{cases}
\tag{5.12}
$$

The other optimization parameters are set to the following values;

$$
\begin{cases}
number\ of\ particles = 50 \\
number\ of\ iterations = 50 \\
c_1 = 2 \\
c_2 = 2 \\
\alpha = 1 \\
\omega = 0.85
\end{cases}
\tag{5.13}
$$

For the sake of comparison, the proposed WADC is compared with the conventional one.

The only difference between the conventional method and the proposed ST-WADC, is that,

J for the conventional design is subjected to the same constrains given in (15) excluding β

bounds.

5.4 Design Procedure

The following steps explain briefly the proposed method implementation:

Step 1*:* Build a detailed power system model.

Step 2: Insert scattering transformation ports between the plant and the controller by implementing the equations set (5.5) which links the scattering-variables V_l, U_l, V_r and U_r, see Figure 5.1.

Step 3: Implementation of PSO algorithm.

Step 4: Use PSO to search for the optimal parameters of the controller as well as the optimal scattering-parameter β.

Step 5: Run the program.

5.5   Summary

This chapter addressed a novel scattering transformation-based wide-area damping controller. The main objective is to design a controller that able to suppress the system oscillations and eradicate the detrimental impact of it while compensating for the remote-area signals communication delay either fixed or time-varying delay. To resolve the destabilizing effect of the communication latency, scattering transformation is inserted in form of two ports between the power system and WADC. In other word, the signals exchanged between the plant and the controller are regulated by set of equations. The deployment of PSO algorithm has incorporated the scattering-parameter constrains in addition to the constrains of the lead-lag controller.

CHAPTER 6

RESULTS AND DISCUSSION

6.1   Introduction

This chapter highlights the result of applying the proposed methods and discusses its effectiveness in improving the damping performance. A set of case-studies is considered to verify the robustness of the proposed controllers under different disturbance scenarios. The results confirm the efficacy of the proposed approaches to greatly enhance the power system stability.

6.2   Application of LQG-WADC

LQG-WADC has been applied in the four-machine system and ten-machine system, respectively. The two case-studies are given as follows:

6.2.1   Four-Machine/Two-Area System

ST-WADC is tested on a classic two-area four-machine system. This system has a factual structure (although it's a fictional system) which has been widely used to carry-out various studies related to low frequency oscillations in power systems. The system is comprised of four synchronous generators with DC excitation system and 11 buses, distributed in two symmetrical areas, connected via two parallel 220-km long tie-lines between bus 7 and bus 9. The system transmits about 400 MW between the areas under normal conditions and vary between $(0 - 500 \text{ MW})$ just by adjusting the loads connected to bus 3 and 5, as

depicted in Figure 6.1. Two-area/Four-machine system. The system has been built in MATLAB/SIMULINK using $SimPowerSystem$ toolbox.
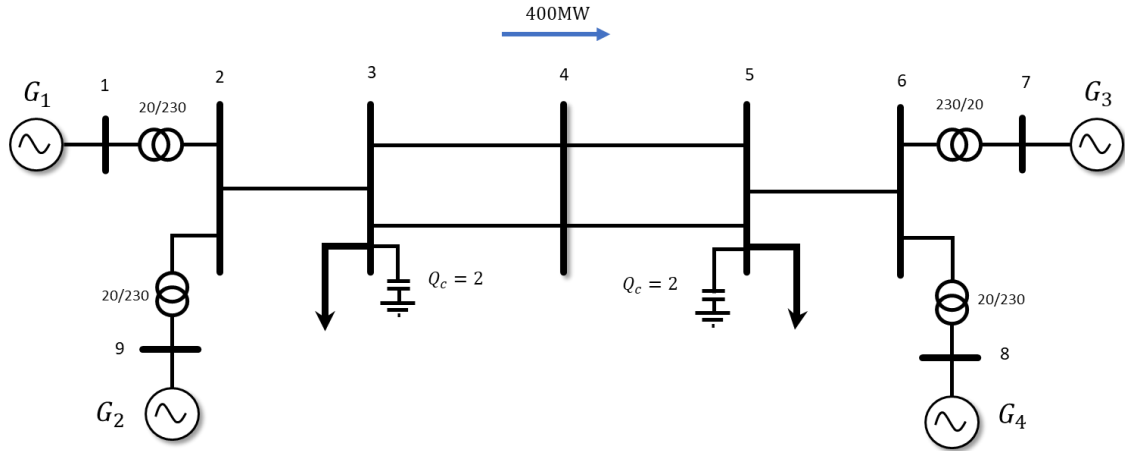
Figure 6.1. Two-area/Four-machine system

6.2.1.1　Full-order Model and Small Signal Analysis

Eigenvalue analysis is conducted for this base case to examine the damping characteristics of the open-loop systems under different operating points. The system exhibits three modes with low damping performance, two local modes and one interarea mode. Interarea mode of an eigenvalue $\lambda = 0.1041 \pm 4.0514i$, frequency $f = 0.7318$ Hz, and damping $\boldsymbol{\zeta} = -0.0106$. The objective of the wide-area controller is to give a satisfactory damping to this mode in particular, rest of the modes are presented in Table 6.1.

FFT algorithm has been developed as well to detect the oscillation modes directly from speed measurements as shown in Figure 6.2, Figure 6.3 and Figure 6.4. Area-1 is represented by speed difference of G1 and G2, and Area-2 by speed difference of G3 and G4. Since our purpose is to mitigate the oscillations between the two areas, the interarea mode can be represented by speed difference of (G1, G2) and (G3, G4). By a quick look

in these plots, it can be observed that the magnitude of the interarea mode is 1.449 which

is relatively large compared to 0.1189 and 0.162 for local modes 1 and 2, respectively.

Table 6.1. Eigenvalue analysis of two-area/four-machine system

Mode index	Mode Type	Eigenvalue	Frequency (Hz)	Damping Ratio, ζ
I	Local Mode 1	$-0.5250 \pm 7.2925i$	1.1385	0.10021
II	Local Mode 2	$-05893 \pm 7.4636i$	1.1870	0.085649
III	Interarea Mode	$0.1041 \pm 4.0514i$	0.7318	-0.010583
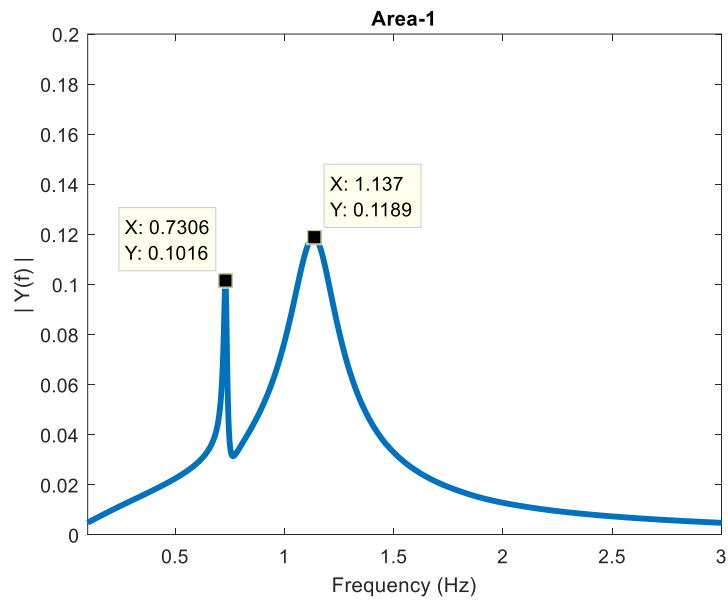
Figure 6.2. FFT for area-1 speeds
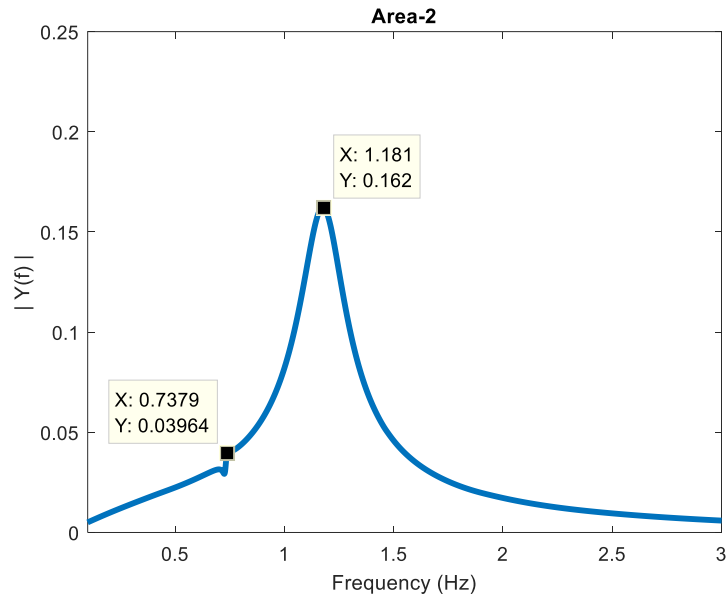
Figure 6.3. FFT for area-2 speeds
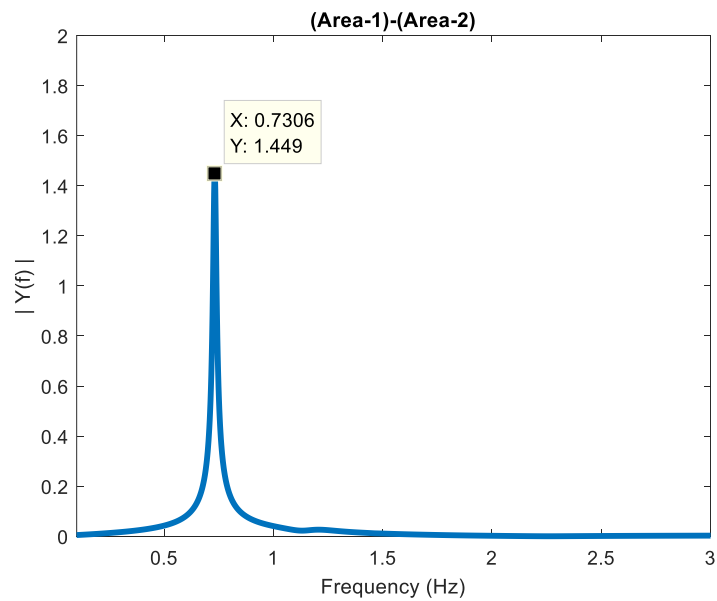
Figure 6.4. FFT for (area-1) -(area-2)

6.2.1.2   Selection of Feedback Signals and Controller Locations

The Geometric Measures decide the effective control signals as well as the optimal controller locations. Figures (6.5) and (6.6) shows the modal controllability/observability

measures for system oscillatory modes. In order to design WADC, optimal location of the controller should be specified according to the mode of controllability, input signal selection according to the mode of observability.

In Figure (6.5) it can be shown that for mode I the maximum controllability measure found in G2, so the PSS should be placed here. In Figure (6.6) G2 has also the maximum observability measure, therefore, the control input signal will be selected from G2 (local signal). The same case for mode II, where the maximum controllability and observability in G4, therefore, PSS will be located there, and the control input signal will be fed-back from G4 (local signal). For mode III the maximum controllability found in G2, so the optimal location for the controller will be there.
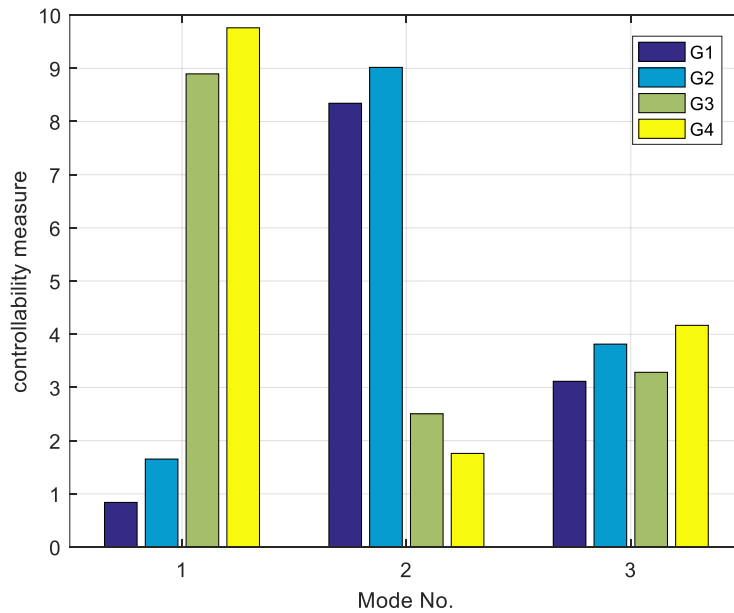
Figure 6.5. The controllability measure for the oscillatory modes
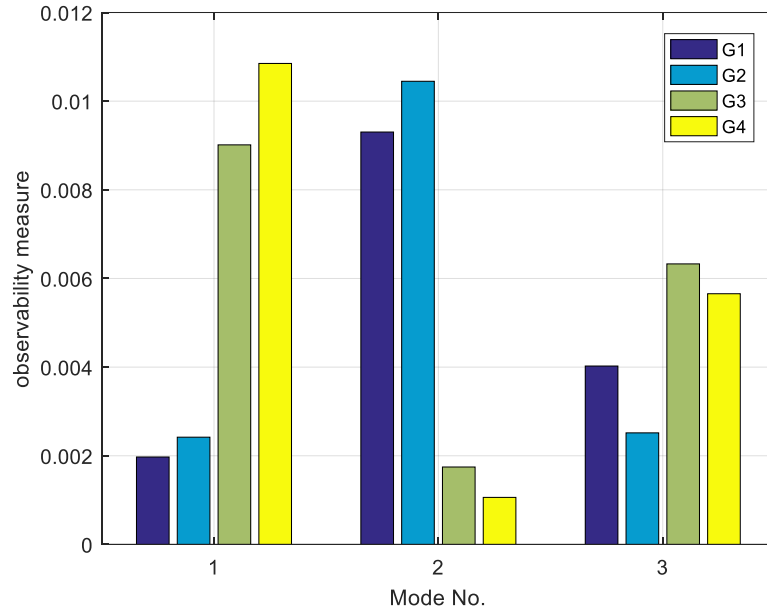
Figure 6.6. The observability measure for the oscillatory modes

The mode shape of the three modes is determined as shown in Figure 6.7 to Figure 6.9. For mode I, G1 swings against G2 locally in area 1. For mode II, G3 swings against G4 locally in area 2. For mode III the swinging between two group of generators, in other word, G1&G2 against G3&G4.
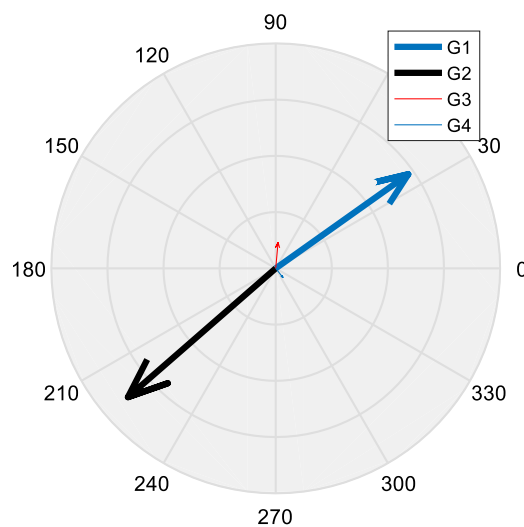
Figure 6.7. Modes shape of local mode 1
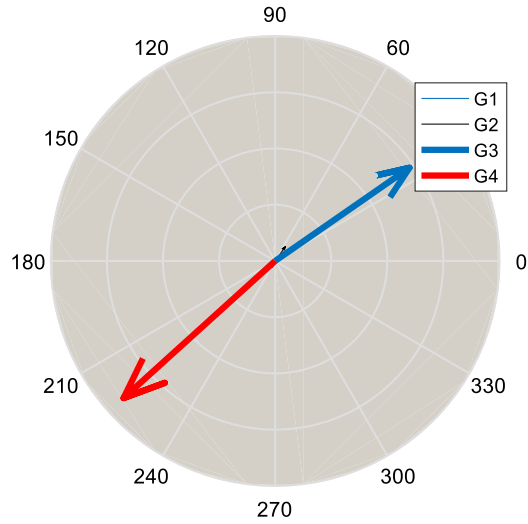
Figure 6.8. Modes shape of local mode 2
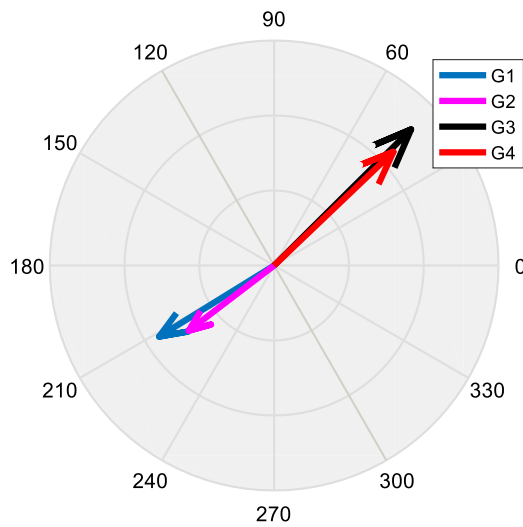
Figure 6.9. Modes shape of the interarea mode

Figure 6.10 illustrates the participation factors of generator speeds to the interarea mode. The most participated state to this mode in area-1 is G1 speed. In area-2 the strongest participant is G3 speed. Therefore, to increase the observability of this mode, a combination of G1 and G3 speed deviations is used as a feedback signal.

$$\Delta y = \Delta \omega_1 - \ \Delta \omega_3 \tag{6.1}$$
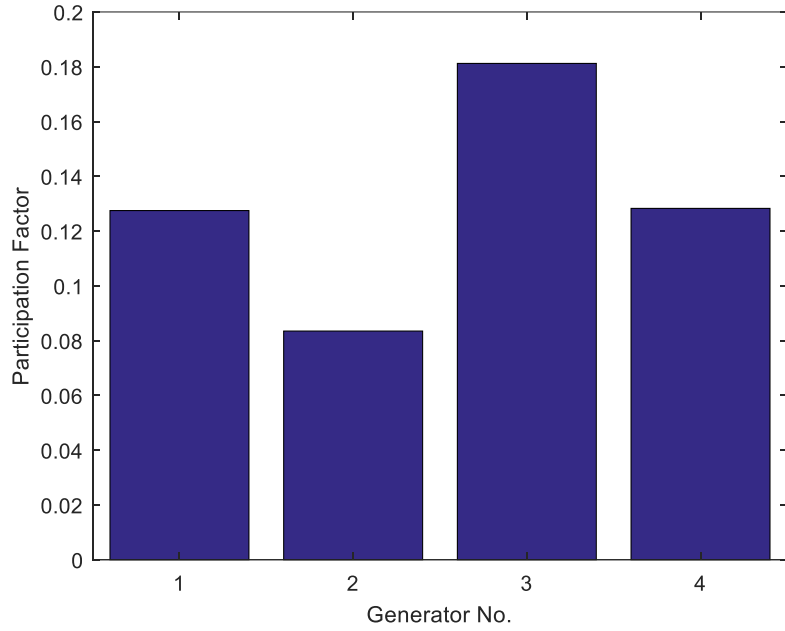
Figure 6.10. Participation factors of generator speeds
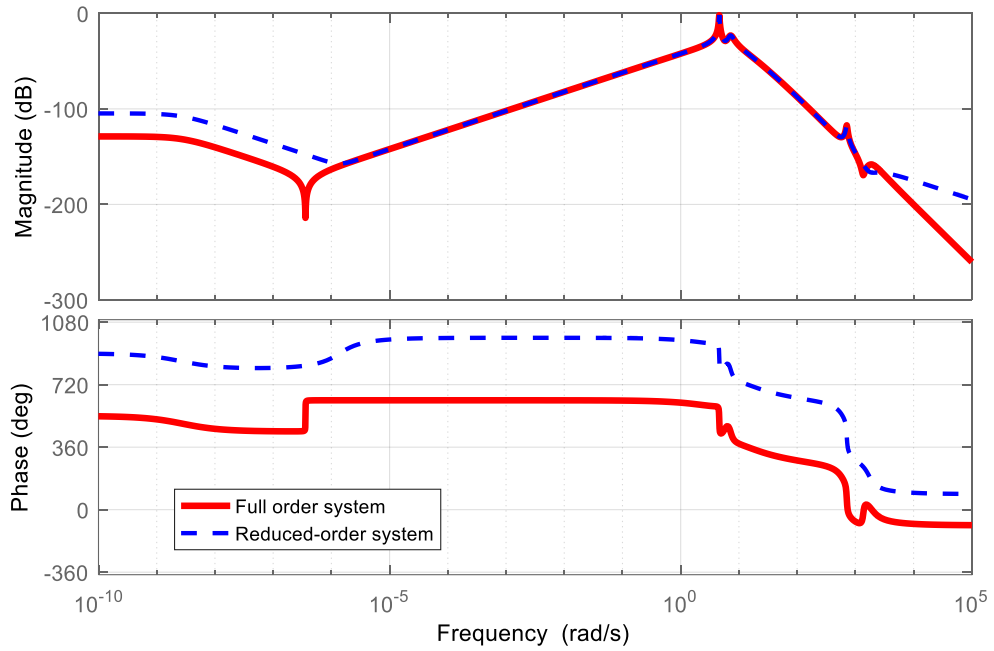
Figure 6.11. Bode plot of full and reduced order system

6.2.1.3 System Order Reduction

The full order of the designed system is 68. The designed controller will be in the same system order plus the order of the scaling functions. That needs a huge computation effort to design such controller. A site from that, the states of interest are the dominant states which reflect the characteristics of the model. Therefore, Schur method for balanced-truncation is used to reduce this 68th order model into 20th order model. The reduced system eigenvalues for the three critical modes are presented in Table 6.2. To validate its characteristic, the corresponding frequency response is depicted in Figure 6.11, it's obvious that the reduced system matches the full order model within 0.1~2 Hz.

Table 6.2. Eigenvalue analysis of full and reduced order systems

Mode	Full Order System			Reduced Order System		
	Eigenvalues	*Frequency (Hz)*	*Damping Ratio, ζ*	*Eigenvalues*	*Frequency (Hz)*	*Damping Ratio, ζ*
Local 1	$-0.5250 \pm 7.2925i$	1.1385	0.10021	$-0.72047 \pm 7.1536i$	1.1385	0.10024
Local 2	$-05.893 \pm 7.4636i$	1.1870	0.085649	$-0.63738 \pm 7.4155i$	1.1802	0.085636
Interarea	$0.1041 \pm 4.0514i$	0.7318	−0.010583	$0.108664 \pm 4.5979i$	0.73177	0.010613

6.2.1.4 LQG Controller Synthesis

The LQG controller is of 20th order equal to the reduced-plant order, then it has been further reduced to a 5th order using Schur method. The bode diagram of the reduced model is depicted in Figure 6.12, the purpose of this step is to eliminate the draw backs of high order controllers because it could result in making the real nonlinear system impotent. Furthermore; this could help speeding up the controller prosses. In addition to that; it could be very difficult and inappropriate to design such a controller in a hardware prototype.

Therefore, the original controller order need to be reduced. Since our dealing with a reduced model, it's hard to find a direct procedure for scaling matrix selection. The state-space realization of the reduced-order controller is presented as:

$$A_k = \begin{bmatrix} -29.1205 & 13.8427 & -4.7463 & -0.9781 & 0 \\ -13.8427 & -2.0047 & 1.2168 & 0.8718 & 0 \\ 4.7463 & 1.2168 & -0.8573 & -7.2637 & 0 \\ -0.9781 & -0.8573 & 7.2637 & -0.0728 & 0 \\ 0 & 0 & 0 & 0 & -2.7968^{-9} \end{bmatrix};$$

$$B_k = \begin{bmatrix} -15.2602 \\ -2.3633 \\ 1.0453 \\ -0.2944 \\ 3.5395^{-8} \end{bmatrix};$$

$$C_k = [15.2602 \quad -2.3633 \quad 1.0453 \quad 0.2944 \quad 2.3901^{-8}];$$

$$D_k = [4.6181];$$
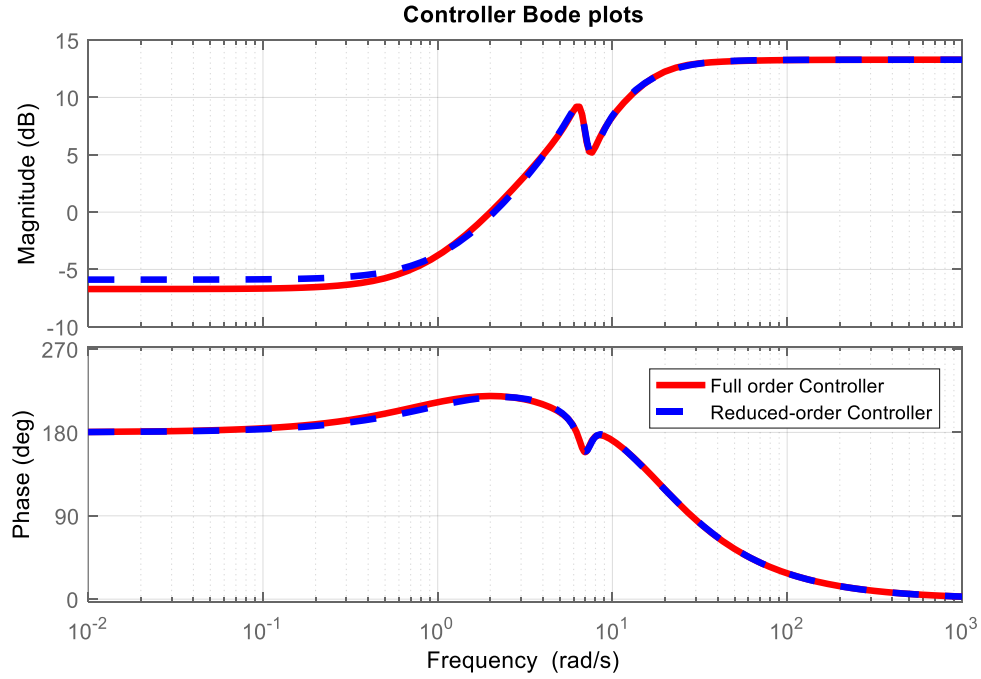
Figure 6.12. Bode plot of full and reduced order controller

6.2.1.5 Conventional Phase Compensation Method

LQG-WADC is compared with the classical WADC which has been designed based on phase compensation method (residue method) [73], [99]. The transfer function of the plant $G(S)$ can be factorized into partial functions with residues R_i and eigenvalue λ_i, such that

$$G(s) = \frac{Y(s)}{U(s)} = C(SI - A)^{-1}B = \sum_{i=1}^{n} \frac{R_i}{S - \lambda_i} \qquad (6.2)$$

where i is the associated mode index. General WADC structure composites of two lead-lag compensators, washout filter and a controller gain. The transfer function of this classical form is formulated as follows:

$$H_{WADC}(s) = K_{WADC} * \frac{T_w s}{1 + T_w s} * \frac{1 + T_1 s}{1 + T_2 s} * \frac{1 + T_3 s}{1 + T_4 s} \qquad (6.3)$$

Where $T1, T2, T3$, and $T4$ are phase-compensation parameters, Tw is washout filter time

constant which is usually chosen between 5-10 s, here it has been selected to be 10s. K_{WADC}

is the controller gain.

By means of residue method, these parameters can be calculated as follows:

$$\phi_i = \pi - \arg(R_i) \qquad (6.4)$$

Where ϕ_i is the amount of phase required compensation. The lead-lag parameters are

determined by the following equations

$$\alpha = \frac{T2}{T1} = \frac{T4}{T3} = \frac{1 - \sin\left(\frac{\phi_i}{2}\right)}{1 - \sin\left(\frac{\phi_i}{2}\right)} \qquad (6.5)$$

$$T_1 = \frac{1}{2\pi f_i \sqrt{\alpha}}, \quad T_2 = \alpha T_1 \qquad (6.6)$$

$$T_3 = \frac{1}{2\pi f_i \sqrt{\alpha}}, \quad T_4 = \alpha T_3 \qquad (6.7)$$

Where f_i represents the frequency of mode i.

6.2.1.6   Nonlinear Time Domain Simulation

To verify the performance, effectiveness, and robustness of the obtained LQG-WADC,

nonlinear time domain simulations is carried out with MATLAB/Simulink. Figure 6.13 to

Figure 6.16 show some of the power system states responses with the presence of LQG-

based wide area control, conventional wide-area control and without wide area control

(open-loop). System is tested in post-fault condition, after applying a three-phase fault in

one of the tie-lines at bus 4 for 4 cycles to initiate the interarea oscillations.
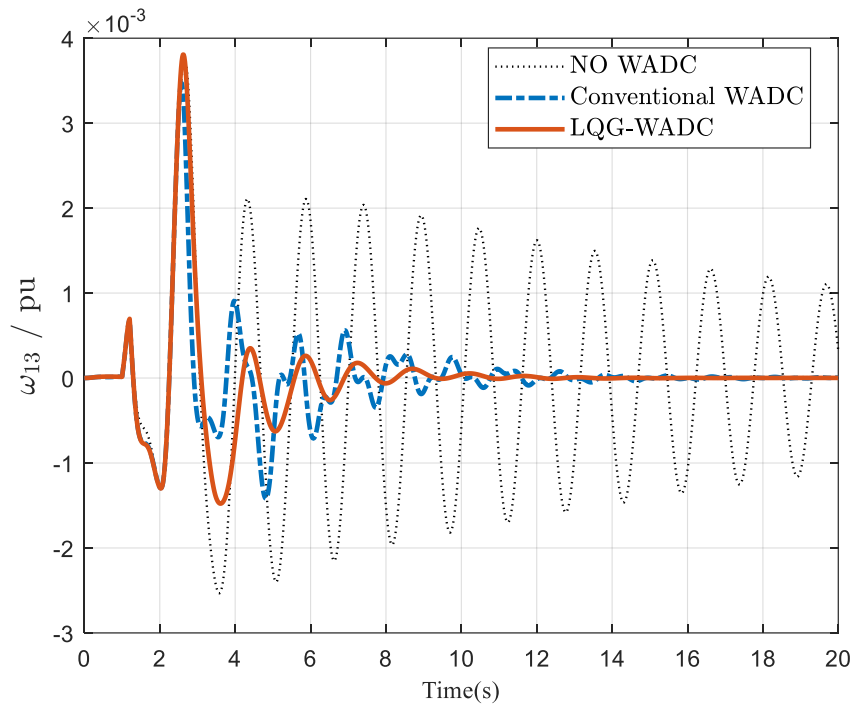
Figure 6.13. Rotor speed deviation (G1-G3) (Controller input signal)
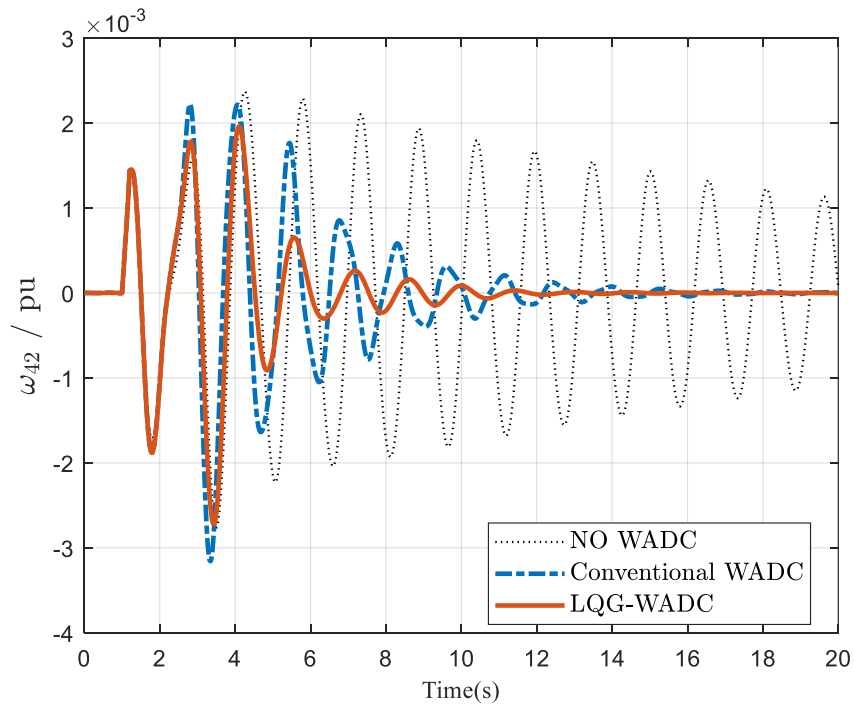
Figure 6.14. Rotor speed deviation (G4-G2)
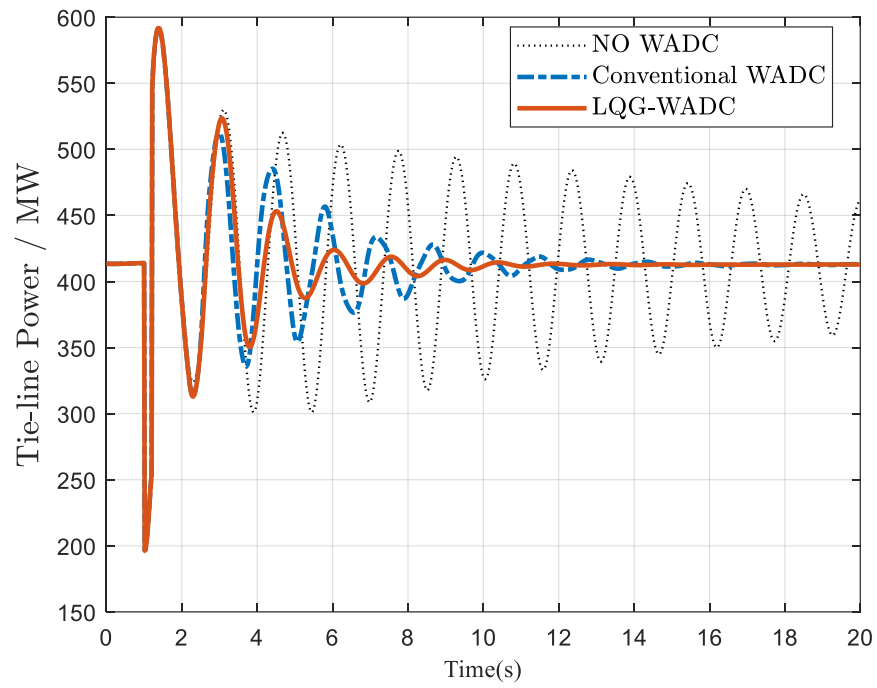
Figure 6.15. Tie-line active power
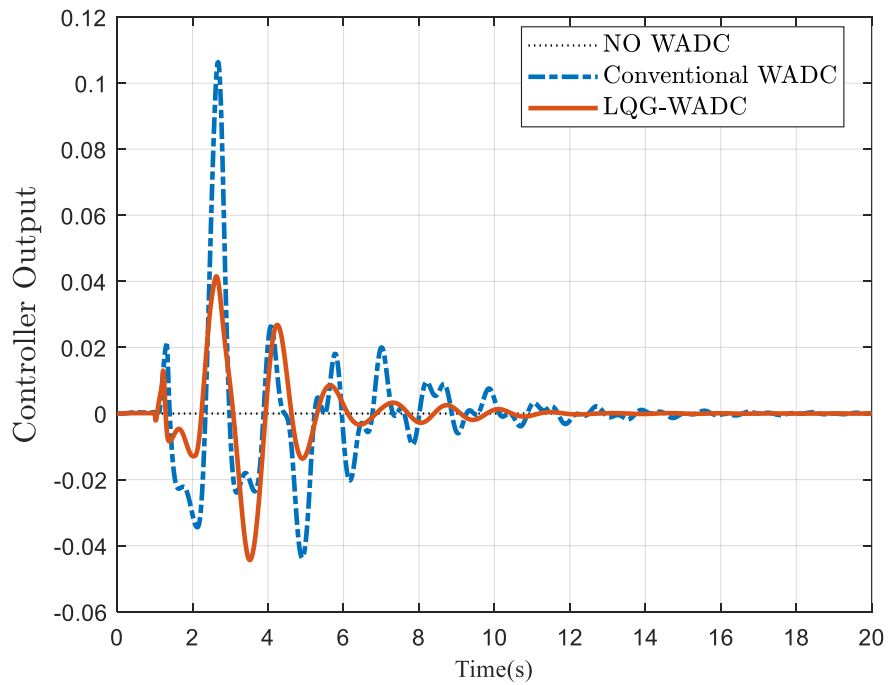
Figure 6.16. Controller output signal

65

6.2.1.7   Discussion

Controller performance is tested with MATLAB/Simulink. Previous Figures shows some of the power system states responses with the presence of wide area control (closed-loop), and without wide area control (open-loop), after applying a three-phase fault in one of the tie-lines at bus 4 for 4 cycles to initiate the interarea oscillations. According to the simulated results, its confirmed that the interarea oscillations have been successfully damped when LQG-WADC is introduced soon after 12 secs compared to 18 secs with the conventional controller and 35-40 secs in the un-controlled case. Figure 6.15 displays the power flow in the tie-line between bus 3 and bus 5. In the beginning the response is highly vacillating, and that owing to nature of the disturbance, while successfully recovered after few seconds. The controller gives a satisfactory action when the fault took place, and improve the damping greatly, compared with the open-loop case. It is demonstrated that LQG-WADC has the capability to eradicate this mischievous system oscillations and improve interarea damping performance. Furthermore; the oscillations settling time is reduced significantly is each case, which perfectly achieve the system damping requirement. Results also demonstrate the robustness of the controller which corresponds to system eigenvalues analysis shown in Table 6.3.

Table 6.3. Eigenvalue analysis for LQG-WADC

Mode		With Convectional WADC		With LQG-WADC	
		Frequency (Hz)	Damping Ratio, ζ	Frequency (Hz)	Damping Ratio, ζ
Local 1		1.5261	0.2146	1.4126	0.2309
Local 2		1.6286	0.1870	1.4542	0.2512
Interarea		0.6832	0.1056	0.6105	0.2331

6.2.2   New England 39-bus test system

To further explore the effectiveness of the proposed strategy, another study has been conducted. The controller has been implemented in New England 39-bus 10-machine test system. This model consists of 46 transmission lines. It has been vastly used to carryout studies related to interarea low frequency oscillations under faults and various perturbations. The generators are represented by six-order model. All generators are equipped with exciters, turbine/governors, and power system stabilizers (two lead-lag compensation blocks) with one slack bus in G2. This system is so stressed with various levels of loading and generation. The single line diagram is depicted in Figure 6.17. (shaded parts represent the coherent areas). The model has been built in MATLAB/SIMULINK.
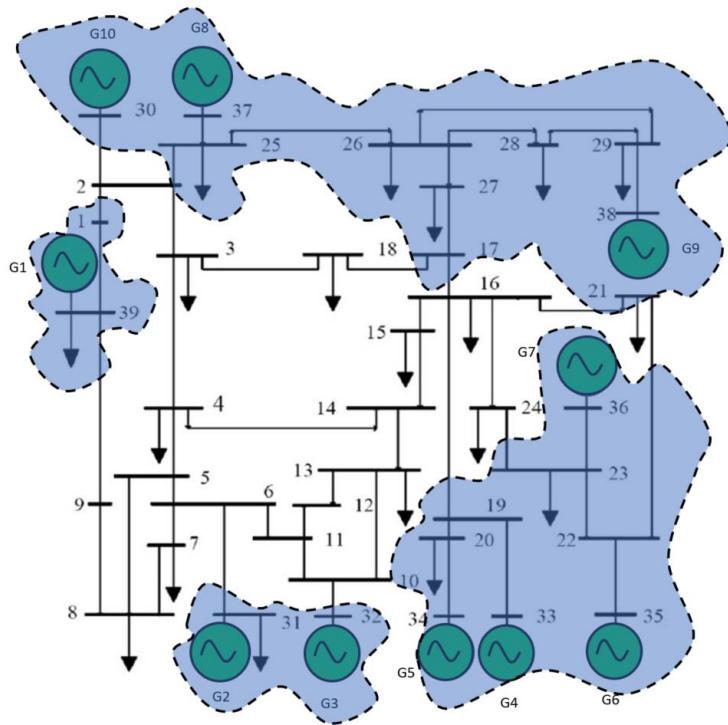
Figure 6.17. Ten-machine system

6.2.2.1   Full-order Model and Small Signal Analysis

Similar to the previous test case, eigenvalue analysis is carried out to evaluate system damping of the open-loop system under various operating points. Linearization results in a LTI system of order 290. The system exhibits three interarea modes and five local modes with very weak damping performance. The local modes are can be appropriately well damped with local controllers (PSS) installation. However, the major attention will be concentrated on Interarea modes. The modes characteristics are shown in Table 6.4 where FFT algorithm has detect the critical modes from speed measurements as shown in Figure 6.18, three interarea modes have been assigned as shown in the Figure 6.19. Apparently; the magnitude of the interarea modes is quite large compared with the local modes magnitudes.

Table 6.4. Small-signal analysis of ten-machine system

Mode		Mode Shape		Freq	Damping Ratio
Interarea 1		10 vs All		0.31631	-0.0213
Interarea 2		(4,5,6,7) vs (2,3), (1,8,9)		0.54372	-0.0266
Interarea 3		(2,3) vs (1,8,9)		0.86565	-0.0125
Local 1		4 vs (5,6,7)		1.7112	0.0445
Local 2		9 vs (1,8)		1.6421	0.0458
Local 3		2 vs 3		1.4297	0.0511
Local 4		5 vs (6,7)		1.2604	0.0413
Local 5		6 vs 7		1.1821	0.0483
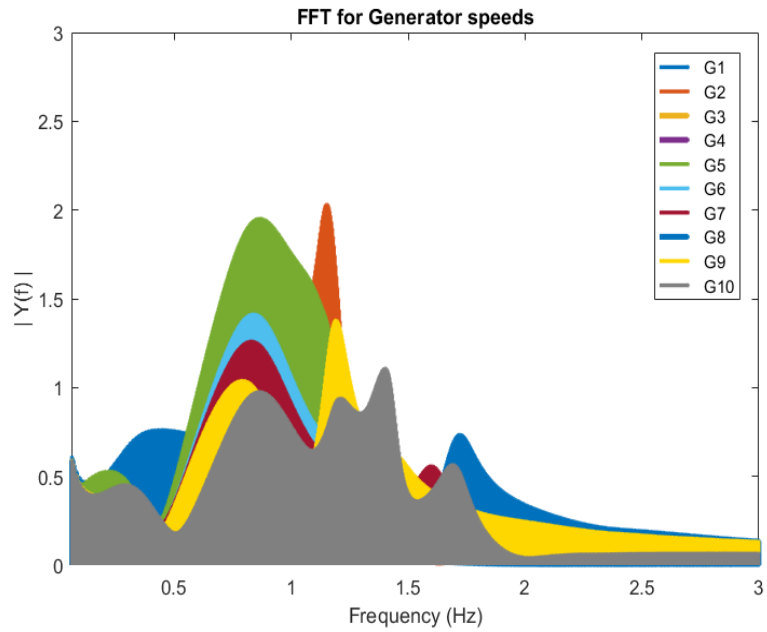
Figure 6.18. FFT analysis of Generator speeds
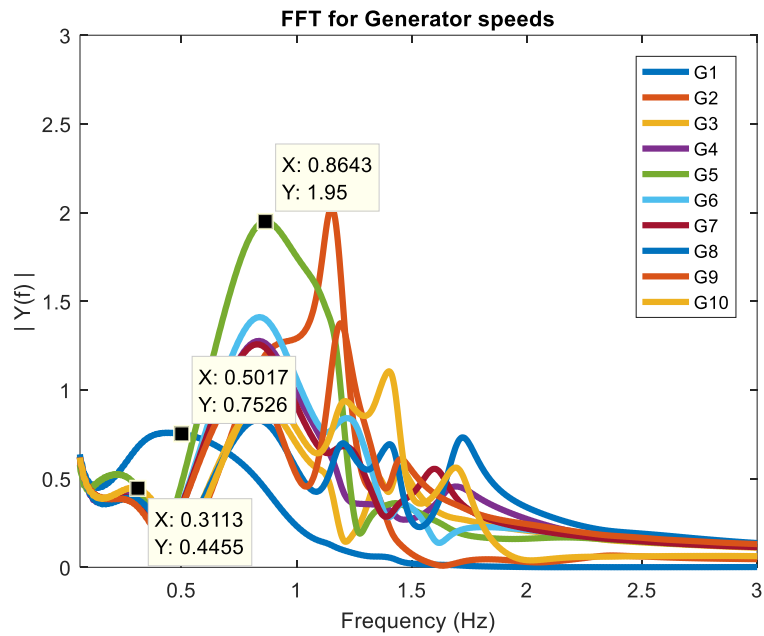
Figure 6.19. Interarea modes identification via FFT

69

6.2.2.2   Selection of Feedback Signals and Controller Locations

Normalized Participation factors are calculated for each interarea mode as shown in Figure 6.20. However, it's not certain that the largest participated state will offer the best control action when used as feedback signal, therefore, residue analysis is used for a proper signals selection. According to system modes shape, it's clear that we have 4 areas with 3 coherent groups. Geometric Measures has been used again to decide which control signal is suitable to be used, in addition to controller location. Several signals have been chosen as a potential candidate signals, including generator speeds and tie-line powers. Eventually, the most observable signal will be chosen as the best candidate. Figure 6.21 shows the modal controllability/observability with respect to interarea modes. It could be seen that G1 has the maximum controllability for mode 1 and mode 3, however, for mode 2, the controllability measures of G5 and G10 are the best (G5 is badly involved in destabilizing this mode due to its high participation). The use of many measurements (from all tie-lies) could improve the damping performance, however, this might increase the communication cost. Therefore, two maximum observable signals will be chosen, according to Figure 6.21 active powers in the tie-lines connecting bus 9 and bus 39 (No.12) and bus 15 and bus 16 (No.13) are the most observable signals. These signals could be enough to reflect the nature of the interarea modes; therefore, they are selected as controller inputs.

Table 6.5. Geometric Measures with Respect to Interarea Modes

Candidate Signal	ω_1	ω_2	ω_3	ω_4	ω_5	ω_6	ω_7	ω_8	ω_9	ω_{10}	P_{8-9}	$\boldsymbol{P_{9-39}}$	$\boldsymbol{P_{15-16}}$	P_{1-39}	P_{16-17}	P_{4-5}
Signal Index	1	2	3	4	5	6	7	8	9	10	11	**12**	**13**	14	15	16
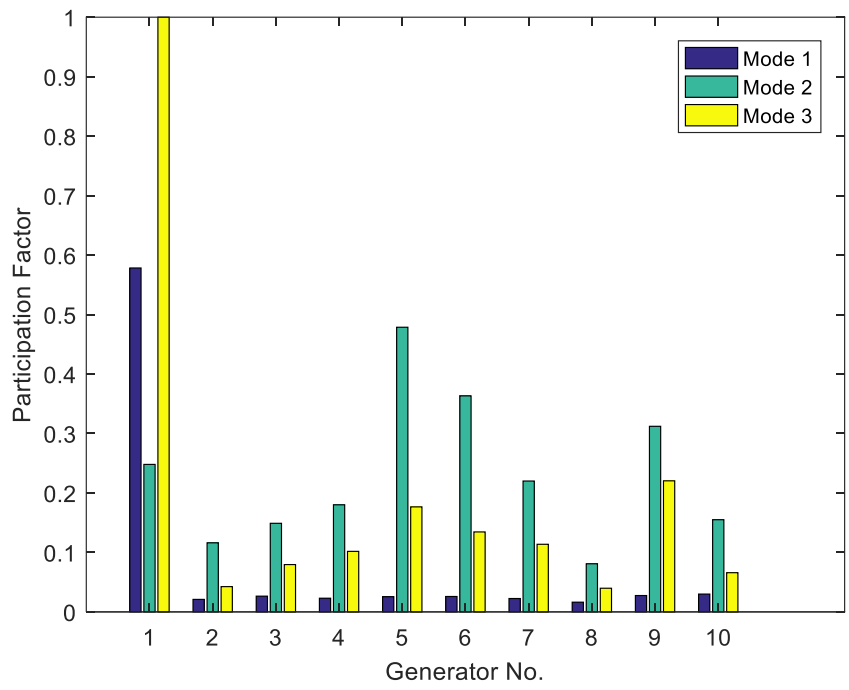
Figure 6.20. Speed participation factors with respect to interarea modes
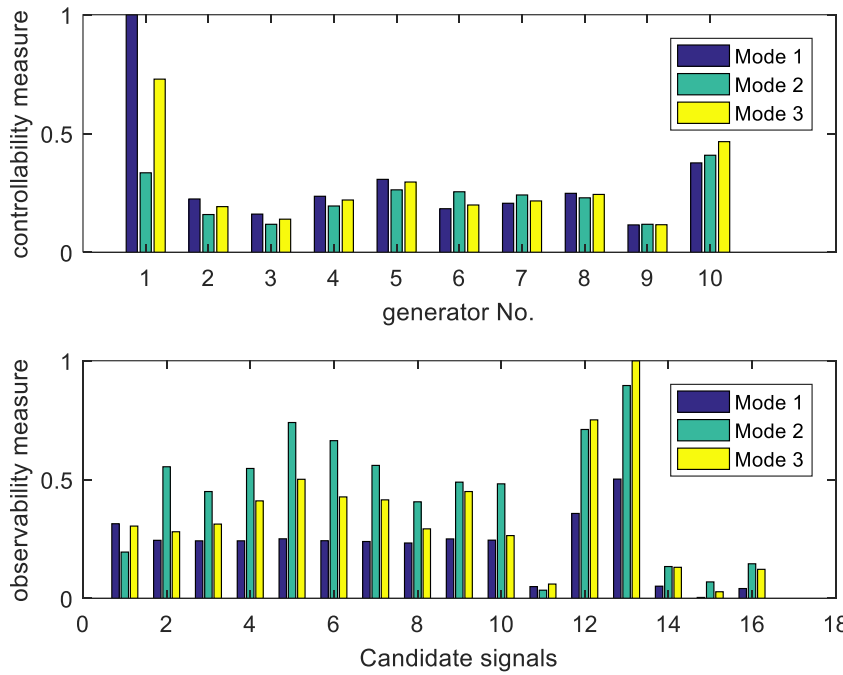
Figure 6.21. Controllability/Observability measures with respect to interarea modes

6.2.2.3   Controller Synthesis

The design procedure is similar to the one that used in the previous case study (two area power system), however in this case, the controller is multi-input/multi-output (MIMO). Two input signals are taken from the tie-lines active powers, and three output signals are distributed to G1, G10, and G5, as shown in Figure 6.22. The controller order will be reduced to the 10th order via Schur method.
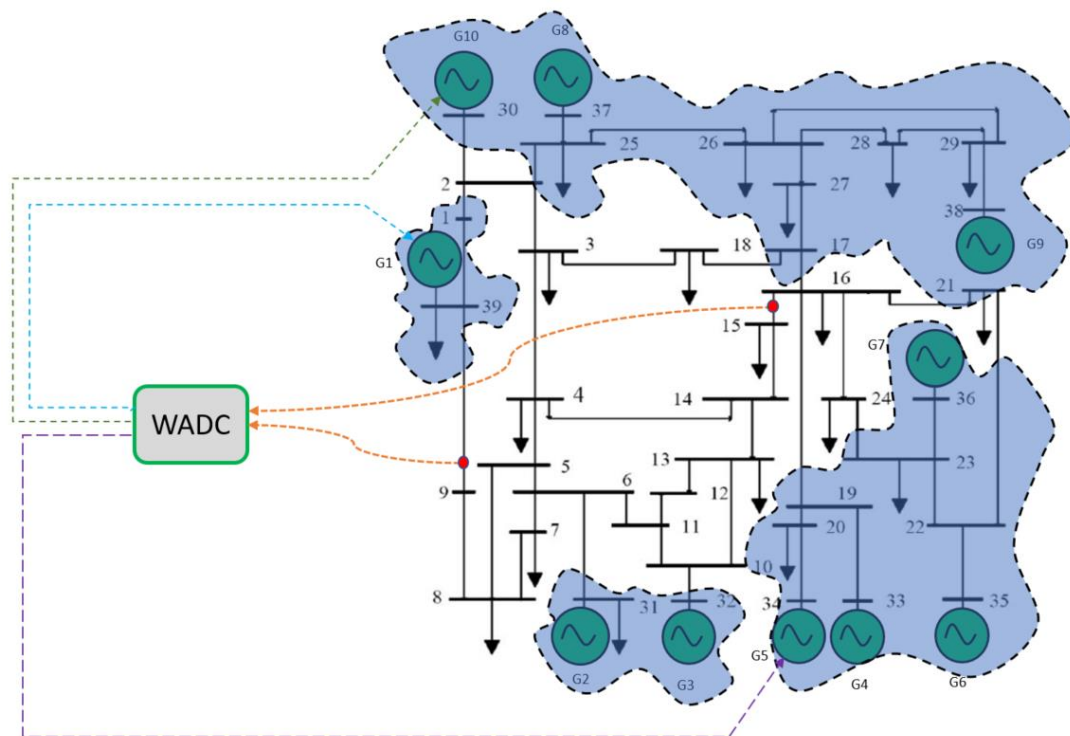
Figure 6.22. Wide-area control in Ten-machine system

6.2.2.4   Conventional Phase Compensation Method

Residue method a gain has been used to identify the parameters of the conventional WADC. The general lead-lag structure given in (6.3) is modified to include three lead-lag blocks

instead of two. Therefore, the transfer function the of classical controller is given as follows:

$$H_{WADC}(s) = K_{WADC} * \frac{T_w s}{1 + T_w s} * \frac{1 + T_1 s}{1 + T_2 s} * \frac{1 + T_3 s}{1 + T_4 s} * \frac{1 + T_5 s}{1 + T_6 s} \qquad (6.8)$$

Where T_5 and T_6 are parameters of the lead-lag controller.

6.2.2.5   Small Signal Analysis and Nonlinear Time Domain Simulation

Small signal analysis is carried out to verify the improved controller performance, Table 6.6 shows a comparison between the open-loop and the closed-loop system (with WADC) in term of damping performance for interarea modes only.

Table 6.6. Small-signal analysis of the conventional design as well as LQG-WADC

Mode	Conventional Design		LQG-Based Design	
	Frequency (Hz)	ζ	Frequency (Hz)	ζ
Interarea 1	0.3365	0.0647	0.3645	0.1005
Interarea 2	0.5824	0.0654	0.5981	0.1563
Interarea 3	0.9244	0.0339	0.9645	0.1353

Nonlinear simulations represented in Figure 6.23 to Figure 6.25 demonstrate the effectiveness of LQG based wide area control in large scale power networks. Compared with uncontrolled and conventional case, the system exhibits an improved damping performance under wide range of operating conditions. A three-phase to ground fault is applied between line 3 and 4 near bus 3 at t=1s and cleared at t=1.1s.

73
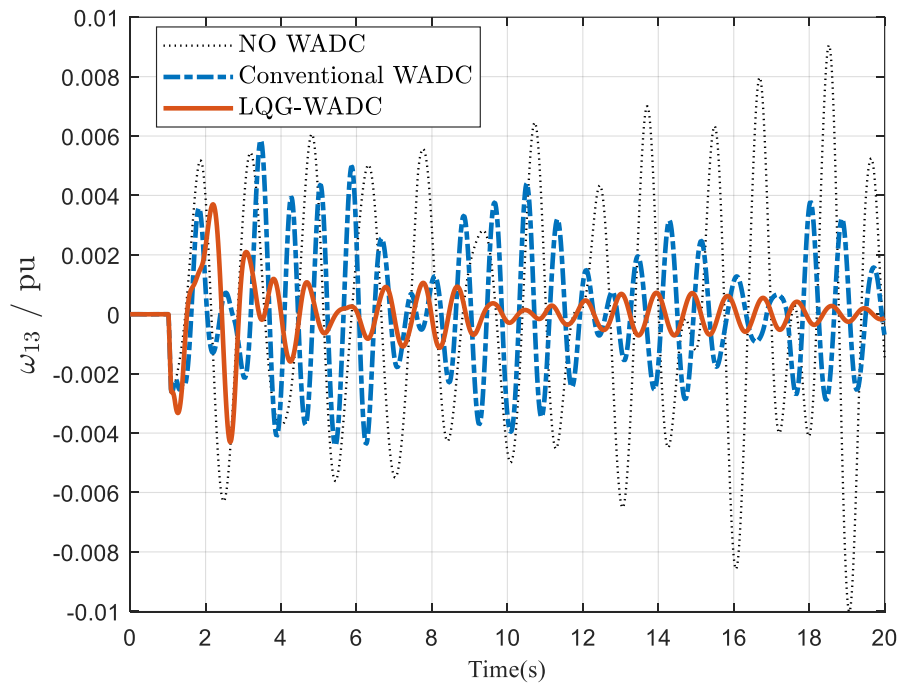
Figure 6.23. Rotor speed deviation (G1-G3) (Controller input signal)
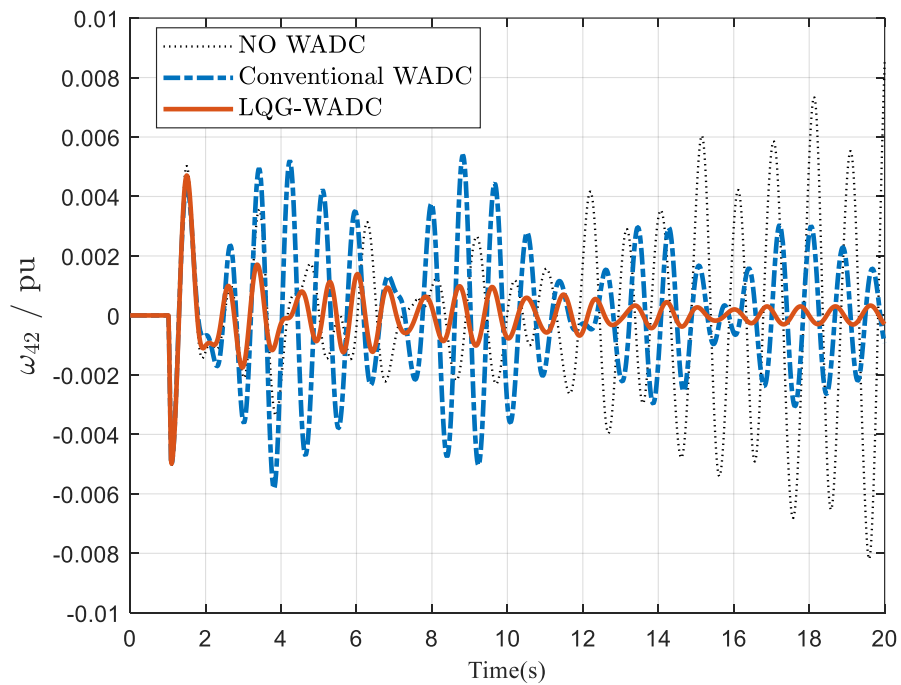
Figure 6.24. Rotor speed deviation (G4-G2) (Controller input signal)
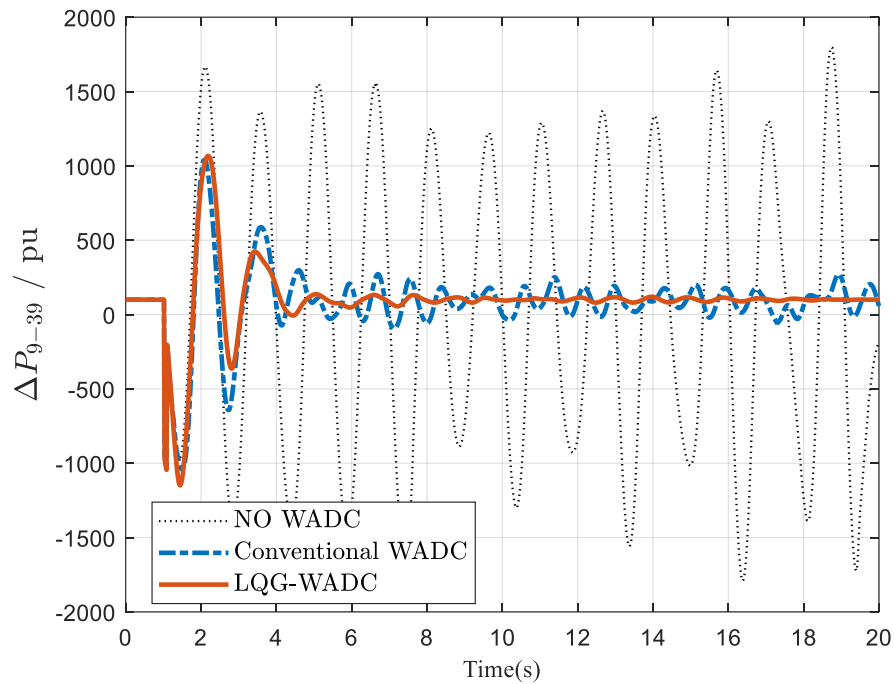
Figure 6.25. Power transfer between bus 9 and 39 (Controller input)

6.2.2.6 Discussion

The power system oscillation arises due to lack of damping torque, which is largely affected by different operating conditions. Typically, in a power system where the transmission of a large amount of active power between two large areas takes place, the decrease of damping torque tends to result in a reduced damping ratio for oscillations. The simulation results in previous Figures show that the proposed damping control scheme is robust enough to operate under various system disturbances, interarea oscillation can be effectively damped, and the system settling time is greatly reduced.

6.3 Application of ST-WADC

ST-WADC has been applied in the four-machine system and ten-machine system, respectively. The two case-studies are given as follows:

6.3.1 Four-Machine/Two-Area System

6.3.1.1 Controller Design

For the conventional design as well as the proposed one, PSO is used to find the controller parameters which are listed in Table 6.7. These parameters are optimized for a time delay of $50\ ms$. Note that there is a new parameter introduced in the proposed scattering transformation design as shown in the table. After several runs, it has been figured out that the best range of scattering-parameter β is between 0.01 and 1. Selecting β value is very sensitive as it might destabilize the system.

Table 6.7: Optimized WADC parameters using PSO

Control Method	K	T_1	T_2	T_3	T_4	β
Conventional WADC	11.2219	1.0088	1.4732	1.6925	0.2787	------
Proposed ST-WADC	5.9503	0.9060	0.1231	2.0000	1.0964	0.084

To examine system performance, three-phase fault is applied at the mid of one of the tie-lines at bus 4, at $t = 1\ sec$ and cleared after 4 cycles. The simulation is done over a time horizon of $20\ sec$.

6.3.1.2 System Response without Delay

When there is no delay, the system response is presented in Figure 6.26 The response with or without scattering transformation is almost identical, in other word, the proposed ST-WADC provides the same damping characteristic with conventional WADC. That means

scattering control hasn't alter system properties when there is no delay (ideal control action). In fact, the proposed controller has acted as a conventional WADC, which indicate that scattering transformation impact has diminished and the two-scattering transformation-ports have canceled each other.
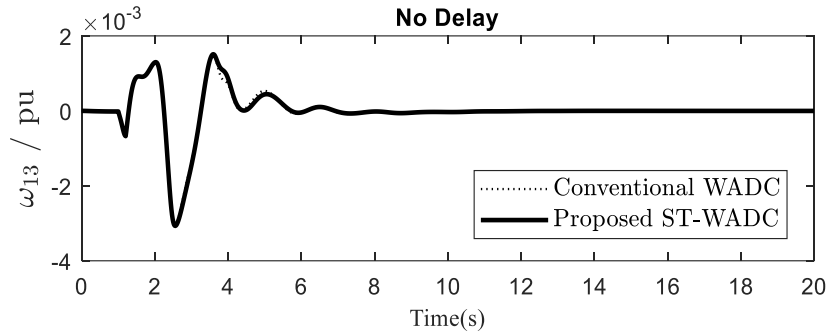
Figure 6.26. System interarea oscillations when there is no delay

6.3.1.3   System Response with Fixed Latency

When delay is introduced, the interarea oscillation is well-damped using the proposed ST-WADC and the system is perfectly stabilized and able to attenuate the oscillations greatly compared to Conventional WADC under the same fault conditions. The performance has been tested under various round-trip delay values with equally backward and forward delays $(T_{D1} = T_{D2} = T/2$, where T is the total time delay). The values of $T = 100\ ms, 200\ ms, 300\ ms, 400\ m$s, and $500\ ms$). As shown in Figure 6.27 the proposed controller can handle large delays and withstand the oscillation unlike the conventional one. As the communication latency gets larger, the performance became rather poor, and the system failed to tolerate the oscillations. Furthermore, system oscillations grew and cause a loss of synchronism between generators and eventually result in system collapse, as shown in Figure 6.27 (d). This result confirms that ST-WADC is robust enough to handle large delays with less conservativeness and less sensitivity to these kinds of delays. The

77

proposed controller outperformed the conventional method in term of settling time and maximum overshoot. Moreover, the time delay effect has slightly appeared in the signals response. The proposed ST-WADC guarantees the delay-independent stability and shows less sensitivity to time delay unlike the conventional PSS-WADC.
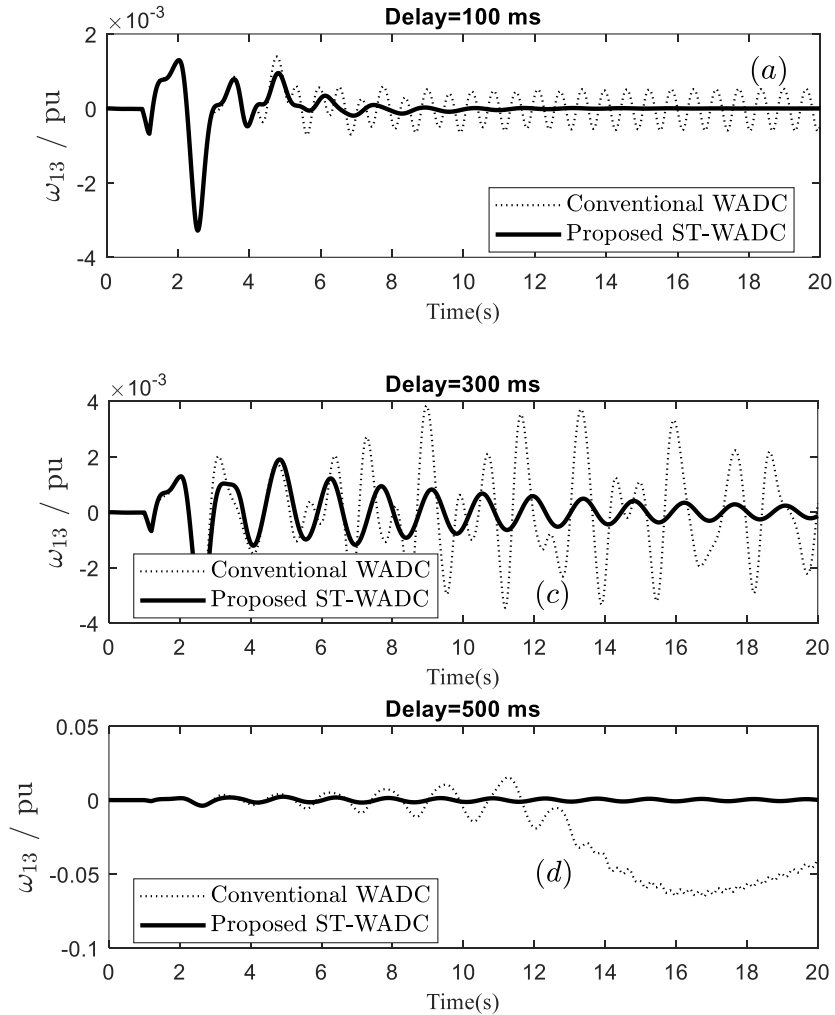
Figure 6.27. Speed deviation response due to three-phase fault with different values of fixed delays

Since all the measured feedback signals are time stamped by PMUs, i.e., the exact signal transmission time is recorded, then, the latency can be computed if the local time at the controller location is available. It's worth to mention that communication latency is not

usually constant, due to some factors such as communication loading, this may cause a delay uncertainty, which should be considered in our design as well. Although the proposed control method has considered constant delays, however, time-varying delays could be tested just to examine the robustness of the controller against feed-back signals latencies with different levels. Here, the control signal is assumed to have a total delay comprised of the fixed delay in addition to a random value. This value has been taken arbitrarily to represent variable time delay, say $200 \pm rand(100)\ ms$ as given in Figure 6.28.
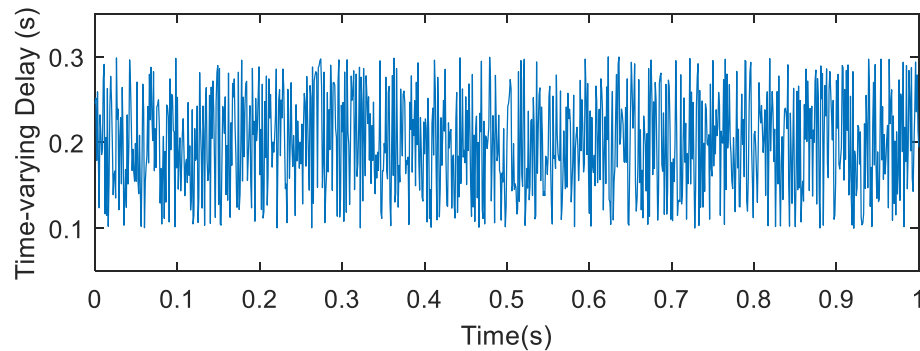
Figure 6.28.   Variable delay in the wide-area signal

Figure 6.29 shows the dynamic system response in the presence of large random communication delays. The effectiveness of the proposed controller is verified by a comparative study between the proposed scheme and another delay-dependent controller in ref [81], considering random delays. As shown in Figure 6.29 it is clear that the performance of ST-WADC is better than the delay-dependent controller in term maximum overshoot and settling-time of the rotor speed deviation signal for different delay values except for time delay of $100\ ms$, for which its observed that the delay dependent controller would outperform. However, when the delay increases, the Preference will be for the proposed controller.

For the conventional design as well as the delay-dependent controller, as the latency increases, the system performance gets worse and totally collapse at $500 \pm 100\ ms$ delay. The proposed WADC is able to preserve system stability for the same delay values. The robustness of ST-WADC is verified against wide-area signal delay that suffers from uncertainty.
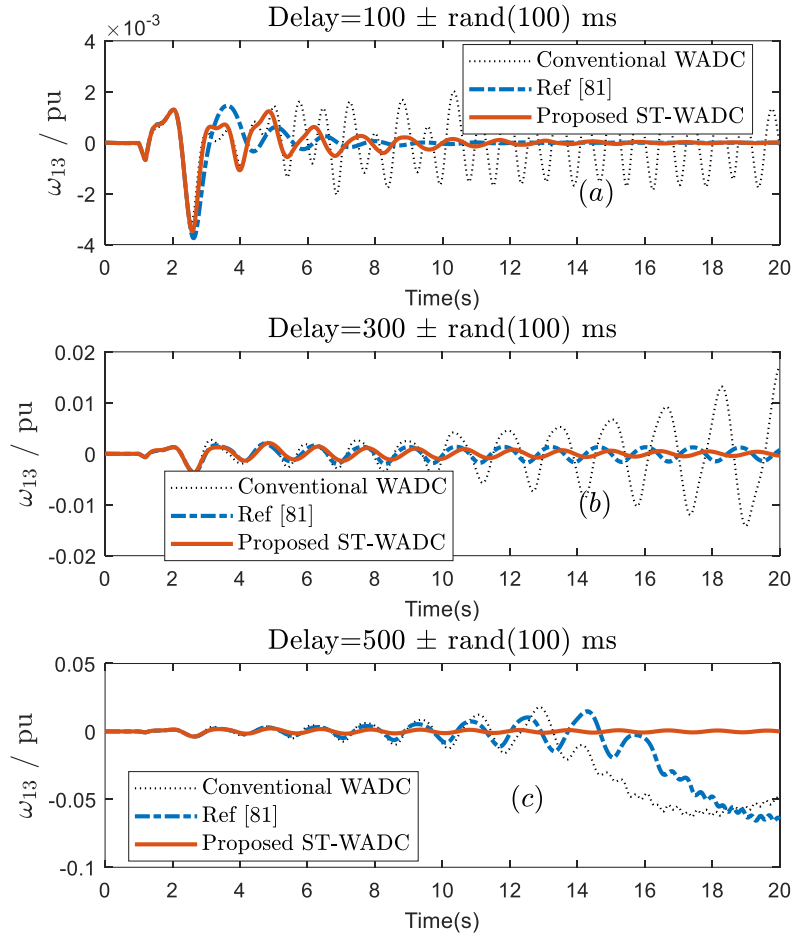
Figure 6.29. Speed deviation response due to three-phase fault with different values of time-varying delays

The state-space representation of the controller designed in ref [81] is:

$$Ak = \begin{pmatrix} -7.032 10^{-10} & -3.665 10^{-7} & -6.41 10^{-6} & -9.356 10^{-6} & 9.012 10^{-6} & 2.297 10^{-6} \\ -6.86 10^{-6} & -7.589 & -9.024 & -15.58 & 16.72 & 4.272 \\ 8.892 10^{-6} & 18.35 & -8.796 & 0.7411 & -8.388 & 0.5876 \\ 7.317 10^{-6} & 12.81 & -2.718 & -1.226 & 2.21 & 0.5985 \\ -5.538 10^{-6} & -12.21 & 12.36 & 0.9454 & -2.38 & -3.176 \\ -2.985 10^{-6} & -2.714 & -6.932 & -2.731 & 5.502 & -9.639 \end{pmatrix}$$

$$Bk = \begin{pmatrix} -9.104 10^{-6} \\ -1.418 \\ -36.34 \\ -11.74 \\ 14.6 \\ -13.6 \end{pmatrix}$$

$$Ck = \begin{pmatrix} -1.012 10^{-5} & -22.58 & 19.04 & -1.056 & 0.315 & 16.12 \end{pmatrix}$$

$$Dk = 57.71$$

Where A_k, B_k, C_k and D_k are the controller state-space matrixes.

6.3.1.4   Performance Index Evaluation

In order to compare the performance of the proposed approach with other methodologies, the following integral of time absolute error (ITAE) performance index is used:

$$ITAE = \int_0^{t_{sim}} t \left(\sum_{i=1}^{n} \sum_{j=1}^{n} |\Delta \omega_{i,j}| \right) . dt , i \neq j \tag{6.9}$$

where n is the number of generators, t_{sim} the time period of simulations and $\Delta \omega$ is the deviation between two different generators $(\omega_i - \omega_j)$. Note that the low value of performance index indicate that this response is relatively better. Here, the performance indexes have been calculated under the same previous fault conditions as shown in Table 6.8. It can be seen that the lowest ITAE value corresponds to ST-WADC for all delay

values (except for $100 \pm 100\ ms$ for which the delay-dependent controller is better), which indicate that this controller offers the best performance among others.

Table 6.8:   Comparative studies between different controllers under a three-phase fault for different values of fixed and random delays

	Fixed Delay			Random Delay		
	$100\ ms$	$300\ ms$	$500\ ms$	$100 \pm 100\ ms$	$300 \pm 100\ ms$	$500 \pm 100\ ms$
Conventional WADC	4.8793	23.9060	1.2917	73.3146	155.4339	139.39
Proposed ST-WADC	0.9439	4.7748	0.0085	21.0753	13.0017	2.02
Ref [81]	------	------	------	1.2237	19.4501	75.14

6.3.2   New England 39-bus Test System

To further explore the effectiveness of the proposed strategy, another study has been conducted. The controller has been implemented in New England 39-bus 10-machine test system shown in Figure 6.17. The model is built in MATLAB/SIMULINK software along with the classical lead-lag structure and the two scattering-ports.

6.3.2.1   Controller Design

The controller is placed in G5 whereas the input the active power deviation of the transmission line between bus 15 and bus 16 (ΔP_{15-16}) is selected as remote-area feed-back signal for ST-WADC. The parameters of the conventional controller and the proposed one has been searched for using PSO algorithm considering nominal communication delay of $100\ ms$. The optimized parameters are given in Table 6.9.

Table 6.9: Optimized WADC parameters via PSO

Control Method	K	T_1	T_2	T_3	T_4	T_5	T_6	β
Conventional WADC	6.2111	0.3714	0.6769	0.6881	1.0839	1.6034	0.3877	------
Proposed ST-WADC	5.5913	0.2574	1.3559	0.9392	0.4527	1.0564	0.2720	0.5081

For gathering the best cost function minimization, the program has been run several times in order to get the best parameters bounds. In this case study, its recommended to have β in the range between 0.01 and 10.

The constrains for K_s, T_1, T_2, T_3 and T_4 are given equation (5.12.The bounds of T_5 and T_6 is $[0.01 - 2]$. To test the efficacy of the proposed approach, nonlinear time domain simulation has been carried out. A three-phase-to-ground fault is applied between line 3 and 4 near bus 3 at $t = 0.5s$ and cleared after 4 cycles. a large change in operating mode is introduced, since this line-in particular- is so stressed compared with other lines. The simulation is carried out over a time horizon of $20 \, sec$. Furthermore, a white noise of $\pm 0.06 \, p.u.$ has been inserted into the wide-area signal, since measurement imperfections always exists, to demonstrate how the proposed controller would act in real-world scenarios

6.3.2.2   System Response without Delay

In no-delay case, the response of active power deviation of line 15 to 16 (ΔP_{15-16}) due to three-phase fault is presented in Figure 6.30, to represent the oscillatory system behavior taking this stressed line as a sample. Similar to previous case study, there is no quite differences in interarea oscillations damping performance between the Conventional designed WADC and the proposed ST-WADC.
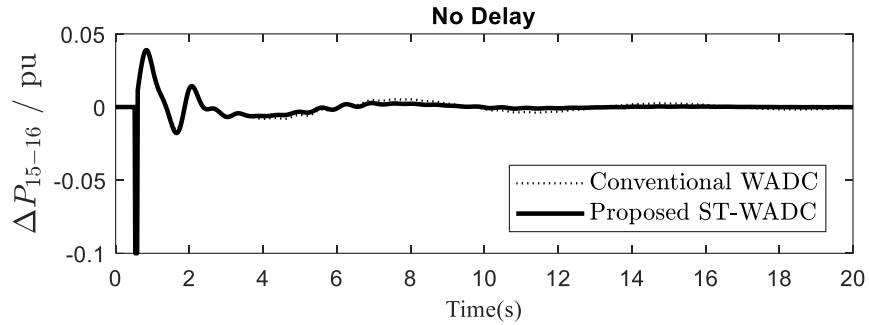
Figure 6.30. System interarea oscillations when there is no delay

6.3.2.3   System Response with Fixed Latency

Active power responses for various communication delay values under the same fault conditions are shown in Figure 6.31. It can be seen that the conventional design is able to control the oscillations till the delay reach a value of $1200\,ms$ then the system failed to tolerate the oscillations and eventually breakdown. Note that the conventional design has been originally designed to compensate for time delays as well. Another thing can be observed from the figures is that ST-WADC has offer a greater delay-compensation ability compared to the classical one and it can provide the desired interarea oscillations damping characteristic for different values of latencies.

84
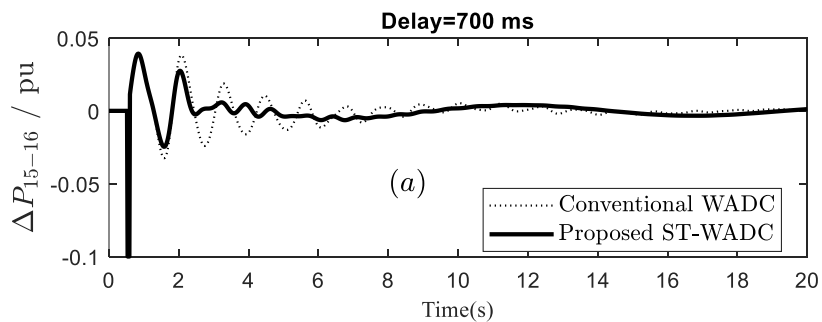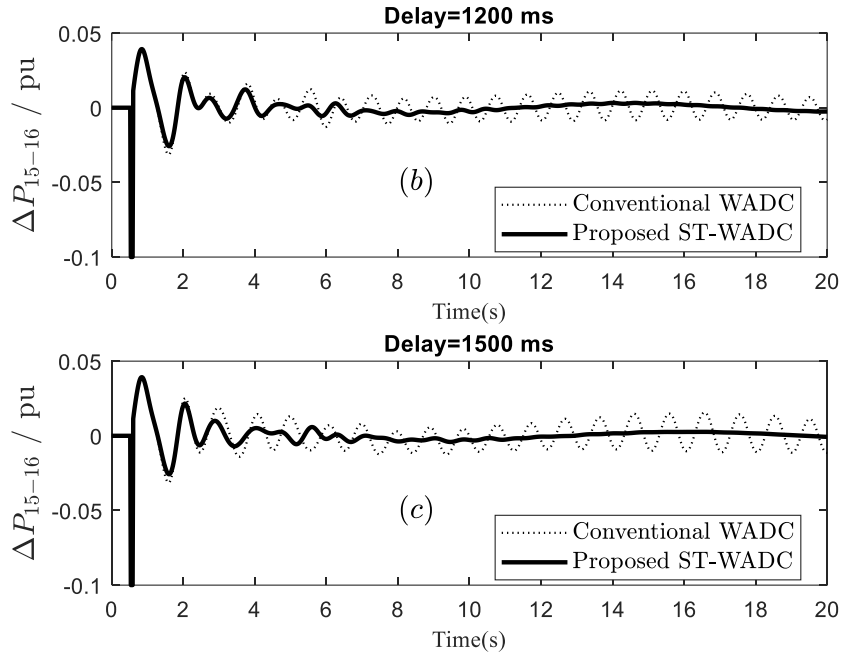
Figure 6.31. Line Power deviation response due to three-phase fault with different values of fixed delays

6.3.2.4 System Response with Random Latency

When Variable random delays are included, the active power response is presented in Figure 6.32, the same random delay described in Figure 6.28. is used in this section as well. its revealed that the proposed damping control scheme is robust enough to operate under severe system disturbances. Interarea oscillations have been effectively damped, and the system settling time is greatly reduced. The response indicate that the proposed approach has the ability to maintain system stability and ensure a satisfactory robustness with communication latency uncertainty. Whereas the conventional tuned WADC cannot effectively damp out the oscillations with the presence of random delays. It's found that when latency value is less than $1000\,ms$ the conventional controller can act well. However, when this value exceeds $1200\,ms$ the conventional control methodology cannot handle it, and a clear degradation of control performance can be observed. Whereas the proposed ST-WADC is able to handle this situation appropriately. That's means the

conventional WADC has less delay-compensation capability compared with ST-WADC which can compensate for latency perfectly and keep the desired damping characteristic.

6.3.2.5 Performance Index Evaluation

For a clear insight of the controller performance, an index-based comparison has been conducted. The same index given in equation (6.9) is used. The lower index indicates the best performance. The values of the indices are presented in Table 6.10. Its observed that the proposed controller gives the lower indices for various delay values, and thus, a significant damping improvement is observed via ST-WADC.

Table 6.10: Comparative studies between different controllers under a three-phase fault for different values of fixed and random delays

	Fixed Delay			Random Delay		
	700 ms	**1200 ms**	**1500 ms**	**700 $\pm$ 100 ms**	**1200 $\pm$ 100 ms**	**1500 $\pm$ 100 ms**
Conventional WADC	133.08	124.54	96.0080	154.70	135.86	109.3465
Proposed ST-WADC	98	56	2.5896	11.76	76	2.8716
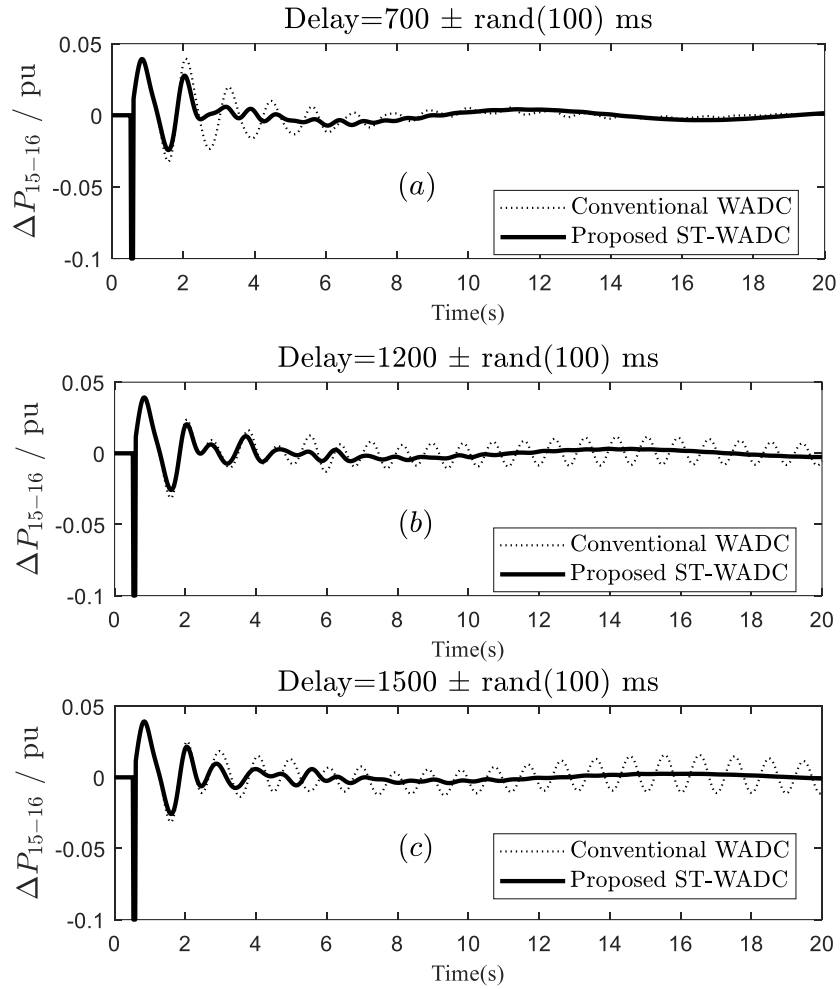
Figure 6.32. Line Power deviation response due to three-phase fault with different values of Variable delays

6.3.3 Optimization of Beta only

In previous part, the controller design has been formulated as an optimization problem whereas the lead-lag compensator parameters have been tuned along with scattering parameter β. In this part the same parameters that has been tuned in the conventional design will be taken as its, while β will be tuned alone. Table 6.11 shows the optimized parameters in each case. The system performance is shown in Figure 6.33 and Figure 6.34

Control Method	K	T_1	T_2	T_3	T_4	β
Conventional WADC	11.2219	1.0088	1.4732	1.6925	0.2787	------
ST-WADC (β only)	11.2219	1.0088	1.4732	1.6925	0.2787	0.1404
ST-WADC (all parameters)	5.9503	0.9060	0.1231	2.0000	1.0964	0.084
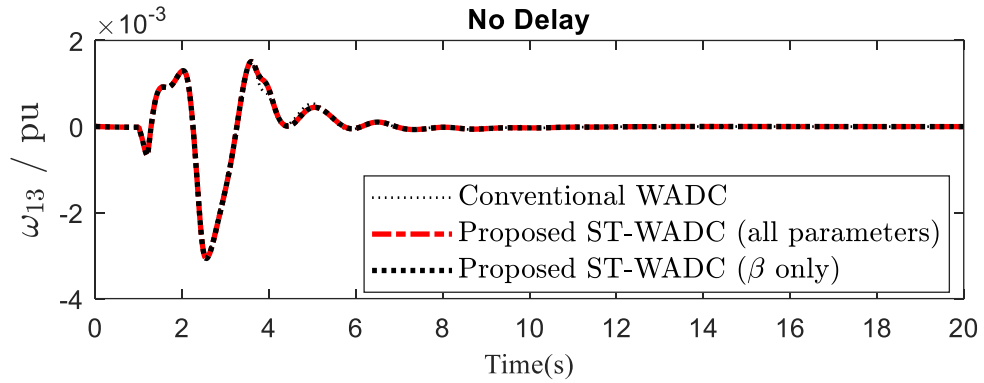
Figure 6.33. System performance when there is no delay

88
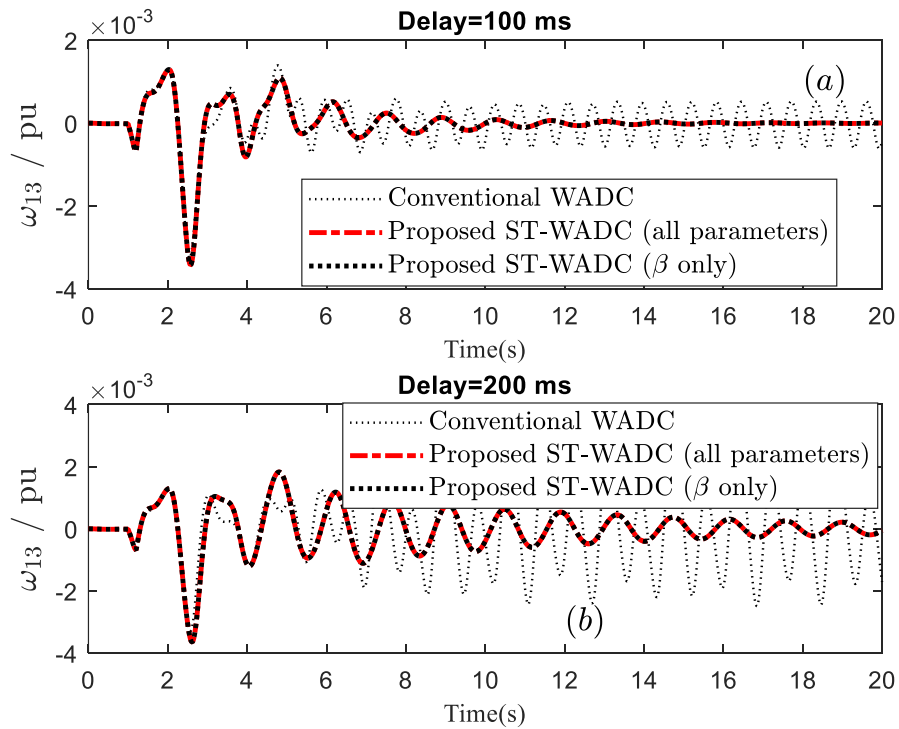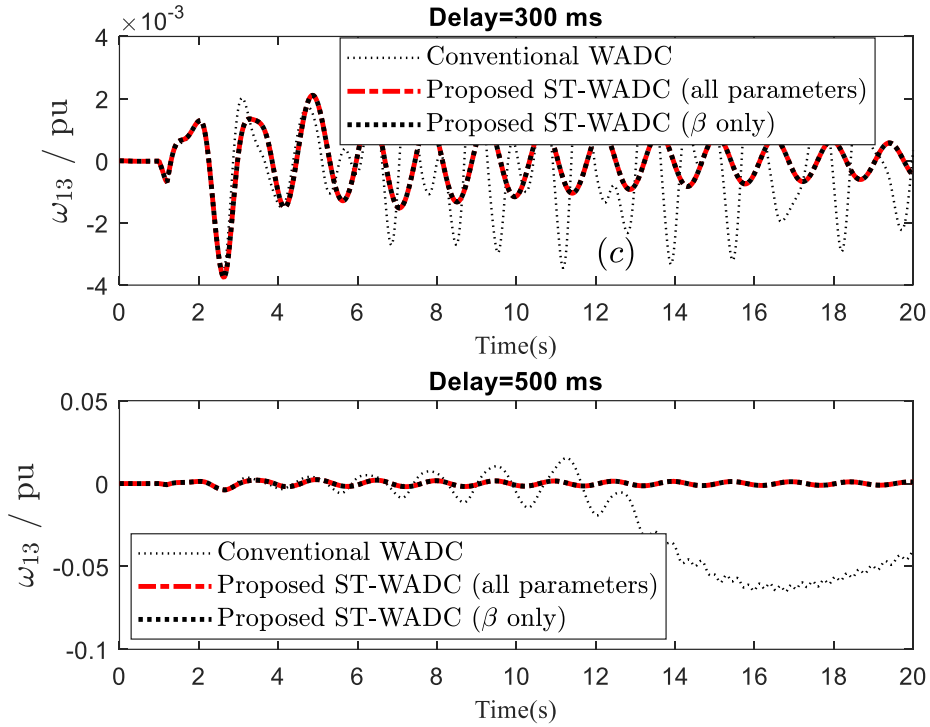
Figure 6.34. System performance in (a) 100 ms (b) 200 ms (c) 300 ms (d) 500 ms

6.3.4 Controller Computation Time

In this part, the time taken by the central processing unit (CPU) on a laptop (Intel Core i5 2.6 GHz, 8-GB RAM) to execute the program is measured by using the *'tic'* and *'toc'* function. **tic** starts a stopwatch timer to measure performance. The function records the internal time at the code execution and display the elapsed time with the **toc** function. **toc** reads the elapsed time from the stopwatch timer started by the **tic** function. Table 6.12. shows the elapsed time by using different controllers.

Table 6.12. Elapsed time for different control methods

Control Method	*Elapsed Time* (s)
Conventional WADC	7.21023
ST-WADC (β only)	3.71892
ST-WADC (all parameters)	3.64092

6.3.5 Advantages of ST-WADC

The simulation results have shown how the proposed ST-WADC perform when communication delay imperfections are considered. The simplicity of the design and the efficacy of the performance offer ST-WADC the ability to outperform other delay-dependent approaches which are complex and require more computation time, and this might be of the interest of various real-world applications. This control methodology however requires only the time of parameters computation and the results are further satisfactory. One of the main benefits of this control methodology over small-gain methodologies is that it does not require a prior knowledge of time-delay value to define the design objectives.

6.4   Summary

In this chapter, the design LQG-WADC is presented. The design is validated through small signal analysis and time domain simulation in MATLAB software. In pursuit of better control performance, the selection of controller inputs (feedback signals) is based on modal residues. Modal analysis has proved the effectiveness of the designed controller to suppress the interarea modes and improve it effectively under multiple nominal and off-nominal operating conditions. Eventually, a novel scattering transformation-based wide-area damping controller. The main objective is to design a controller that is able to suppress the system oscillations while compensating for the signals communication delay either fixed or time-varying delay. To resolve the destabilizing effect of the communication latency, scattering transformation is inserted in form of two ports between the power system and WADC.

CHAPTER 7

REAL-TIME SIMULATION

7.1   Introduction

This chapter illustrates an experimental validation of the proposed ST-WADC design on RTDS (real time digital simulator). It has a significant feature over traditional simulation software such as MATLAB and PSCAD/EMTDC which is "online hard real-time simulation". This allows RTDS to be interfaced with power system hardware equipment, such as commercial relay and external controller in real-time. Compared with conventional simulation packages, RTDS is computationally faster, time-saving and more accurate. It is a super computer that performs real-time simulation using parallel computation. It is capable of performing time-domain simulation at real-time speed using time steps less than 50 microseconds. Such fast computation let RTDS able to simulate power system phenomena in the range of 0 to 3 kHz with high accuracy and reliability.

RTDS consists of custom hardware and software, specifically designed to perform real time electromagnetic transient simulations. The hardware is bundled into modular units called racks that allow easy expansion of the simulator's computing capability as required. The RTDS software is the link to the simulator hardware. The main elements of the software are the graphical user interface (GUI), RSCAD and the libraries of power and control system component models. RSCAD represents a family of software tools consisting of individual modules that accomplish the different tasks involved in operating the

91

simulator. Through RSCAD, simulation projects and cases can be organized and shared. RSCAD has the ability to; assemble circuit diagrams using predefined or user-defined power and control system component models; automate or interact with simulator operation to analyze and post-process simulation results. So, power system network to be simulated is constructed RSCAD. This software has a large library containing many power system component and control models. The RSCAD software has different models, the main two modules are; draft and run-time. The draft module is used for building the network and parameters entry. The run-time module is used to control the operation of RTDS. Using run-time, user can perform a lot actions; such as starting and stopping of simulation, initiating system disturbances, changing some of the system set points, on-line monitoring and measuring of power system quantities, and other control functions.

The RTDS is currently applied to many areas of development, testing and a lot of studies such as; protection and control system, general AC and DC system operations and behavior, feasibility studies, and for demonstration and training purposes.

Due to the limited number of racks (modular units that allow easy expansion of the simulator's computing capability as required) in the laboratory (only 2 racks), this work will not involve Ten-machine system in RTDS, therefore, the simulation is carried out in Two-area system only.

To test the effectiveness of the proposed control strategy, experimental work has been performed in a hardware platform. The experimental setup is shown in Figure 7.1 the proposed ST-WADC is built in d-SPACE/DS1103, while RTDS is used to simulate the rest of the plant. The digital signals are transmitting back and forth between RTDS-RACK

and d-SPACE board through their input/output ports. The dSPACE library should be-first-interfaced with MATLAB/SIMULAINK library, then certain blocks can be used for signal sending and receiving from DS1103 board. After implementing the controller in MATLAB/SIMULAINK, it is downloaded to the d-SPACE processor using (**Build Model**) command and then the controller is ready to be used.
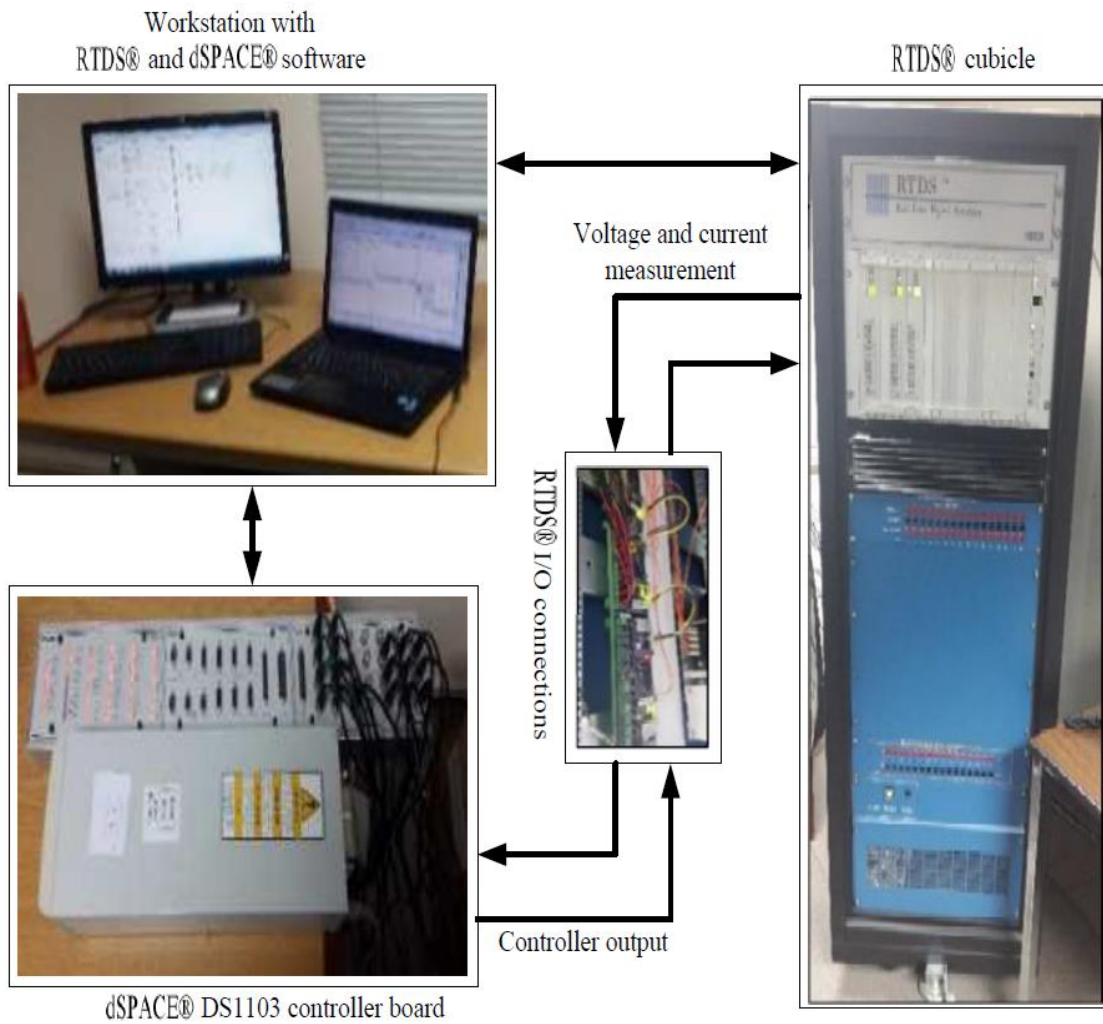
Figure 7.1. Experimental setup

7.2   Application on Two-Area Four-Machine system

Similar to MATLAB simulation, here, same system in built in RTDS, modal analysis including participation factor calculation and residues analysis are well-elaborated in chapters 3 and 6.

Figure 7.2 shows graphical representation of the two-area power system Run-time module. This representation gives flexibility and easy interface with the system and allowed the user to select different form of results, such as numerical values, trends, plots, meters and other measurements display means. On-line flow of MW and MVAR can be shown also on each branch of the circuit.

To run the simulation, the circuit built in the previous section needs to be compiled first from RSCAD/Draft and then the case can be load into RSCAD/Run-time module. Run-time is used to control the simulation case being performed on the RTDS hardware. Simulation control; including start/stop commands, set point adjustment, fault application, etc. are performed through the Runtime Operator's Console. Additionally, meters and plots can be created to monitor various system quantities such as bus voltages, line currents, generators rotor speed, generators power output, etc.

The system is exposed to large disturbance represented by three-phase fault located in one of the lines connecting bus 4 and bus 5, the fault starts at t=1, and last for 4 cycles. Figure 7.3 to Figure 7.7 show the system response in real-time.
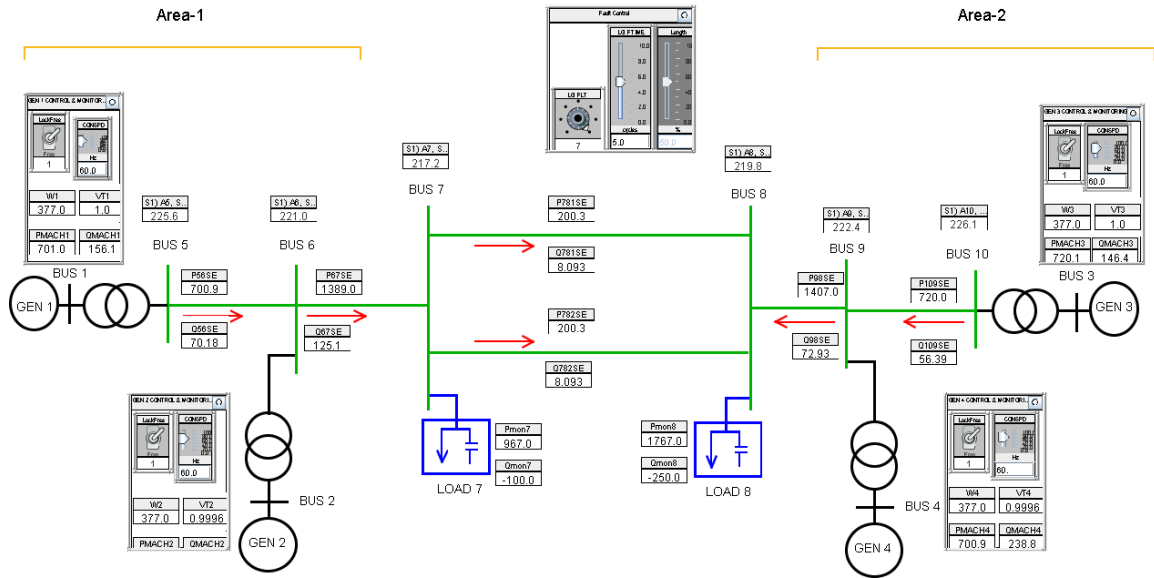
Figure 7.2. Two-area power system represented graphically at run-time
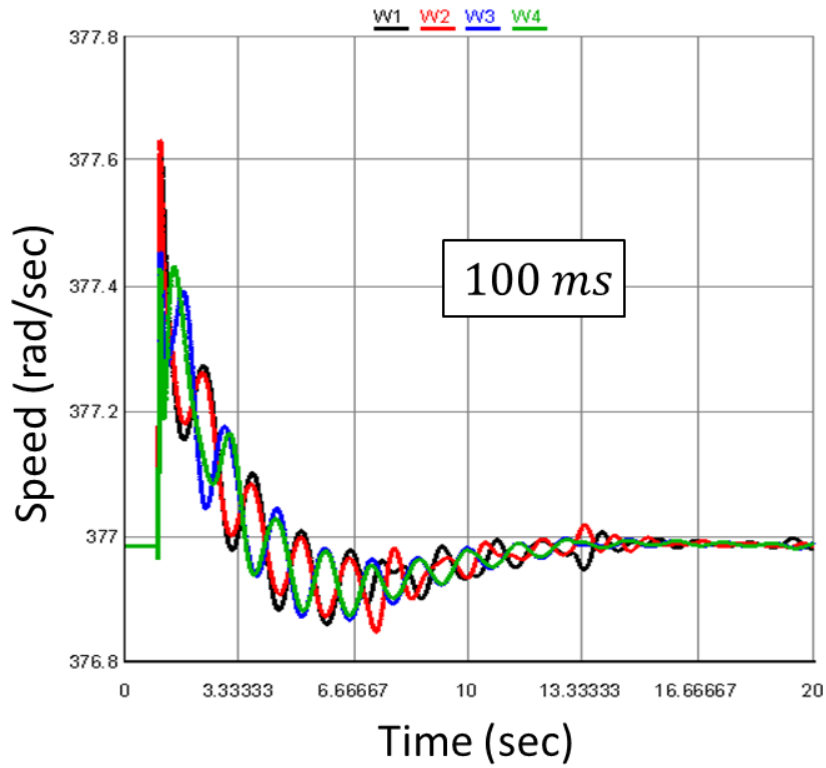
Figure 7.3. Machines speed without ST-WADC under 100 ms delay

95
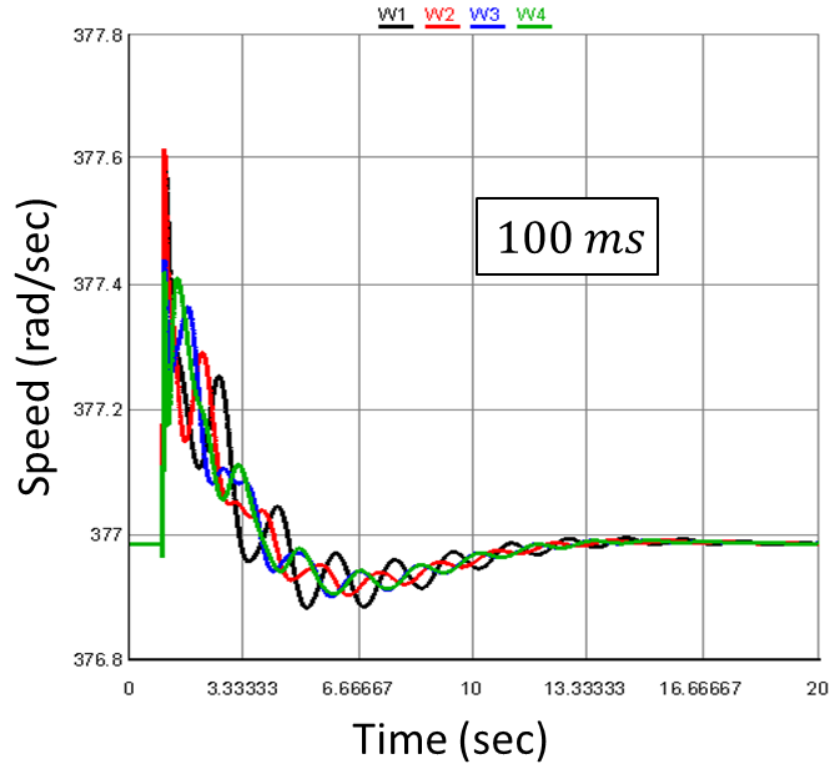
Figure 7.4. Machines speed with ST-WADC under 100 ms delay
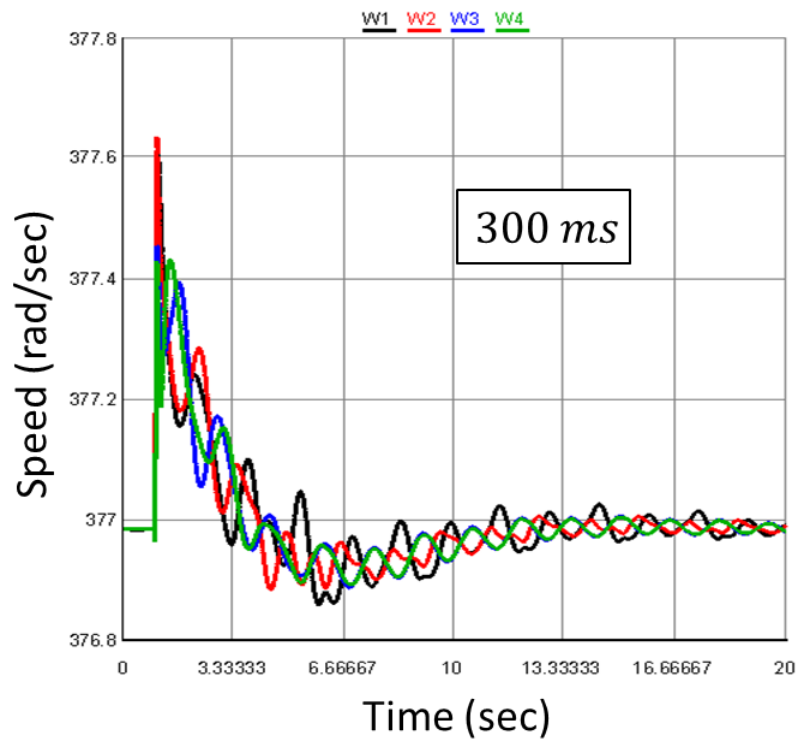
Figure 7.5.   Machines speed without ST-WADC under 300 ms delay

96
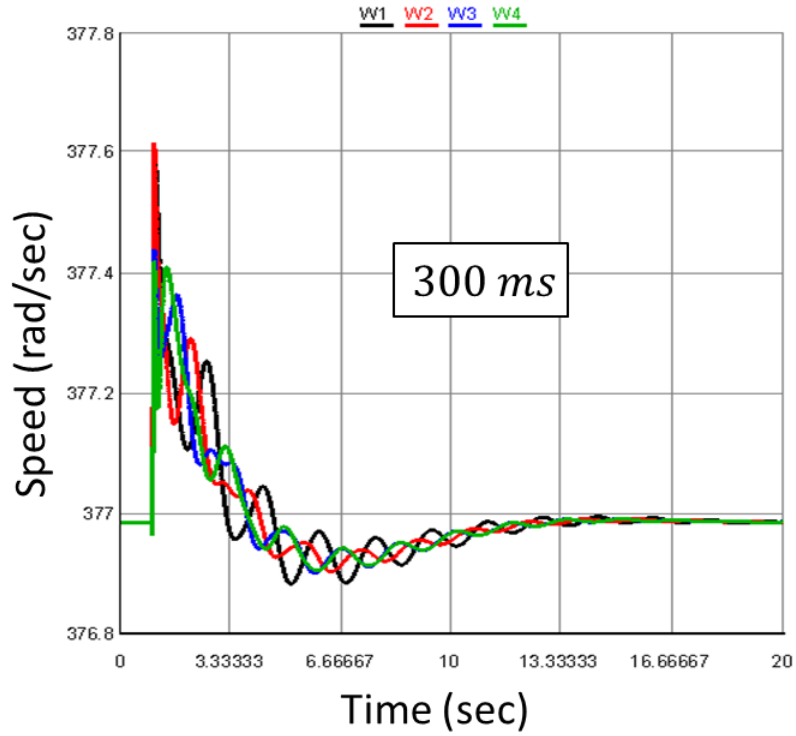
Figure 7.6. Machines speed with ST-WADC under 300 ms delay
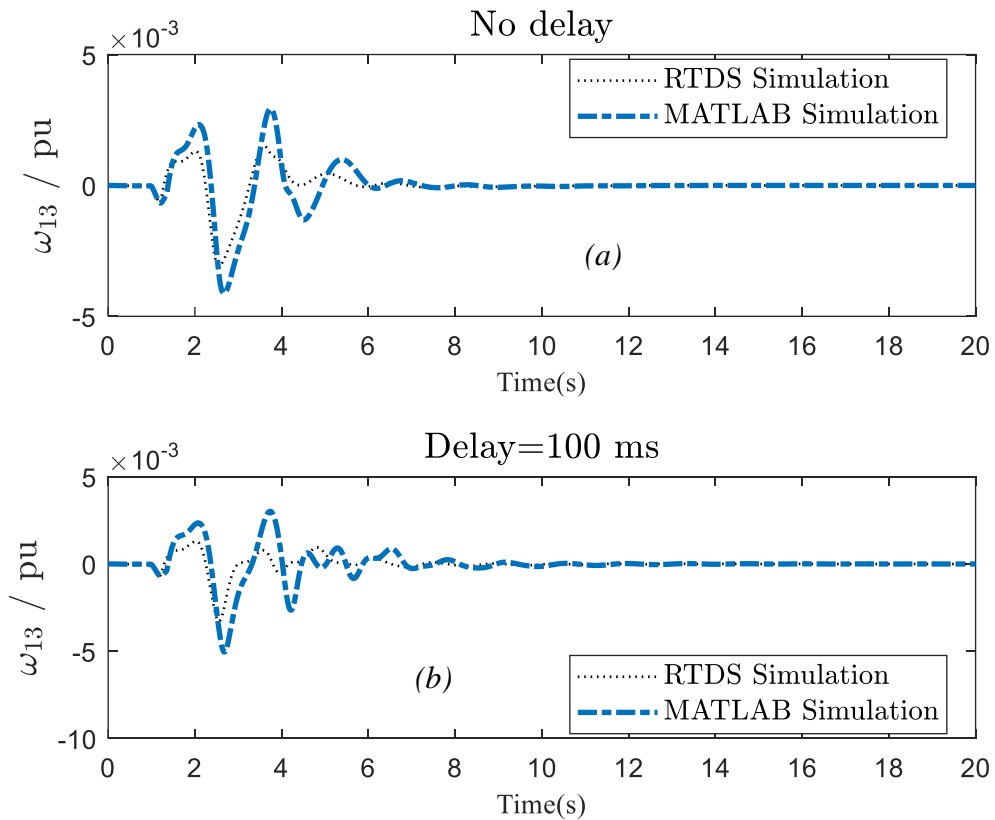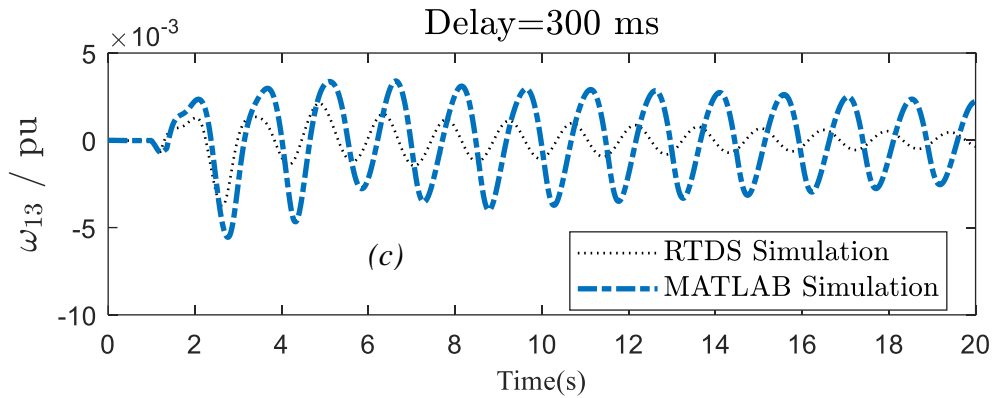
Figure 7.7. Comparison between MATLAB and RTDS results in (a) No delay (b) 100 ms (c) 300 ms

7.3   Summary

This chapter addresses the real-time implementation of the proposed ST-WADC based wide area controller via RTDS. The designed system has been modeled using RSCAD software, and the controller has been built in d-SPACE board. Each component modeled dynamically using either IEEE standard models or different standard that's available in the RSCAD library. Eventually, comparison between MATLAB and RTDS results has been carried out. System response shows an acceptable mismatch between both MATLAB and RTDS results.

CHAPTER 8

CONCLUSION & FUTURE WORK

8.1　Conclusion

Interarea oscillation has the potential to deteriorate power system stability, furthermore, reliability and security, and its known as a major reason of many famous blackouts worldwide. In this work, a design of a new wide-area control scheme based on linear quadratic gaussian theory in discussed. The controller performance with respect to interarea oscillations at different locations is evaluated through residue analysis. The designed controller is tested in two study systems. Linear analysis in addition to MATLAB nonlinear simulation as well as some experimental work, has demonstrated the capability of the proposed controller to effectively handle multiple system disturbances in multiple operating conditions, and it was robust enough to eradicate the system oscillations perfectly. Some notes could be reported from the simulation results, summarized as follows:

- Geometric measures of controllability/observability are used to select the best controller locations and the best feedback signals.
- Tie-line active powers in addition to speed signals are considered as a potential stabilizing signals candidate with respect to interarea modes.
- for small scale power network such as two-system, one signal might be enough to be taken as a wide area control signal. However, in large scale systems such as ten

machine systems, it's anticipated to have multiple stabilizing signals for an acceptable control performance.

- The centralized LQG based wide area controller shows good results which cannot be produced based only on the local decentralized controllers.

- In this work, a new WADC design is proposed based on scattering transformation with unknown time latency. The proposed controller is capable to improve the damping of interarea oscillations as well as providing active compensation of communication latencies in feedback control signals. The proposed ST-WADC is a conventional lead-lag controller tuned via particle swarm optimization (PSO) algorithm. The proposed method is successfully applied to two different multi-machine power systems. Simulation studies are conducted in MATLAB/SIMULINK to demonstrate the efficiency of the proposed control strategy.

8.2   Future Work

Even thought, the proposed method has shown auspicious results, however, its early to end this work in this point, some aspects that might be considered in future for further study are presented as follows:

- FACTS devices based on wide area measurements: the research could be extended to design a wide-area controller that provides the control signal to a FACTS device instead of providing the signals through generator excitation system. By using this

approach, it's expected to have more damping, thus, those devices are used to control line power flow.

- Time delay: due to many factors such as communication process, transmission, and wide-area signals synchronization, usually a time delay will take place, and thus could lead to inaccurate synchronization as well as some stability issues, so, it's needed to be considered by researchers in the control design.

- Using a decentralized control (distributed control) scheme could lead to less time-delays and less hardware equipment.

- Design of a systematic way of wide-area controller parameters tuning, instead of using linear control techniques which deal with a certain operating condition.

- In future, fault identification and isolation using wide-area measurements could be done, to gain an efficient way of faults detection.

- The future research may focus on the design of double fed induction generator-based ST-WADC (DFIG-ST-WADC) to improve system dynamic behavior through feeding the remote signal to rotor side-convertor of DFIG while considering large control signal delays.

APPENDIX A

This Appendix represents the Two-area system data

A.1 Machines Data

Gen.	D	H (MW.s /MVA)	Xd (pu)	Xq (pu)	X'd (pu)	X'q (pu)	T'do (s)	T'qo (s)	KA	TA
1	0	55.575	0.2	0.19	0.033	0.061	8	0.4	200	0.01
2	0	55.575	0.2	0.19	0.033	0.061	8	0.4	200	0.01
3	0	58.5	0.2	0.19	0.033	0.061	8	0.4	200	0.01
4	0	58.5	0.2	0.19	0.033	0.061	8	0.4	200	0.01

A.2 Bus Data

Bus no.	Type	Voltage (pu)	Angle	Generation P (MW)	Generation Q (MVAR)	Load P (MW)	Load Q (MVAR)
1	1	1.03	0	0	0	0	0
2	2	1.01	0	700	0	0	0
3	2	1.03	0	719	0	0	0
4	2	1.01	0	700	0	0	0
5	3	1.00	0	0	0	0	0
6	3	1.00	0	0	0	0	0
7	3	1.00	0	0	0	967	100
8	3	1.00	0	0	0	1767	250
9	3	1.00	0	0	0	0	0
10	3	1.00	0	0	0	0	0

A.3 Transmission Lines Data

Line no.	From	To	R	X	B
1	1	5	0	0.0576	0.00
2	2	6	0	0.0625	0.00
3	3	10	0	0.0586	0.00
4	4	9	0	0.0850	0.088
5	5	6	0.0025	0.025	0.021875
6	6	7	0.001	0.01	0.00875
7	7	8	0.011	0.11	0.385
8	8	9	0.001	0.01	0.00875
9	9	10	0.0025	0.025	0.021875

APPENDIX B

This Appendix represents the Ten Machine system data

B.1 Machines Data

Machine Number	1	2	3	4	5	6	7	8	9	10
Bus Number	39	31	32	33	34	35	36	37	38	30
Base MVA	1000	1000	1000	1000	1000	1000	1000	1000	1000	1000
x_l *(pu)*	0.0300	0.3500	0.3040	0.2950	0.5400	0.2240	0.3220	0.2800	0.2980	0.125
r_a *(pu)*	0	0	0	0	0	0	0	0	0	0
x_d *(pu)*	0.2	2.95	2.495	2.62	6.7	2.54	2.95	2.9	2.106	1
x'_d *(pu)*	0.06	0.697	0.531	0.436	1.32	0.5	0.49	0.57	0.57	0.31
x''_d *(pu)*	0.01	0.01	0.01	0.01	0.01	0.01	0.01	0.01	0.01	0.01
T'_{do} *(sec)*	7	6.56	5.7	5.69	5.4	7.3	5.66	6.7	4.79	10.2
T''_{do} *(sec)*	0.003	0.003	0.003	0.003	0.003	0.003	0.003	0.003	0.003	0.003
x_q *(pu)*	0.19	2.82	2.37	2.58	6.2	2.41	2.92	2.8	2.05	0.69
x'_q *(pu)*	0.08	1.7	0.876	1.66	1.66	0.814	1.86	0.911	0.587	0.08
x''_q *(pu)*	0.03	0.03	0.03	0.03	0.03	0.03	0.03	0.03	0.03	0.03
T'_{qo} *(sec)*	0.7	1.5	1.5	1.5	0.44	0.4	1.5	0.41	1.96	1.5
T''_{qo} *(sec)*	0.005	0.005	0.005	0.005	0.005	0.005	0.005	0.005	0.005	0.005
H *(sec)*	50	3.03	3.58	2.86	2.6	3.48	2.64	2.43	3.45	4.2
d_o *(pu)*	0	0	0	0	0	0	0	0	0	0
d_1 *(pu)*	0	0	0	0	0	0	0	0	0	0

B.2 Excitation System Data

T_r (sec)	K_A	T_A (sec)	T_b (sec)	T_c (sec)	V_t (pu)	E_{min}	E_{max}
0.01	200	0.015	10	1	1.03	-5	5
0.01	200	0.015	10	1	1.03	-5	5
0.01	200	0.015	10	1	1.03	-5	5
0.01	200	0.015	10	1	1.03	-5	5
0.01	200	0.015	10	1	1.03	-5	5
0.01	200	0.015	10	1	1.03	-5	5
0.01	200	0.015	10	1	1.03	-5	5
0.01	200	0.015	10	1	1.03	-5	5
0.01	200	0.015	10	1	1.03	-5	5
0.01	200	0.015	10	1	1.03	-5	5

B.3 Transmission Lines Data

Line No	From	To	R	X	B
1	2	0.0035	0.0411	0.6987	0
1	39	0.001	0.025	0.75	0
2	3	0.0013	0.0151	0.2572	0
2	25	0.007	0.0086	0.146	0
2	30	0	0.0181	0	1.025
3	4	0.0013	0.0213	0.2214	0
3	18	0.0011	0.0133	0.2138	0
4	5	0.0008	0.0128	0.1342	0
4	14	0.0008	0.0129	0.1382	0
5	8	0.0008	0.0112	0.1476	0
6	5	0.0002	0.0026	0.0434	0
6	7	0.0006	0.0092	0.113	0
6	11	0.0007	0.0082	0.1389	0
7	8	0.0004	0.0046	0.078	0
8	9	0.0023	0.0363	0.3804	0
9	39	0.001	0.025	1.2	0
10	11	0.0004	0.0043	0.0729	0
10	13	0.0004	0.0043	0.0729	0
10	32	0	0.02	0	1.07
12	11	0.0016	0.0435	0	1.006
12	13	0.0016	0.0435	0	1.006
13	14	0.0009	0.0101	0.1723	0
14	15	0.0018	0.0217	0.366	0
15	16	0.0009	0.0094	0.171	0
16	17	0.0007	0.0089	0.1342	0
16	19	0.0016	0.0195	0.304	0
16	21	0.0008	0.0135	0.2548	0
16	24	0.0003	0.0059	0.068	0
17	18	0.0007	0.0082	0.1319	0
17	27	0.0013	0.0173	0.3216	0
19	33	0.0007	0.0142	0	1.07
19	20	0.0007	0.0138	0	1.06
20	34	0.0009	0.018	0	1.009
21	22	0.0008	0.014	0.2565	0
22	23	0.0006	0.0096	0.1846	0
22	35	0	0.0143	0	1.025
23	24	0.0022	0.035	0.361	0
23	36	0.0005	0.0272	0	1
25	26	0.0032	0.0323	0.513	0
25	37	0.0006	0.0232	0	1.025

26	27	0.0014	0.0147	0.2396	0
26	28	0.0043	0.0474	0.7802	0
26	29	0.0057	0.0625	1.029	0
28	29	0.0014	0.0151	0.249	0
29	38	0.0008	0.0156	0	1.025
31	6	0	0.025	0	1

B.4 Bus Data

Bus no.	Type	Voltage (pu)	Angle	Generation		Load	
				P (MW)	Q (MVAR)	P (MW)	Q (MVAR)
1	3	1.048	-9.43	0	0	0	0
2	3	1.0505	-6.89	0	0	0	0
3	3	1.0341	-9.73	0	0	3.22	0.024
4	3	1.0116	-10.53	0	0	5	1.84
5	3	1.0165	-9.38	0	0	0	0
6	3	1.0172	-8.68	0	0	0	0
7	3	1.0067	-10.84	0	0	2.338	8.4
8	3	1.0057	-11.34	0	0	5.22	1.76
9	3	1.0322	-11.15	0	0	0	0
10	3	1.0235	-6.31	0	0	0	0
11	3	1.0201	-7.12	0	0	0	0
12	3	1.0072	-7.14	0	0	0.085	0.88
13	3	1.0207	-7.02	0	0	0	0
14	3	1.0181	-8.66	0	0	0	0
15	3	1.0194	-9.06	0	0	3.2	1.53
16	3	1.0346	-7.66	0	0	3.294	3.23
17	3	1.0365	-8.65	0	0	0	0
18	3	1.0343	-9.49	0	0	1.58	0.3
19	3	1.0509	-3.04	0	0	0	0
20	3	0.9914	-4.45	0	0	6.8	1.03
21	3	1.0337	-5.26	0	0	2.74	1.15
22	3	1.0509	-0.82	0	0	0	0
23	3	1.0459	-1.02	0	0	2.475	0.846
24	3	1.0399	-7.54	0	0	3.086	-0.922
25	3	1.0587	-5.51	0	0	2.24	0.472
26	3	1.0536	-6.77	0	0	1.39	0.17
27	3	1.0399	-8.78	0	0	2.81	0.755
28	3	1.0509	-3.27	0	0	2.06	0.276
29	2	1.0505	-0.51	0	0	2.835	1.269
30	2	1.0475	-4.47	2.5	1.3621	0	0

31	2	1.04	0	5.7293	1.7036	0.092	0.046
32	2	0.9831	1.63	6.5	1.759	0	0
33	2	0.9972	2.18	6.32	1.0335	0	0
34	2	1.0123	0.74	5.08	1.64	0	0
35	2	1.0493	4.14	6.5	2.0884	0	0
36	2	1.0635	6.83	5.6	0.9688	0	0
37	2	1.0278	1.26	5.4	-0.0444	0	0
38	2	1.0265	6.55	8.3	0.1939	0	0
39	1	1.03	-10.96	10	0.6846	11.04	2.5

References

[1]   A. R. Messina, Ed., *Inter-area Oscillations in Power Systems*. Boston, MA: Springer US, 2009.

[2]   Q. Wei, W. Guo, N. He, and M. Yang, "A new method to eliminate low-frequency oscillations," in *IEEE Power and Energy Society General Meeting*, 2013.

[3]   S. Bifaretti, P. Zanchetta, A. Watson, L. Tarisciotti, and J. C. Clare, "Advanced power electronic conversion and control system for universal and flexible power management," *IEEE Trans. Smart Grid*, vol. 2, no. 2, pp. 231–243, 2011.

[4]   B. Mwinyiwiwa, Z. Wolanski, and B. T. Ooi, "High power switch mode linear amplifiers for flexible AC transmission system," *IEEE Trans. Power Deliv.*, vol. 11, no. 4, pp. 1993–1998, 1996.

[5]   M. Moazzami, R. A. Hooshmand, A. Khodabakhshian, and M. Yazdanpanah, "Blackout prevention in power system using flexible AC transmission system devices and combined corrective actions," *Electr. Power Components Syst.*, vol. 41, no. 15, pp. 1433–1455, 2013.

[6]   M. K. Mahdiyeh Eslami, Hussain Shareef, Azah Mohamed, "A Survey on Flexible AC Transmission Systems (FACTS)," *Przegląd Elektrotechniczny*, vol. 88, no. 1, pp. 1–11, 2012.

[7]   K. T. Tan, P. L. So, Y. C. Chu, and M. Z. Q. Chen, "A Flexible AC Distribution System Device for a Microgrid," *IEEE Trans. Energy Convers.*, vol. 28, no. 3, pp. 601–610, 2013.

[8]   Jiangmeng Zhang and D. Chen, "On the application of Phasor Measurement Units to power system stability monitoring and analysis," in *2012 IEEE Power and Energy Conference at Illinois*, 2012, pp. 1–6.

[9]   G. Rogers, *Power System Structure and Oscillations*. Boston, MA: Springer US, 2000.

[10]   Wei Yao, Lin Jiang, Jinyu Wen, Qinghua Wu, and Shijie Cheng, "Wide-Area Damping Controller for Power System Interarea Oscillations: A Networked Predictive Control Approach," *IEEE Trans. Control Syst. Technol.*, vol. 23, no. 1, pp. 27–36, Jan. 2015.

[11]   Y. Chompoobutrgool, L. Vanfretti, and M. Ghandhari, "Survey on power system stabilizers control and their prospective applications for power system damping using Synchrophasor-based wide-area systems," *Eur. Trans. Electr. Power*, vol. 21, no. 8, pp. 2098–2111, Nov. 2011.

[12]   R. Yousefian and S. Kamalasadan, "An approach for real-time tuning of cost

functions in optimal System-Centric Wide Area Controller based on Adaptive Critic Design," in *IEEE Power and Energy Society General Meeting*, 2014, vol. 2014–Octob, no. October.

[13] R. Yousefian and S. Kamalasadan, "System-centric control architecture for wide area monitoring and control of power system," in *2013 IEEE PES Innovative Smart Grid Technologies (ISGT)*, 2013, pp. 1–7.

[14] J. H. Chow, Ed., *Power System Coherency and Model Reduction*, vol. 94. New York, NY: Springer New York, 2013.

[15] Y. Li, D. Yang, F. Liu, Y. Cao, and C. Rehtanz, *Interconnected Power Systems*. Berlin, Heidelberg: Springer Berlin Heidelberg, 2016.

[16] M. Klein, G. J. Rogers, and P. Kundur, "A fundamental study of inter-area oscillations in power systems," *IEEE Trans. Power Syst.*, vol. 6, no. 3, pp. 914–921, 1991.

[17] M. A. Abido, "Analysis and assessment of STATCOM-based damping stabilizers for power system stability enhancement," *Electr. Power Syst. Res.*, vol. 73, no. 2, pp. 177–185, 2005.

[18] C. E. Ugalde-Loo, E. Acha, and E. Licéaga-Castro, "Multi-machine power system state-space modelling for small-signal stability assessments," *Appl. Math. Model.*, vol. 37, no. 24, pp. 10141–10161, 2013.

[19] J. A. Suul, J. Beerten, and S. D'Arco, "Frequency-dependent cable modelling for small-signal stability analysis of VSC-HVDC systems," *IET Gener. Transm. Distrib.*, vol. 10, no. 6, pp. 1370–1381, 2016.

[20] J. Sun, "Small-signal methods for AC distributed power systems-A review," *IEEE Transactions on Power Electronics*, vol. 24, no. 11. pp. 2545–2554, 2009.

[21] D. J. Lee and L. Wang, "Small-signal stability analysis of an autonomous hybrid renewable energy power generation/energy storage system part I: Time-domain simulations," *IEEE Trans. Energy Convers.*, vol. 23, no. 1, pp. 311–320, 2008.

[22] W. Gao and J. Ning, "Wavelet-based disturbance analysis for power system wide-area monitoring," *IEEE Trans. Smart Grid*, vol. 2, no. 1, pp. 109–118, 2011.

[23] J. J. Sanchez-Gasca, "Performance comparison of three identification methods for the analysis of electromechanical oscillations," *IEEE Trans. Power Syst.*, vol. 14, no. 3, pp. 995–1002, 1999.

[24] C. Geng, F. Wang, J. Zhang, and Z. Jin, "Modal parameters identification of power transformer winding based on improved Empirical Mode Decomposition method," *Electr. Power Syst. Res.*, vol. 108, pp. 331–339, 2014.

[25] S. You, J. Guo, G. Kou, Y. Liu, and Y. Liu, "Oscillation mode identification based on wide-area ambient measurements using multivariate empirical mode

decomposition," *Electr. Power Syst. Res.*, vol. 134, pp. 158–166, 2016.

[26] A. Prince, N. Senroy, and R. Balasubramanian, "Targeted approach to apply masking signal-based empirical mode decomposition for mode identification from dynamic power system wide area measurement signal data," *IET Gener. Transm. Distrib.*, vol. 5, no. 10, p. 1025, 2011.

[27] K. Mandadi and B. Kalyan Kumar, "Identification of Inter-Area Oscillations Using Zolotarev Polynomial Based Filter Bank with Eigen Realization Algorithm," *IEEE Trans. Power Syst.*, vol. 31, no. 6, pp. 4650–4659, 2016.

[28] A. R. Messina and V. Vittal, "Extraction of dynamic patterns from wide-area measurements using empirical orthogonal functions," *IEEE Trans. Power Syst.*, vol. 22, no. 2, pp. 682–692, 2007.

[29] K. M. K. Mei, S. M. Rovnyak, and C.-M. O. C.-M. Ong, "Dynamic event detection using wavelet analysis," *2006 IEEE Power Eng. Soc. Gen. Meet.*, no. 1, pp. 1–7, 2006.

[30] S. Han, Z. Xu, B. Sun, and L. He, "Dynamic characteristic analysis of power system interarea oscillations using HHT," *Int. J. Electr. Power Energy Syst.*, vol. 32, no. 10, pp. 1085–1090, 2010.

[31] S. Y. Sun, H. C. Shu, J. Dong, and Z. J. Liu, "Analysis of low frequency oscillation mode based on PMU and PRONY method," *Asia-Pacific Power Energy Eng. Conf. APPEEC*, no. 3, pp. 1–4, 2009.

[32] P. Tripathy, S. C. Srivastava, and S. N. Singh, "An improved Prony method for identifying low frequency oscillations using synchro-phasor measurements," *2009 Int. Conf. Power Syst. ICPS '09*, 2009.

[33] H. T. Yang and C. C. Liao, "A de-noising scheme for enhancing wavelet-based power quality monitoring system," *IEEE Trans. Power Deliv.*, vol. 16, no. 3, pp. 353–360, 2001.

[34] R. Yan and R. X. Gao, "Hilbert-huang transform-based vibration signal analysis for machine health monitoring," *IEEE Trans. Instrum. Meas.*, vol. 55, no. 6, 2006.

[35] Z. K. Peng, P. W. Tse, and F. L. Chu, "An improved Hilbert-Huang transform and its application in vibration signal analysis," *J. Sound Vib.*, vol. 286, no. 1–2, pp. 187–205, 2005.

[36] F. R. Schleif, H. D. Hunkins, G. E. Martin, and E. E. Hattan, "Excitation Control to Improve Powerline Stability," *IEEE Trans. Power Appar. Syst.*, vol. 2, no. 6, pp. 1426–1434, 1968.

[37] F. Demello and C. Concordia, "Concepts of Synchronous Machine Stability as Affected by Excitation Control," *IEEE Trans. Power Appar. Syst.*, vol. PAS-88, no. 4, pp. 316–329, 1969.

[38] M. A. Mahmud, H. R. Pota, M. Aldeen, and M. J. Hossain, "Partial feedback linearizing excitation controller for multimachine power systems to improve transient stability," *IEEE Trans. Power Syst.*, vol. 29, no. 2, pp. 561–571, 2014.

[39] J. P. Bayne, P. Kundur, and W. Watson, "Static exciter control to improve transient stability," *IEEE Trans. Power Appar. Syst.*, vol. 94, no. 4, pp. 1141–1146, 1975.

[40] P. Zhao, W. Yao, J. Wen, L. Jiang, S. Wang, and S. Cheng, "Improved synergetic excitation control for transient stability enhancement and voltage regulation of power systems," *Int. J. Electr. Power Energy Syst.*, vol. 68, pp. 44–51, 2015.

[41] H. Zhang, F. Shi, and Y. Liu, "Enhancing optimal excitation control by adaptive fuzzy logic rules," *Int. J. Electr. Power Energy Syst.*, vol. 63, pp. 226–235, 2014.

[42] D. K. Chaturvedi and O. P. Malik, "Neurofuzzy power system stabilizer," *IEEE Trans. Energy Convers.*, vol. 23, no. 3, pp. 887–894, 2008.

[43] F. M. Hughes, O. Anaya-Lara, N. Jenkins, and G. Strbac, "A power system stabilizer for DFIG-based wind generation," *IEEE Trans. Power Syst.*, vol. 21, no. 2, pp. 763–772, 2006.

[44] D. Chitara, K. R. Niazi, A. Swarnkar, and N. Gupta, "Cuckoo Search Optimization Algorithm for Designing of Multimachine Power System Stabilizer," *IEEE Trans. Ind. Appl.*, pp. 1–1, 2018.

[45] H. Wu, K. S. Tsakalis, and G. T. Heydt, "Evaluation of Time Delay Effects to Wide-Area Power System Stabilizer Design," *IEEE Trans. Power Syst.*, vol. 19, no. 4, pp. 1935–1941, 2004.

[46] Y. Li, C. Rehtanz, S. Rüberg, L. Luo, and Y. Cao, "Wide-area robust coordination approach of HVDC and FACTS controllers for damping multiple interarea oscillations," *IEEE Trans. Power Deliv.*, vol. 27, no. 3, pp. 1096–1105, 2012.

[47] H. Ni, G. T. Heydt, and L. Mili, "Power system stability agents using robust wide area control," *Power Syst. IEEE Trans.*, vol. 17, no. 4, pp. 1123–1131, 2002.

[48] J. Deng, C. Li, and X. P. Zhang, "Coordinated Design of Multiple Robust FACTS Damping Controllers: A BMI-Based Sequential Approach with Multi-Model Systems," *IEEE Trans. Power Syst.*, vol. 30, no. 6, pp. 3150–3159, 2015.

[49] B. Chaudhuri, R. Majumder, and B. C. Pal, "Wide-area measurement-based stabilizing control of power system considering signal transmission delay," *IEEE Trans. Power Syst.*, vol. 19, no. 4, pp. 1971–1979, 2004.

[50] D. Dotta, A. S. e Silva, and I. C. Decker, "Wide-area measurements-based two-level control design considering signal transmission delay," *IEEE Trans. Power Syst.*, vol. 24, no. 1, pp. 208–216, 2009.

[51] R. Majumder, B. Chaudhuri, and B. C. Pal, "Implementation and test results of a wide-area measurement-based controller for damping interarea oscillations

considering signal-transmission delay," *Gener. Transm. Distrib. IET*, vol. 1, no. 1, pp. 1–7, 2007.

[52]   G. L. Yu, B. H. Zhang, H. Xie, and C. G. Wang, "Wide-area measurement-based nonlinear robust control of power system considering signals' delay and incompleteness," in *2007 IEEE Power Engineering Society General Meeting, PES*, 2007.

[53]   Y. Li, F. Liu, C. Rehtanz, L. Luo, and Y. Cao, "Dynamic output-feedback wide area damping control of HVDC transmission considering signal time-varying delay for stability enhancement of interconnected power systems," *Renew. Sustain. Energy Rev.*, vol. 16, no. 8, pp. 5747–5759, 2012.

[54]   Z. Liu, G. Hailati, and J. Wang, "Stabilizing control of wide-area power system with signal transmission delay based on Hamiltonian functional method," *Aust. J. Electr. Electron. Eng.*, vol. 12, no. 3, pp. 259–266, 2015.

[55]   S. Ray and G. K. Venayagamoorthy, "Real-time implementation of a measurement-based adaptive wide-area control system considering communication delays," *IET Gener. Transm. Distrib.*, vol. 2, no. 1, p. 62, 2008.

[56]   J. W. Stahlhut, T. J. Browne, G. T. Heydt, and V. Vittal, "Latency viewed as a stochastic process and its impact on wide area power system control signals," *IEEE Trans. Power Syst.*, vol. 23, no. 1, pp. 84–91, 2008.

[57]   F. Bai, L. Zhu, Y. Liu, X. Wang, K. Sun, Y. Ma, M. Patel, E. Farantatos, and N. Bhatt, "Design and implementation of a measurement-based adaptive wide-area damping controller considering time delays," *Electr. Power Syst. Res.*, vol. 130, pp. 1–9, 2016.

[58]   G. Cai, D. Yang, and C. Liu, "Adaptive wide-area damping control scheme for smart grids with consideration of signal time delay," *Energies*, vol. 6, no. 9, pp. 4841–4858, 2013.

[59]   W. Li, H. Li, and A. Monti, "Using co-simulation method to analyze the communication delay impact in agent-based wide area power system stabilizing control," *Proc. 2011 Gd. Challenges Model. Simul. Conf.*, pp. 356–361, 2011.

[60]   M. R. Shakarami and I. F. Davoudkhani, "Wide-area power system stabilizer design based on Grey Wolf Optimization algorithm considering the time delay," *Electr. Power Syst. Res.*, vol. 133, pp. 149–159, 2016.

[61]   R. Hadidi and B. Jeyasurya, "Reinforcement learning based real-time wide-area stabilizing control agents to enhance power system stability," *IEEE Trans. Smart Grid*, vol. 4, no. 1, pp. 489–497, 2013.

[62]   B. Yang and Y. zhang Sun, "A new wide area damping controller design method considering signal transmission delay to damp interarea oscillations in power system," *J. Cent. South Univ.*, vol. 21, no. 11, pp. 4193–4198, 2014.

[63] V. A. F. de Campos and J. J. da Cruz, "Robust hierarchized controllers using wide area measurements in power systems," *Int. J. Electr. Power Energy Syst.*, vol. 83, pp. 392–401, 2016.

[64] W. Yao, L. Jiang, J. Wen, Q. H. Wu, and S. Cheng, "Wide-Area Damping Controller of FACTS Devices for Inter-Area Oscillations Considering Communication Time Delays," vol. 29, no. 1, pp. 318–329, 2014.

[65] M. G. Safonov and R. Y. Chiang, "A Schur Method for Balanced-Truncation Model Reduction," *IEEE Trans. Automat. Contr.*, vol. 34, no. 7, pp. 729–733, 1989.

[66] N. Kishor, L. Haarla, J. Seppänen, and S. R. Mohanty, "Fixed-order controller for reduced-order model for damping of power oscillation in wide area network," *Int. J. Electr. Power Energy Syst.*, vol. 53, no. 1, pp. 719–732, 2013.

[67] M. Bhadu, G. N. Sudha, N. Senroy, and I. Narayan Kar, "Robust linear quadratic Gaussian-based discrete mode wide area power system damping controller," *IET Gener. Transm. Distrib.*, vol. 10, no. 6, pp. 1470–1478, 2016.

[68] R. Shah, N. Mithulananthan, and K. Y. Lee, "Large-scale PV plant with a robust controller considering power oscillation damping," *IEEE Trans. Energy Convers.*, vol. 28, no. 1, pp. 106–116, 2013.

[69] B. Naduvathuparambil, M. C. Valenti, and A. Feliachi, "Communication delays in wide area measurement systems," in *Proceedings of the Thirty-Fourth Southeastern Symposium on System Theory (Cat. No.02EX540)*, 2002, pp. 118–122.

[70] S. Wang, X. Meng, and T. Chen, "Wide-area control of power systems through delayed network communication," *IEEE Trans. Control Syst. Technol.*, vol. 20, no. 2, pp. 495–503, 2012.

[71] C. Lu, X. Zhang, X. Wang, and Y. Han, "Mathematical Expectation Modeling of Wide-Area Controlled Power Systems with Stochastic Time Delay," *IEEE Trans. Smart Grid*, vol. 6, no. 3, pp. 1511–1519, 2015.

[72] H. Lin, S. S. Veda, S. S. Shukla, L. Mili, and J. Thorp, "GECO: Global event-driven co-simulation framework for interconnected power system and communication network," *IEEE Trans. Smart Grid*, vol. 3, no. 3, pp. 1444–1456, 2012.

[73] M. E. Aboul-Ela, A. A. Sallam, J. D. McCalley, and A. A. Fouad, "Damping controller design for power system oscillations using global signals," *IEEE Trans. Power Syst.*, vol. 11, no. 2, pp. 767–773, 1996.

[74] S. Zhang and V. Vittal, "Design of wide-area power system damping controllers resilient to communication failures," *IEEE Trans. Power Syst.*, vol. 28, no. 4, pp. 4292–4300, 2013.

[75] Y. Chompoobutrgool and L. Vanfretti, "Using PMU signals from dominant paths in power system wide-area damping control," *Sustain. Energy, Grids Networks*, vol. 4, pp. 16–28, 2015.

[76]   A. E. Leon, J. M. Mauricio, A. Gomez-Exposito, and J. A. Solsona, "Hierarchical wide-area control of power systems including wind farms and FACTS for short-term frequency regulation," *IEEE Trans. Power Syst.*, vol. 27, no. 4, pp. 2084–2092, 2012.

[77]   A. E. Leon and J. A. Solsona, "Power oscillation damping improvement by adding multiple wind farms to wide-area coordinating controls," *IEEE Trans. Power Syst.*, vol. 29, no. 3, pp. 1356–1364, 2014.

[78]   B. Yang and Y. Sun, "A novel approach to calculate damping factor based delay margin for wide area damping control," *IEEE Trans. Power Syst.*, vol. 29, no. 6, pp. 3116–3117, 2014.

[79]   B. Yang and Y. Sun, "Damping factor based delay margin for wide area signals in power system damping control," *IEEE Trans. Power Syst.*, vol. 28, no. 3, pp. 3501–3502, 2013.

[80]   Y. Li, Y. Zhou, F. Liu, Y. Cao, and C. Rehtanz, "Design and Implementation of Delay-Dependent Wide-Area Damping Control for Stability Enhancement of Power Systems," *IEEE Trans. Smart Grid*, vol. 8, no. 4, pp. 1831–1842, 2017.

[81]   W. Yao, L. Jiang, Q. H. Wu, J. Y. Wen, and S. J. Cheng, "Delay-dependent stability analysis of the power system with a wide-area damping controller embedded," *IEEE Trans. Power Syst.*, vol. 26, no. 1, pp. 233–240, 2011.

[82]   N. R. Chaudhuri, S. Ray, R. Majumder, and B. Chaudhuri, "A new approach to continuous latency compensation with adaptive phasor power oscillation damping controller (POD)," *IEEE Trans. Power Syst.*, vol. 25, no. 2, pp. 939–946, 2010.

[83]   X. Wu, P. Li, C. Lu, J. Wu, and J. He, "Design and experiment of wide area HVDC supplementary damping controller considering time delay in China southern power grid," *IET Gener. Transm. Distrib.*, vol. 3, no. 1, pp. 17–25, 2009.

[84]   D. Roberson and J. F. OBrien, "Variable Loop Gain Using Excessive Regeneration Detection for a Delayed Wide-Area Control System," *IEEE Transactions on Smart Grid*, 2017.

[85]   V. Belevitch, *Classical Network Theory*, G. F. Fran. San Francisco, CA: Holden-Day, 1968.

[86]   R. J. Anderson and M. W. Spong, "Bilateral Control of Teleoperators with Time Delay," *IEEE Trans. Automat. Contr.*, vol. 34, no. 5, pp. 494–501, 1989.

[87]   T. Matiakis, S. Hirche, and M. Buss, "Control of networked systems using the scattering transformation," *IEEE Trans. Control Syst. Technol.*, vol. 17, no. 1, 2009.

[88]   P. Kundur, "Power system stability and control," *McGraw-Hill*. pp. 45–138, 1994.

[89]   Y. Yu, S. Grijalva, J. J. Thomas, L. Xiong, P. Ju, and Y. Min, "Oscillation Energy Analysis of Inter-Area Low-Frequency Oscillations in Power Systems," *IEEE*

Trans. Power Syst., vol. 31, no. 2, pp. 1195–1203, 2016.

[90] K. Liao, Z. He, Y. Xu, G. Chen, Z. Y. Dong, and K. P. Wong, "A Sliding Mode Based Damping Control of DFIG for Interarea Power Oscillations," *IEEE Trans. Sustain. Energy*, vol. 8, no. 1, pp. 258–267, 2017.

[91] T. E. Duncan, "Linear-exponential-quadratic gaussian control," *IEEE Trans. Automat. Contr.*, vol. 58, no. 11, pp. 2910–2911, 2013.

[92] A. Bryson and M. Reyhanoglu, "Applied Linear Optimal Control: Examples and Algorithms," *Applied Mechanics Reviews*, vol. 56, no. 4. p. B55, 2003.

[93] A. S. Musleh, S. M. Muyeen, A. Al-Durra, I. Kamwa, M. A. S. Masoum, and S. Islam, "Time-Delay Analysis of Wide-Area Voltage Control Considering Smart Grid Contingences in a Real-Time Environment," *IEEE Trans. Ind. Informatics*, vol. 14, no. 3, pp. 1242–1252, 2018.

[94] H. Ye, Q. Mou, and Y. Liu, "Calculation of Critical Oscillation Modes for Large Delayed Cyber-Physical Power System Using Pseudo-Spectral Discretization of Solution Operator," *IEEE Trans. Power Syst.*, vol. 32, no. 6, pp. 4464–4476, Nov. 2017.

[95] H. K. Khalil, "Noninear Systems," *Prentice-Hall, New Jersey*, vol. 2, no. 5. pp. 1–5, 1996.

[96] Tilemachos Matiakis, Sandra Hirche, and M. Buss, "The scattering transformation for networked control systems," in *Proceedings of 2005 IEEE Conference on Control Applications, 2005. CCA 2005.*, pp. 705–710.

[97] J. Kennedy and R. Eberhart, "Particle swarm optimization," in *Proceedings of ICNN'95 - International Conference on Neural Networks*, vol. 4, pp. 1942–1948.

[98] M. A. Abido, "Optimal design of power-system stabilizers using particle swarm optimization," *IEEE Trans. Energy Convers.*, vol. 17, no. 3, pp. 406–413, Sep. 2002.

[99] M. S. El-Moursi, B. Bak-Jensen, and M. H. Abdel-Rahman, "Novel STATCOM controller for mitigating SSR and damping power system oscillations in a series compensated wind park," *IEEE Trans. Power Electron.*, vol. 25, no. 2, pp. 429–441, 2010.

Vitae

Name   :Ahmed Husham Ahmed Mohamed

Nationality   :Sudanese

Date of Birth   :1/11/1994

 Email   :ahisham500@gmail.com

Address   :Dammam, Saudi Arabia (31261)

Khartoum ZIP Code   : 11111

Academic Background   :Bachelor of Science (B.Sc.) degree in Electrical Engineering from Sudan university of science & technology (SUST), Khartoum, Sudan in 2014.

Publications (Under Review+Accepted)

Ahmed Husham Mohamed, and M. Abido, "**Delay-independent Approach for Wide-Area Damping Control Using Scattering Transformation**", currently under review in IEEE Transactions on Power Systems.

Ahmed Husham, Luqman Maraaba and Ammar Elagab,"**Optimal Tuning of SSSC-based Supplemental Damping Controller Employing RCGA"** IEEE Conference (*Accepted*)

Ammar Elagab, Ibrahim Alamin and Ahmed Husham, **"Power Quality Issues Due to connecting an Electric Train To a Power Supply System Through V/V Transformer"** IEEE conference (*Accepted*)